AEDC-TR-66-88

FILM AND TRANSPIRATION COOLING OF NOZZLE THROATS

H. C. Roland, P. F. Pasqua,
and P. N. Stevens
Nuclear Engineering Department
The University of Tennessee

June 1966

PROPERTY OF U.S. AIR FORCE
AEDC TECHNICAL LIBRARY

TECHNICAL REPORTS
FILE COPY

Distribution of this document is unlimited.

ARNOLD ENGINEERING DEVELOPMENT CENTER
AIR FORCE SYSTEMS COMMAND
ARNOLD AIR FORCE STATION, TENNESSEE

NOTICES

When U. S. Government drawings specifications, or other data are used for any purpose other than a definitely related Government procurement operation, the Government thereby incurs no responsibility nor any obligation whatsoever, and the fact that the Government may have formulated, furnished, or in any way supplied the said drawings, specifications, or other data, is not to be regarded by implication or otherwise, or in any manner licensing the holder or any other person or corporation, or conveying any rights or permission to manufacture, use, or sell any patented invention that may in any way be related thereto.

Qualified users may obtain copies of this report from the Defense Documentation Center.

References to named commercial products in this report are not to be considered in any sense as an endorsement of the product by the United States Air Force or the Government.

FILM AND TRANSPIRATION COOLING OF NOZZLE THROATS

H. C. Roland, P. F. Pasqua,
and P. N. Stevens
Nuclear Engineering Department
The University of Tennessee

FOREWORD

The work reported herein was sponsored by Headquarters, Arnold Engineering Development Center (AEDC), Air Force Systems Command (AFSC), Arnold Air Force Station, Tennessee, under Program Element 62410034, Project 7778, Task 777805.

The results of research were obtained by the Nuclear Engineering Department, University of Tennessee, under Contract AF40(600)-981. The manuscript was submitted for publication on March 29, 1966.

The reproducibles used in the reproduction of this report were supplied by the author.

This technical report has been reviewed and is approved.

GORDON M. GRAY
Lt Col, USAF
Chief, Tripltee Program Office
DCS/Civil Engineering

ORSON A. ISRAELSEN
Colonel, USAF
DCS/Civil Engineering

ABSTRACT
of
FILM AND TRANSPIRATION COOLING
of
NOZZLE THROATS

Analytical studies were made of liquid film cooling, gas film cooling, and liquid or gas transpiration cooling of hypersonic nozzles. Experimental studies of gas film cooling were performed on a small nozzle using air as both the mainstream and coolant gases. Based on the experimental results obtained and the development of satisfactory calculational techniques to implement the analyses given in the present study, the following conclusions were drawn:

1. Gas film cooling can be used to measurably lower the wall temperatures and the wall heat fluxes in the converging section and at the throat of a high-pressure high-temperature nozzle. Some gross mixing occurs at the injection point, the exact amount being some as yet undetermined function of the injection geometry, the relative velocities of the main gas stream and the coolant stream at the injection point, and the entering velocity profiles and turbulence conditions.

2. A straightforward boundary layer type analysis was developed and programmed which predicts with reasonable accuracy the nozzle wall temperatures and wall heat fluxes in the converging section and at the throat for gas film cooled nozzles.

3. Calculational techniques have been developed and programmed for predicting the effectiveness of liquid film cooling and liquid or gas transpiration cooling in nozzles. These techniques should be checked against experimental data before they are used for design purposes, however.

TABLE OF CONTENTS

LIST OF FIGURES

FIGURE PAGE

LIST OF TABLES

CHAPTER I
INTRODUCTION

I. GENERAL DISCUSSION

Recent technological developments have caused an increased interest in analytical and experimental studies of film and transpiration cooling. Military rocket and space research has brought about extensive investigations into the problems of rocket nozzle design. In particular, greater specific thrust can be achieved by using higher combustion chamber pressures and temperatures, however this requires better nozzle throat cooling in order to reduce corrosion, oxidation, and thermal stresses. Another problem involves the surfaces of re-entry vehicles which must be protected from the extremely high heat loads encountered. Experimental studies utilizing wind tunnels which simulate re-entry conditions provide the most direct approach to this problem. Wind tunnel systems designed to provide these test conditions must use air at extremely high stagnation pressures and temperatures resulting in extremely high heat loads at the nozzle throat which must be protected by proper heat transfer design.

Examination of ordinary backside cooling of the nozzle throat shows that it may become inadequate for two principal reasons: (1) Exceedingly high static pressure of the coolant may be required to prevent boiling (for conventional liquid coolants) with the subsequent danger of burnout, (2) backside cooling cannot reduce the heat load to the nozzle surface so it cannot alleviate the problem of thermal stresses.

It has been proposed, therefore, that rocket combustion chambers and nozzles, re-entry vehicles, high-pressure high-temperature wind tunnel nozzles and other devices with the same problems be protected by film or transpiration cooling or a combination of one of these with backside cooling. Film cooling refers to the injection of a liquid or gas into a system in such a manner that it forms a relatively thin protective layer over the surface to be cooled. The liquid or gas is injected at one or more discrete locations on the surface through holes or slots. Transpiration cooling refers to the injection of a liquid or gas through a porous surfece to cool it. Gas film cooling by injection through holes approaches transpiration cooling as the size of the holes decreases and the number increases, however, in actual practice the two are usually well distinguished. Figure 1 shows the two systems diagrammatically.

It is instructive to consider the desirable properties for film and transpiration coolants. In order to maintain a low surface temperature with liquids they should have a low saturation temperature at the static pressure in the chamber. They should also have a high heat of vaporization and a high specific heat capacity in the vapor state. This reduces the amount of coolant required. The primary requirement for a gaseous coolant, from a thermal standpoint, is that it have a high heat capacity. This indicates that light gases, such as helium and hydrogen should make good coolants for gas film and transpiration cooling. There are other requirements to be considered, however. The introduction of the coolant into the system must not produce effects

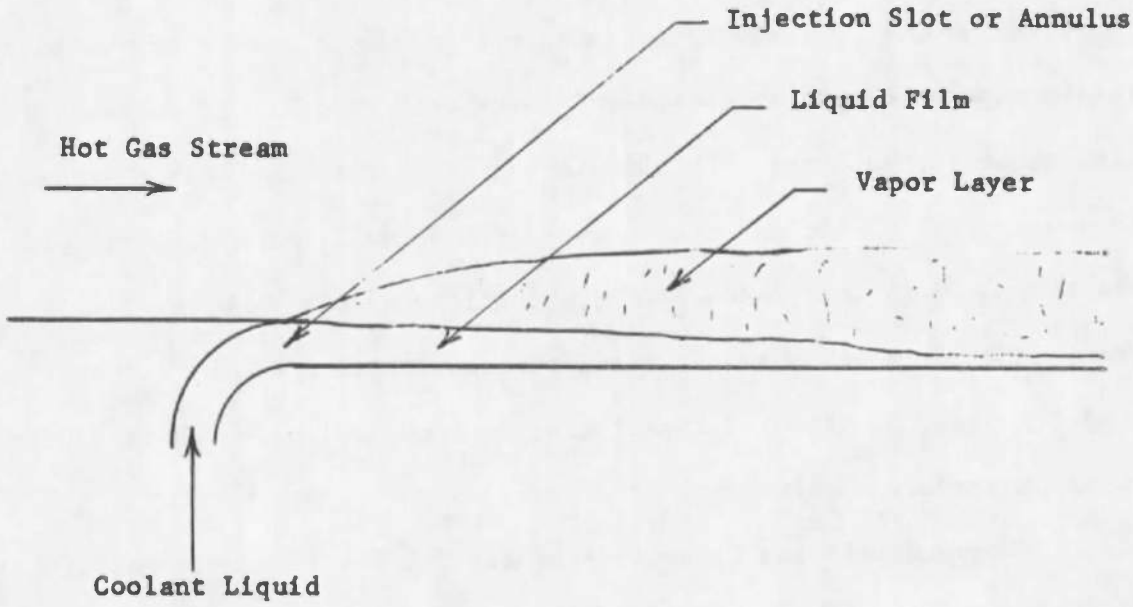

Liquid Film Cooling

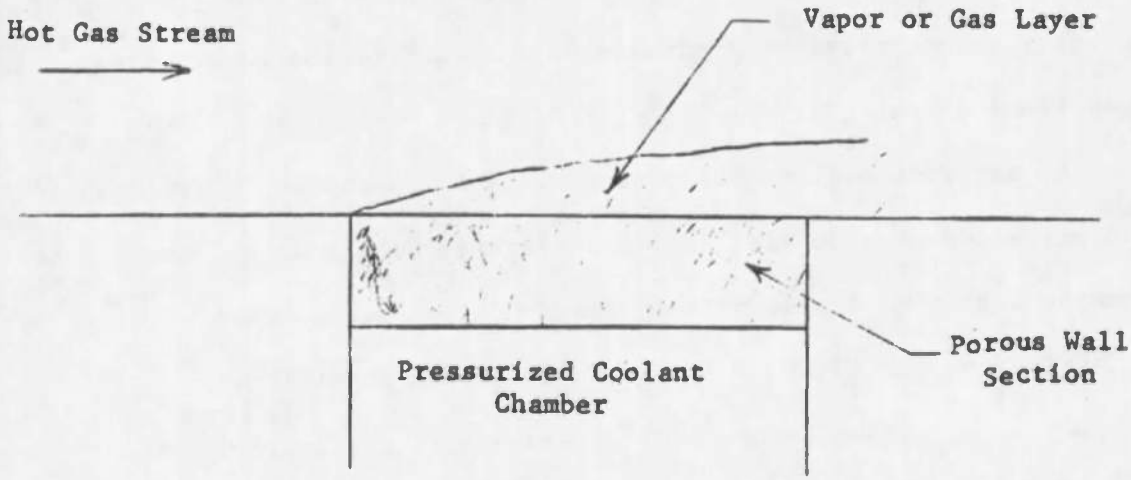

Transpiration Cooling

Fig. 1 Diagram of Liquid Film Cooling and Transpiration Cooling

which destroy the usefulness of the system. This would not severely limit the choice of coolants for a rocket nozzle or a re-entry vehicle, but it must be carefully considered for a wind tunnel. If possible wind tunnels should test vehicles in the atmosphere in which they are to operate. The main gas stream thus will normally be air. Nitrogen might be used in some cases. If the cooling process requires injection of an amount which is a significant fraction of the main gas mass flow rate of the wind tunnel the required coolant would thus have to be either air or nitrogen.

In both film and transpiration cooling the protective effect of the heat absorption by the coolant is augmented by the heat transfer blocking action of the coolant gas as it moves into the main stream. This "blowing" action at the wall or coolant film surface reduces the velocity and temperature gradients at the surface and thus decreases the heat transfer rate.

Backside cooling may be used with film cooling. This combination reduces the nozzle liner temperature and allows the cooling of a greater nozzle wall area by the same amount of film coolant. It is more effective for liquid films under the following conditions:

1. The film saturation temperature is considerably higher than the backside coolant temperature.
2. There is a high thermal conductance between the coolant film and the backside coolant.

II. REVIEW OF PREVIOUS STUDIES

Analytical and experimental studies of nozzle heat transfer rates have been made by a number of investigators; however, studies of heat transfer with extremely high heat loads using nozzles instrumented to give a good profile of the heat transfer rate are not available. In the present study such a nozzle was used.

Analytical and experimental studies of film and transpiration cooling have also been made by many investigators. The Bibliography contains references to several of these studies. An extensive review of the literature on film cooling studies up to 1957 is given in Graham and Bucrow's "Film Cooling, Its Theory and Application," (16). Librizzi and Cresci's "Transpiration Cooling of a Turbulent Boundary Layer in an Axisymetric Nozzle" (24) lists a large amount of work which has been done on film and transpiration cooling since 1957. A careful examination of these references, however, disclosed that none of these analyses is directly applicable to the present problem.

Since the present solution to these problems is based on adaptation of previous works (except for gas film cooling), a somewhat more extensive review of these works is in order.

A widely used equation for rapid calculation of heat transfer coefficients in nozzle throats without film or transpiration cooling was developed by Bartz (2). He started from the basic premise, based on more elaborate boundary layer calculations performed earlier (3) that for a turbulent boundary layer the dominant variable factor is the mass flow rate, i.e.

$$h \sim (\rho u)^m \tag{1}$$

He then rewrote Eq. (1) in the form

$$Nu = C(Re)^m (Pr)^n \tag{2}$$

which is the same form as the widely used Dittus-Boelter equation for correlation of fully developed turbulent heat transfer in pipe flow. By regrouping the variables in Eq. (2), assuming $\mu \sim T^{\omega}$, $\rho \sim \frac{1}{T}$, c_p and Pr constant, and introducing a factor (D_*/r_c) to account for curvature effects at the throat, Bartz was able to write Eq. (2) in the form

$$h = \left(\frac{C}{D_*^{.2}}\right)\left(\frac{\mu^{.2} c_p}{Pr^{.6}}\right)\left(\frac{P_o g_c}{u_*}\right)^{.8}\left(\frac{D_*}{r_c}\right)^{.1}\left(\frac{A_*}{A}\right)^{.9}\sigma \tag{3}$$

in which

$$\sigma = \frac{1}{\left[\frac{1}{2}\frac{T_w}{T_o}\left(1 + \frac{k-1}{2}M^2\right) + \frac{1}{2}\right]^{.8-\omega/5}\left(1 + \frac{k-1}{2}M^2\right)^{\omega/5}} \tag{4}$$

The constant C in the equation was determined from experimental data for heat transfer at nozzle throats to be 0.0265 in a nozzle with contraction and expansion half angles of 30 and 15 degrees, respectively. This is only slightly higher than that usually given for the constant C when Eq. (3) is applied to fully developed turbulent pipe flow, namely 0.023. An examination of the velocity profiles for turbulent flow with negative axial pressure gradients (39) shows that the pressure gradient has the effect of increasing the wall shear stress, and thus an increase in the heat transfer coefficient is to be expected.

Emmons (13) developed a simplified analysis for liquid film cooling of a cylindrical rocket motor combustion chamber with backside cooling. It was based on the following assumptions:

1. The gas stream pressure and velocity do not vary appreciably in the axial direction.
2. The wall temperature does not vary appreciably in the axial direction.
3. The temperature of the liquid film surface exposed to the hot gas is at all points equal to the saturation temperature of the liquid.
4. Temperature gradients in the radial direction through the liquid film are small.
5. The liquid film temperature does not vary rapidly in the axial direction.
6. The heat transfer coefficient between the gas stream and the liquid film is constant and is based on a steady state analysis.
7. The amount of liquid in the film varies linearly with the distance in the axial direction.

In the case studied by Emmons these were all reasonable assumptions provided the coolant film was injected at the local saturation temperature. It may be noted immediately, however, that several of these assumptions are not reasonable for the case of injection of a coolant liquid well below saturation temperature into a high pressure, high temperature nozzle gas stream. In a supersonic nozzle there are

large axial variations in static pressure, film temperature, heat transfer coefficient, film thickness, and film shear stress. The rate of evaporation is not constant and thus the film mass flow rate does not vary linearly with axial distance. To accurately predict the required film cooling for a nozzle using Emmons' approach it was thus necessary to remove the restrictions of the above assumptions.

III. PLAN OF THE PRESENT INVESTIGATIONS

Objectives. The objectives of the present investigation were to perform analytical and experimental studies of heat transfer rates and required coolant injection rates for a hypersonic nozzle with gas film cooling and to make analytical studies of heat transfer rates and required coolant flow rates for a hypersonic nozzle with liquid film and transpiration cooling.

Theoretical Investigations. For liquid film cooling and transpiration cooling the results of previous investigations, particularly those outlined above, were examined, suitably modified and combined in a finite difference stepwise calculation through the nozzle. This was programmed for solution using an IBM 7040 digital computer.

For gas film cooling a method of solution was programmed which consisted of determining the diffusivities of momentum and heat based on a two-region universal pipe velocity profile for turbulent flow; then performing layerwise momentum and energy balances to determine

the temperature profile and heat transfer rate at the wall. This program was also run on the IBM 7040 digital computer and the results correlated with the experimental results.

Experimental Investigations. A temperature instrumented nozzle was constructed for the experimental part of this study. It was instrumented to measure the outside nozzle wall temperatures at one-eighth inch intervals along the nozzle. These temperature readings, along with known flow conditions in the backside cooling annulus, gave sufficient information to calculate local heat transfer rates. The nozzle was also constructed with an air film injector which injected a controlled film of coolant air along the convergent section of the nozzle. Using the experimental information, a comparison could be made to the theoretical heat fluxes and temperature profiles for various nozzle flow conditions.

CHAPTER II
GAS FILM COOLING

I. GENERAL DISCUSSION

A large number of investigators have worked on solutions of the equations of continuity of mass, momentum, and energy. Bird, Stewart and Lightfoot (7), Bennett and Myers (5), and other authors include in their books many of the available solutions. Other solutions are available in the journals concerning fluid flow and heat transfer. A careful study shows that closed type analytical solutions have been accomplished for only a relatively few rather special cases. With the development of high speed computing equipment numerical methods of solution for the more difficult cases are now feasible. The present investigator decided to make use of such capability in the study of film and transpiration cooling.

For gas film cooling a simplified model was adopted which disregards diffusion or mixing of the coolant gas with the mainstream gas. Since $Pr \sim 1$ for most gases it was necessary to solve for the developing velocity and temperature profiles simultaneously. This was done by making certain assumptions about the viscosity and thermal conductivity for individual gas layers and then making layerwise momentum and energy balances over each axial increment.

Libby and Pallone (23) worked out and published in 1954 a rather extensive integral method for handling the calculation of velocity and enthalpy profiles for a gas film introduced into a laminar compressible boundary layer. Sixth degree polynomials were used to describe the velocity and enthalpy profiles. Since the species concentration equation was not used the injected fluid was assumed to be the same as the mainstream fluid. The polynomial coefficients were chosen without particular regard for the asymptotic (far downstream) results and thus the solution is not asymptotically correct. The numerical results do indicate a strong effect of the injected fluid for some distance downstream from the point where injection ceases.

Baron (1) worked out and published in 1956 an extension of the Libby and Pallone method. He included the species concentration equation for a binary fluid boundary layer and adjusted the form of the polynomials so as to assure correct asymptotic solutions.

Neither of these solutions is applicable to the present case of nozzle throat cooling with injection into a turbulent boundary layer.

Emmons (13) and Hatch and Papell (17) used a very crude flow model for tangential coolant gas injection into turbulent pipe flow. The coolant gas was assumed to form a layer at the wall with no diffusion or mixing with the mainstream. A heat transfer coefficient h was used to calculate the heat transfer rate to the coolant layer from the mainstream and from the coolant layer to the nozzle wall. The heat transfer coefficient was calculated from the mainstream conditions as though the coolant layer were not present. It may be noted immediately that this model, besides its other deficiencies, is not asymptotically correct. It predicts a downstream heat transfer rate which is only one half the correct rate for the far downstream value.

II. GAS FILM THEORETICAL ANALYSIS

The approach taken in the present investigation was to solve the continuity, momentum, and energy balance equations for the boundary layer written in finite difference form, for turbulent mainstream flow with tangential injection of a turbulent coolant gas.

The necessary assumptions are:

1. The coolant injection is a low percentage of the mainstream flow rate and has little effect on the expansion process of the mainstream.
2. The injected film is turbulent and a laminar sublayer is immediately established.
3. The laminar sublayer thickness and the eddy diffusivities of momentum and heat may be calculated from the two region universal turbulent velocity profile equations.
4. The ratio of the eddy diffusivities of momentum and heat is a constant. As a preliminary assumption this constant is taken to be one.
5. The wall shear stress may initially be calculated using the Blasius turbulent - smooth pipe - flow formula.

Based on the above assumptions the coolant and mainstream gases near the wall may be divided into finite layers parallel to the wall and finite increments axially along the surface. The velocity and temperature profiles are then calculated in a stepwise fashion through the nozzle. The coordinate system is thus one which moves with the fluid.

As was stated above, the analysis depends upon the solution of the continuity, momentum, and energy equations. The continuity equation is satisfied by assigning a fixed amount of fluid to each layer except for the laminar sublayer and the neighboring turbulent layer. The exchange between these layers is calculated at each

increment and thus continuity assured.

A steady state momentum balance for the coolant layer at the coolant-mainstream interface as shown in Figure 2, is written as*

$$\left[\begin{array}{l}\text{Pressure forces}\\ \text{in } \Delta \text{ direction}\\ \text{on coolant layer 1}\end{array}\right] + \left[\begin{array}{l}\text{Inertia forces}\\ \text{in } \Delta \text{ direction}\\ \text{on coolant layer 1}\end{array}\right] + \left[\begin{array}{l}\text{Shear forces on}\\ \text{top and bottom of}\\ \text{coolant layer 1}\end{array}\right] = 0 \quad (5)$$

Using the notation shown in Figure 2, noting that primed quantities refer to the coolant stream and subscripts refer to layer positions, the resulting mathematical momentum equation is

$$\left[\pi d_1' \delta_1' (p_1 - p_2)\right] + \left[\frac{w_1'}{g_c}(v'_{1_1} - v'_{2_1})\right] + \left[\frac{\pi d_1' \Delta (v1_1 + v2_1 - v'2_1 - v'1_1)}{\frac{\delta_1}{\rho_1 \varepsilon_1} + \frac{\delta_1'}{\rho_1' \varepsilon_1'}} + \frac{\pi d_1' \Delta (v'1_2 + v'2_2 - v'1_1 - v'2_1)}{\frac{\delta_1'}{\rho_1' \varepsilon_1'} + \frac{\delta_2'}{\rho_2' \varepsilon_2'}}\right] = 0 \quad (6)$$

*The differential equation and development is shown in Appendix G.

Solving Eq. (6) for the coolant velocity at the outlet of the first layer, $v'2_1$ gives

$$v'2_1 = \frac{\frac{w'_1}{g_c}\, v'1_1 + A(v1_1 + v2_1 - v'1_1) + B(v'1_2 + v'2_2 - v'1_1) + P}{\frac{w'_1}{g_c} + A + B} \tag{7}$$

where

$$A = \frac{\pi d_1 \Delta}{\frac{\delta_1}{\rho_1 \varepsilon_1} + \frac{\delta'_1}{\rho'_1 \varepsilon'_1}} \tag{8}$$

$$B = \frac{\pi d'_1 \Delta}{\frac{\delta'_1}{\rho'_1 \varepsilon'_1} + \frac{\delta'_2}{\rho'_2 \varepsilon'_2}} \tag{9}$$

$$P = \pi(d'_1)(\delta'_1)(p_1 - p_2) \tag{10}$$

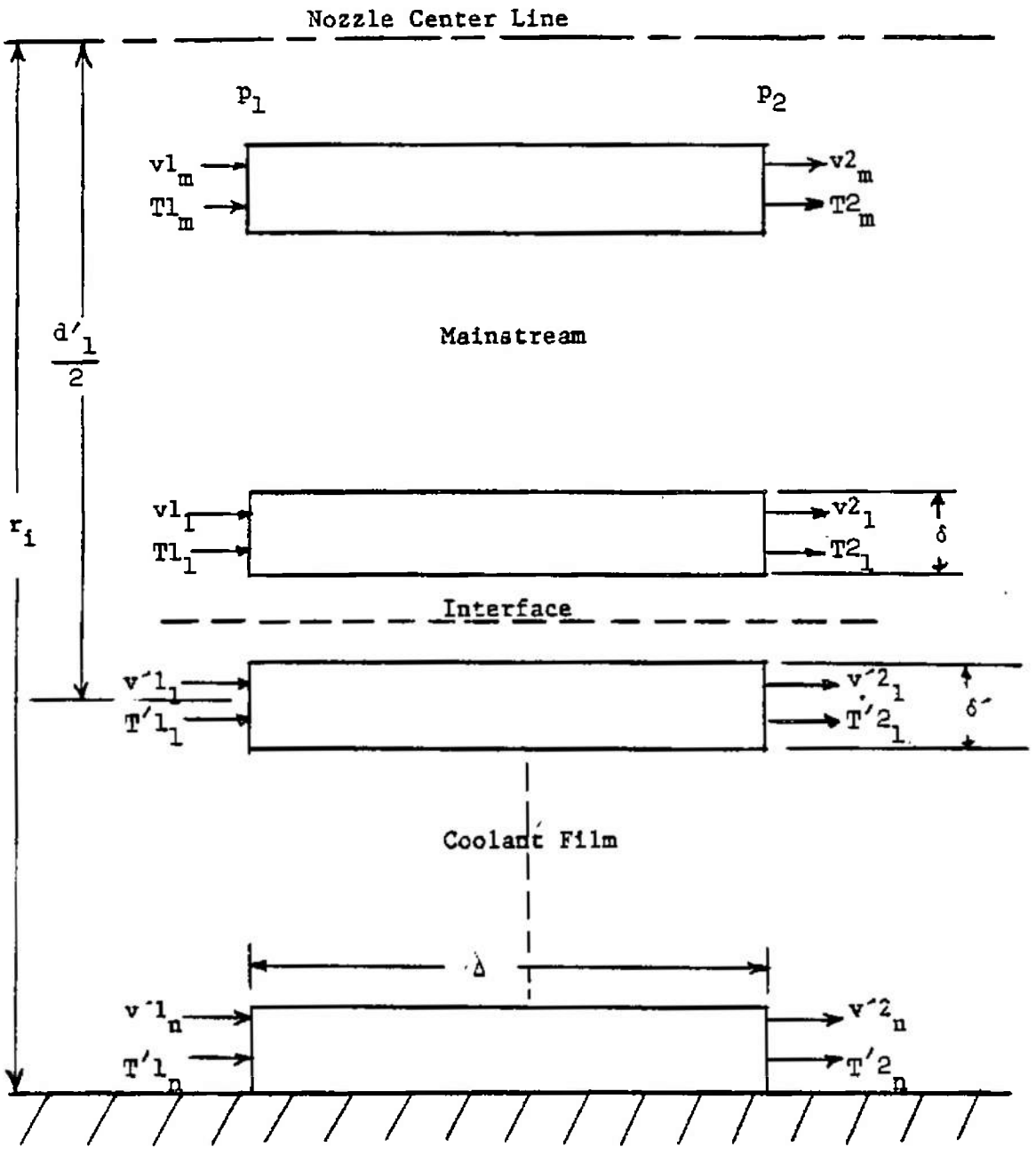

Fig. 2 Velocity and Temperature Notation for Gas Film by Layers and Increments

A set of such equations is written for the fluid layers in the coolant from the coolant-mainstream interface to the nozzle wall. Another set is written for the mainstream fluid layers from the coolant-mainstream interface to a point in the mainstream where there is negligible variation in exit velocity between layers. The wall boundary condition requires zero velocity at the wall. The mainstream boundary condition may be handled either by using enough layers of fluid so they contain several times the mass flow rate of the coolant or by specifying a smaller number of layers and adding layers if the chosen number does not cover the velocity boundary layer. The outer mainstream fluid layer is then fixed at the mainstream velocity calculated from frozen flow conditions established by an isentropic expansion with a constant ratio of specific heats. The Gauss-Siedel method of successive substitution is used to solve the equations iteratively.

In order to make the above calculations, the diffusivity of momentum must be evaluated at each layer. In the laminar sublayer, $0<y^+<10$, the molecular diffusivity of momentum is used. In the turbulent core assumption 3 is used and the eddy diffusivities calculated from the universal velocity profile equation for this region, which is:

$$\frac{u}{u^*} = 2.5 \ln \frac{yu^*}{\upsilon} + 5.5 \tag{11}$$

Differentiating Eq. (11) with respect to y gives:

$$\frac{du}{dy} = 2.5 \frac{u^*}{y} \tag{12}$$

Now for the turbulent core

$$\frac{\tau g_c}{\rho} = \epsilon \frac{du}{dy} = (u^*)^2 \tag{13}$$

thus

$$\epsilon = \frac{\frac{\tau g_c}{\rho}}{\frac{du}{dy}} \tag{14}$$

Assuming the velocity boundary layer terminates near the wall

$$\tau = \tau_w \tag{15}$$

so

$$\epsilon = \frac{(u^*)y}{2.5} \tag{16}$$

or

$$\epsilon = 0.4\, u^*(r_i - r) \tag{17}$$

In the notation of Figure 2, page 16, Eq. (17) becomes

$$\epsilon_i' = 0.4\, u^*\left(r_i - \frac{d'_1}{2}\right) \tag{18}$$

or

$$\epsilon_i = 0.4\, u^*\left(r_i - \frac{d_1}{2}\right) \tag{19}$$

In order to evaluate the diffusivities using either Eq. (18) or Eq. (19), u^* and thus τ_w is required at each increment. Assumption 5 is used to evaluate τ_w for the initial increment, i.e.

$$\tau_w = .053\ (Re)^{-.2}\ \frac{\rho u^2}{2g_c} \tag{20}$$

Following the initial increment, τ_w may be evaluated at each successive increment either from Eq. (20) or from the wall velocity gradient at the exit of the previous increment.

Energy balance equations are written for the same fluid layers in order to calculate temperatures at the exit of the increments - (Refer to Figure 2 for notation). The steady state energy equation for the coolant layer at the coolant-mainstream interface is written as

[Enthalpy change in Δ direction of coolant layer 1] + [Kinetic energy change in Δ direction of coolant layer 1]
+ [Energy transfer from gas layer 1 to coolant layer 1 by diffusion] + [Energy transfer from coolant layer 2 to coolant layer 1 by diffusion]
+ [Work at boundaries on coolant layer 1. Shear stress effects] = 0 (21)

The mathematical statement of Eq. (21) is

$$\left[w'c'(T'1_1 - T'2_1)\right] + \left[\frac{w'(v'1_1^2 - v'2_1^2)}{2g_cJ}\right]$$

$$+\left[\frac{\pi d_1\Delta(T1_1 + T2_1 - T'1_1 - T'2_1)}{\frac{\delta_1}{\rho_1c_1\varepsilon_1\psi} + \frac{\delta'}{\rho'c'\varepsilon'\psi}}\right]$$

$$+\left[\frac{\pi d'\Delta(T'1_2 + T'2_2 - T'1_1 - T'2_1)}{\frac{\delta'}{\rho'c'\varepsilon'\psi} + \frac{\delta'_2}{\rho'_2c'_2\varepsilon'_2\psi}}\right]$$

$$+\left[\frac{\pi d'\Delta\delta'\rho'\varepsilon'(v1_1 + v2_1 - v'1_2 - v'2_2)^2}{Jg_c(2\delta' + \delta'_2 + \delta_1)^2}\right] = 0 \qquad (22)$$

Solving Eq. (22) for $T'2_1$, the exit temperature of the first coolant layer gives:

$$T'2_1 = \frac{T'1_1(w'c' - A - B) + A(T1_1 + T2_1) + B(T'1_2 + T'2_2) + E + F}{w'c' - A + B} \qquad (23)$$

where

$$A = \frac{\pi d_1'\Delta}{\frac{\delta_1}{\rho_1c_1\varepsilon_1\psi} + \frac{\delta'}{\rho'c'\varepsilon'\psi}} \qquad (24)$$

$$B = \frac{\pi d_1' \Delta}{\frac{\delta_1'}{\rho_1' c_1' \epsilon_1' \psi} + \frac{\delta_1'}{\rho_2' c_2' \epsilon_2' \psi}} \tag{25}$$

$$E = \frac{w_1'(v'^2_{1_1} - v'^2_{2_1})}{2Jg_c} \tag{26}$$

$$F = \frac{\pi d_1' \Delta \delta_1' \rho_1' \epsilon_1' (v1_1 + v_{2_1} - v'1_2 - v'2_2)^2}{Jg_c(2\delta_1' + \delta_2' + \delta_1)^2} \tag{27}$$

Since the energy equations contain the entrance and exit velocities, the velocity solution is performed first using layer properties based on the exit temperatures from the preceding increment. The velocity equations are dependent on temperature only through the variation of the fluid properties with temperatures. If desired the fluid properties could be re-evaluated after completion of the temperature iteration.

When the velocity iteration is completed the temperature iteration is performed in like manner by successive substitution.

The analysis described above has been programmed in Fortran IV language for execution on a digital computer. The program is included in Appendix C.

Included in the program are provisions for wall shear stress

calculation either from the Blasius Equation or from the past increment, multiple injection calculations, and provision for approaching a transpiration calculation by injecting a very small amount of coolant at each increment. New coolant layers are added for the multiple injection calculation. The fluid is added at a specified increment, or increments and the wall side coolant layer is recalculated and layers added as needed. Provision is made for backside cooling in the case of single and multiple injection, while an adiabatic wall may be specified for any type injection.

III. EXPERIMENTAL INVESTIGATION

Design Requirements. An examination of some published data for film cooled nozzles (6), (19), (24), (25), indicated that in most cases either insufficient data are available to make a detailed comparison with the present analysis or the fluid stagnation conditions are not in the range of present interests. Therefore an instrumented nozzle was designed and fabricated for this investigation. The general geometrical requirements for this nozzle were that it have an entrance diameter of 1.5 inches, a throat diameter of 0.5 inches, and an expansion angle of 15°. Additional requirements were that it be mechanically designed to handle air as the expanding fluid with stagnation pressure up to ∿ 50 atmospheres and stagnation temperatures up to ∿ 10,000 °R. In order to make the required correlation with the analytical study, instrumentation for the nozzle was required to produce data necessary for calculation of

the local nozzle wall inside temperature and heat loads as distributed axially through the nozzle.

Nozzle Design. Details of the materials study, stress analysis and backside cooling problems have been previously published (27). It was found that the combination of high thermal stresses and hoop stresses in the nozzle could best be handled in the range of interest by using a thin walled nozzle liner turned from copper-zirconium alloy. In higher pressure and heat load regions of the nozzle the wall thickness was 0.040 inches. Downstream from the throat the liner gradually thickened to approximately 0.15 inches near the exit. The liner was surrounded by a steel split sleeve turned to provide a backside coolant flow channel of constant flow area around the liner. The liner and sleeve were surrounded by a steel cylindrical outer casing. The outer casing was provided with passages for thermocouple lead access to the nozzle liner through the split sleeve.

Twenty-four duplex copper-constantan thermocouples were led in on each side of the liner, passing through a narrow slot milled in the split sleeve, through small holes drilled in a positioning rib, and attached to the nozzle liner with 600 ^{o}F. softening temperature solder. The thermocouples started 0.875 inches upstream from the point of smallest radius in the nozzle and were spaced 0.125 inches apart on the liner surface. O-ring seals were provided on either side of the thermocouple passage.

A full-scale sectional view of the liner, sleeve, and casing showing the thermocouple installation, is given in Figure 3.

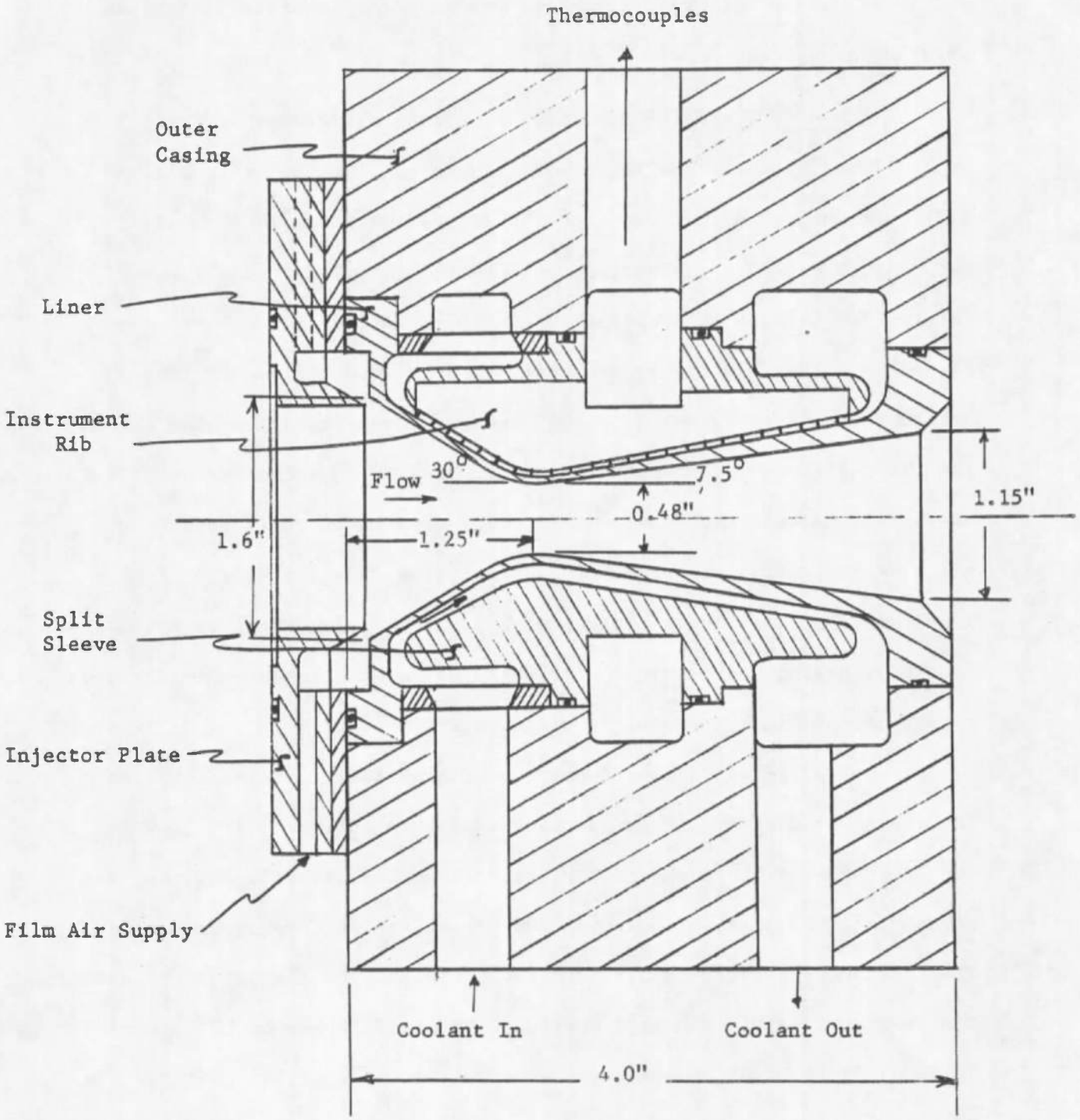

Fig. 3 Nozzle Assembly

Film Injector Design. An injector plate was designed to match the nozzle liner and casing. It consisted of a single piece turned from copper-zirconium and drilled to provide 18 coolant flow passages evenly spaced about the circumference. These coolant passages discharged into a small plenum chamber just before the film entrance annulus. Provision was made for varying the film injection slot width by placing spacer shims between the injector plate and the nozzle casing. Figure 4 shows a sectional view of the injector plate.

Stilling Chamber Design. Experience with the previous instrumented nozzle (27) showed that the nozzle wall heat load was somewhat lower than that anticipated. There was also a swirl component of velocity of the mainstream gas. A possible reason for the low heat flux in the first experiments was a "natural" film cooling effect caused by the peaking of the temperature at the centerline of the arc heater tube. This, together with the centrifugal effect of the swirl flow, would tend to produce lower temperatures near the wall and thus lower heat fluxes. In order to remove the mainstream swirl and provide a more uniform temperature profile at the nozzle entrance, a stilling chamber was designed, fabricated, and installed between the arc air heater and the film injector station. This chamber consisted of a brass liner 0.125 inches thick and a steel outer casing. It was cylindrical in shape with an inside diameter of ∿5 inches and an inside length of ∿8 inches. The liner consisted of a cylindrical sleeve and two curved end pieces. Cooling water passages were provided between

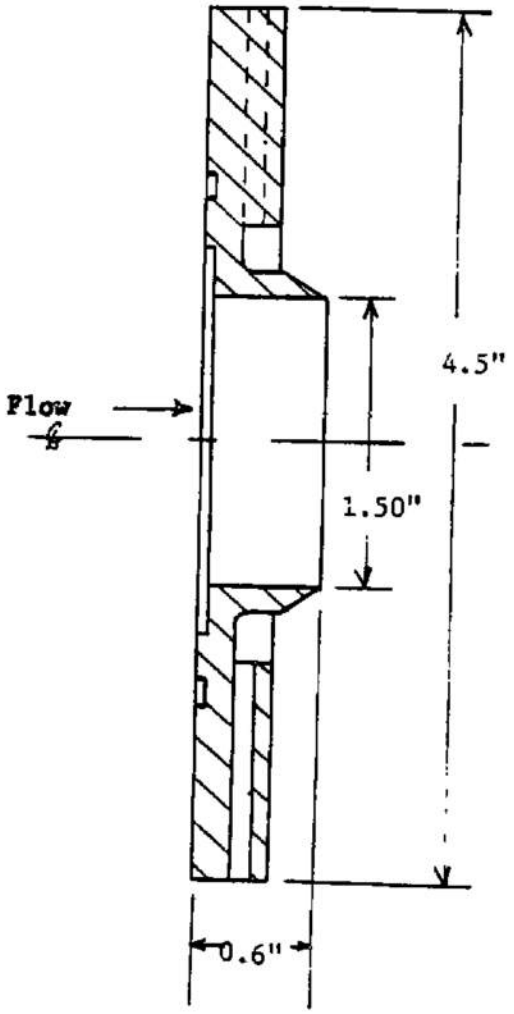

Fig. 4 Injection Plate

the casing and the liner and a pressure tap was provided at the downstream end. Figure 5 shows a half-scale sectional view of the stilling chamber.

Arc Air Heater. The air for expansion through the nozzle was heated by passage through an electric arc heater supplied by the Linde Company, Indianapolis, Indiana. The heater has a capacity of 1.3 pounds per second of air flow at pressures up to ~1400 psia with a 3/8 inch diameter constrictor nozzle. Energy can be supplied to the air up to a maximum rate of ~4 megawatts. The air heater, stilling chamber, injection plate, and nozzle are shown assembled in Figure 6.

Instrumentation. The expefiment was set up to be operated remotely due to the high pressures and temperatures involved. Instrumentation for the operation of the air supply and air heater was designed by the staff at Arnold Engineering Development Center and will not be further discussed in the present report. Instrumentation for the stilling chamber, injection station and nozzle consisted of temperature and flow measuring equipment for water and air as supplied to the particular pieces of equipment.

Water flow rate to the stilling chamber was measured by a calibrated flow rate meter. The inlet to exit temperature difference of the stilling chamber cooling water was measured by thermistors. The pressure at the stilling chamber exit was measured by a pressure transducer.

Air mass flow rate to the coolant injector was established by choked flow through a venturi. The inlet temperature was measured by

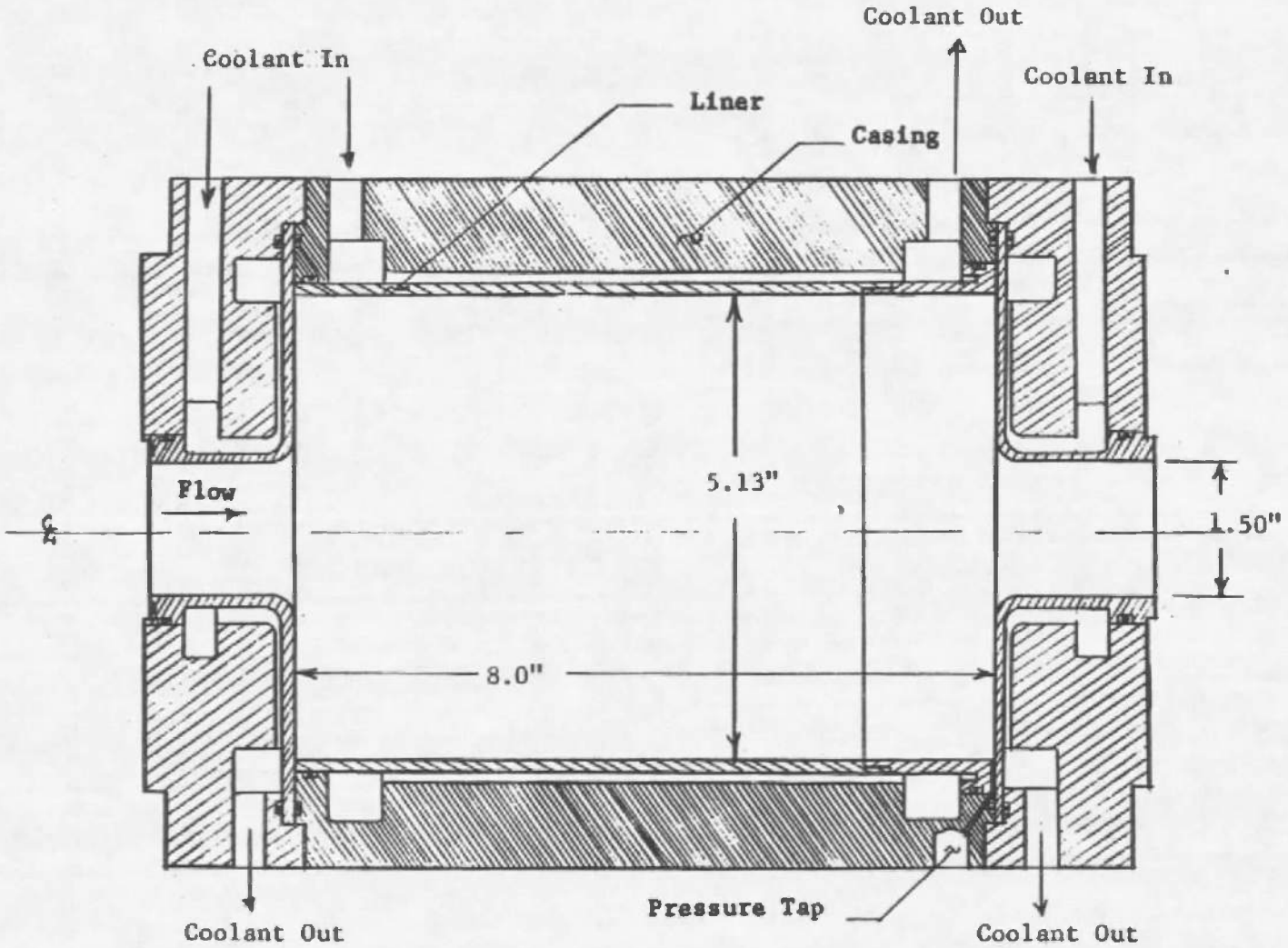

Fig. 5 Stilling Chamber Assembly

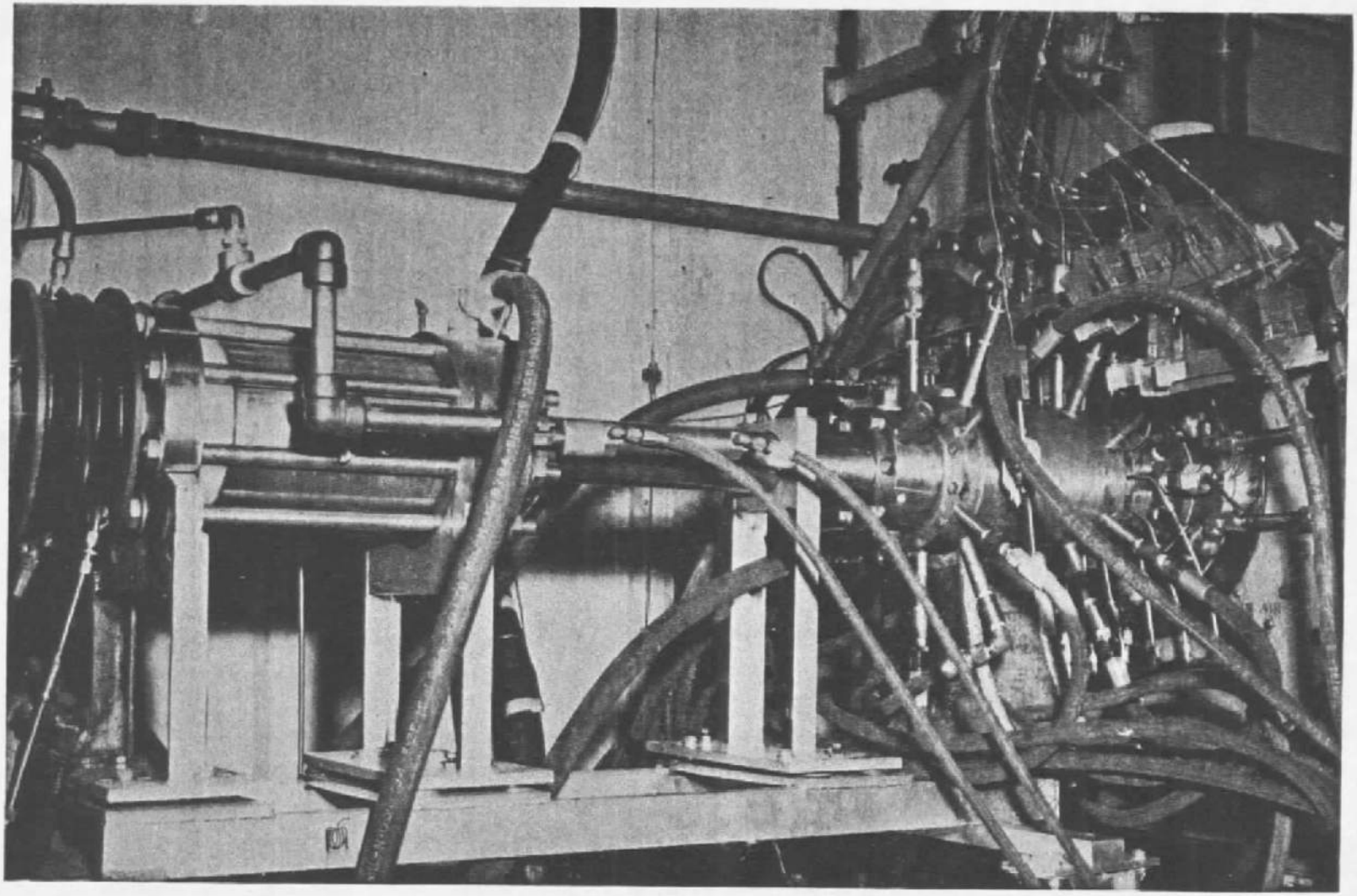

Fig. 6 Photograph of Experimental Assembly

a thermocouple.

Water flow rate to the nozzle backside coolant channel was measured by a calibrated flow rate meter. The inlet-to-exit temperature difference was measured by thermistors. The nozzle wall thermocouple leads were attached to an automatic scanning Austin system.

Experimental Procedure. The experimental nozzle was fabricated and assembled at The University of Tennessee, Knoxville, Tennessee, under the supervision of the investigator. It was then taken to the Arnold Engineering Development Center, Tullahoma, Tennessee, where the actual operation of the experiments was performed by a group now called the experimenter.

The investigator specified gas film cooling ratios of approximately 20%, 10%, and 5% with mass flow rates ranging from 0.4 lbm./sec. to 0.6 lbm./sec. and three enthalpy values ranging up to the maximum value available from the heater at the given flow rate. In addition to the cases at the above film cooling ratios the nozzle was operated for the first run with a gas film cooling ratio of 27.4%.

The gas film injection slot was adjusted for each film cooling ratio. In the range of pressures and temperatures of the test cases the mainstream inlet velocity was from 100 to 250 ft./sec. To minimize mixing of the film with the mainstream gas at injection the slot was adjusted to give film inlet velocities of approximately 150 ft./sec.* For air injected at approximately room temperature this required a slot width

*This film velocity approximately matches the mainstream velocity at the location of injection.

of 0.002 inches for each 5% of coolant. Spacing shims 0.004 inches in thickness were provided by the investigator and one shim was inserted for each 5% coolant ratio. Due to the 30^{o} convergent angle of the nozzle each shim increased the slot width 0.002 inches.

When a test case was run an ambient scan of all the thermocouples was first recorded. The heater was then fired and the thermocouples were scanned approximately 20 times during the run. Since steady state for this system was reached very quickly the thermocouple readings during the data taking period were constant to within approximately 5 ^{o}F. except for a few runs when the heater was slightly unstable over a few scanning periods.

The stagnation enthalpy of the gas was calculated by the experimenter using an energy balance for the system including the air heater and the stilling chamber. This balance included the input electrical energy to the heater, the energy removed in cooling the heater and the stilling chamber, and the change of energy of the mainstream gas.

The raw instrument readings recorded on tape were reduced to pressure, temperature, and flow rate values by the experimenter using standard programs and then furnished to the present investigator.

IV. DISCUSSION OF RESULTS

The described analysis was programmed in Fortran IV language for execution on a digital computer. The program is included in Appendix C. Experiments with the gas film cooled, instrumented nozzle were run at film cooling ratios of approximately 30%, 20%, 10%, and 5% of the mainstream flow rate. Table I summarizes the experimental conditions for all the cases run.

Experimental Results. From the twenty-eight cases run five were selected for analytical correlation. They were chosen to include cases from each of the film cooling ratios given above, and in addition two pairs were chosen because their stagnation conditions were close to the same while they had different film cooling ratios. From Table I the cases chosen were H1-1, H2-2, H6-2, H5-2, and H9-2. Cases H1-1 and H5-2, while differing some in stagnation pressure and temperature represent approximately the same severity of heat loading on the nozzle.

water pressure ?

TABLE I
SUMMARY OF ORIGINAL DATA FOR GAS FILM COOLING EXPERIMENTS

AEDC* Case Number	Mainstream Stagnation Pressure (psia	Mainstream Stagnation Temperature (^{o}K.)	Mainstream Mass Flow Rate (lbm./sec.)	Film Coolant Mass Flow Rate (lbm./sec.)	Film Coolant Inlet Temperature (^{o}F.)	Backside Coolant Flow Rate (gpm.)	Backside Coolant Inlet Temp. (^{o}F.)	Backside Coolant ΔT (^{o}F.)
H1-1	349	3840	0.394	0.108	69.0	41.5	65.0	2.57
H2-1	341	3160	0.412	0.080	49.5	32.0	70.0	4.64
H2-2	373	3660	0.419	0.082	52.5	32.0	66.0	7.34
H2-3	373	3910	0.419	0.092	55.0	32.0	70.5	8.37
H3-1	409	3290	0.496	0.094	65.5	30.6	71.5	5.31
H3-2	434	3660	0.504	0.096	65.5	30.7	71.5	8.81
H3-3	447	3800	0.498	0.095	65.5	30.7	71.5	10.13
H4-1	473	3180	0.606	0.110	69.0	34.1	72.0	4.41
H4-2	492	3320	0.605	0.108	69.0	35.7	72.0	6.74
H4-3	511	3620	0.605	0.108	69.0	34.2	72.0	8.68
H5-1	299	3180	0.401	0.039	55.0	30.1	73.0	5.75
H5-2	312	3450	0.409	0.039	57.5	30.1	73.0	8.18
H5-3	324	3930	0.401	0.039	60.0	38.4	73.0	7.29
H6-1	381	3120	0.517	0.049	60.0	49.2	73.0	4.73
H6-2	407	3460	0.525	0.049	63.0	49.2	73.0	6.14
H6-3	413	3760	0.525	0.049	67.0	49.4	73.0	7.03
H7-1	432	2920	0.603	0.059	52.0	55.7	71.0	3.45
H7-2	470	3280	0.603	0.059	52.0	56.3	71.0	5.50
H7-3	490	3600	0.603	0.059	52.0	55.8	71.0	6.40
H8-1	284	3110	0.401	0.020	61.0	51.6	78.0	3.39
H8-2	301	3440	0.401	0.020	61.0	51.6	78.0	4.56
H8-3	313	3720	0.403	0.020	61.0	52.0	78.0	5.22

*Arnold Engineering Development Center

TABLE I (Concluded)

AEDC* Case Number	Mainstream Stagnation Pressure (psia.)	Mainstream Stagnation Temperature (^{o}K.)	Mainstream Mass Flow Rate (lbm./sec.)	Film Coolant Mass Flow Rate (lbm./sec.)	Film Coolant Inlet Temperature (^{o}F.)	Backside Coolant Flow Rate (gam.)	Backside Coolant Inlet Temp. (^{o}F.)	Backside Coolant ΔT (^{o}F.)
H9-1	372	3130	0.526	0.023	61.0	51.7	74.0	4.43
H9-2	402	3450	0.538	0.023	61.0	51.9	74.0	6.26
H9-3	421	3710	0.545	0.024	61.0	52.0	78.0	6.81
H10-1	425	2960	0.580	0.028	55.0	51.4	78.0	5.74
H10-2	437	3330	0.581	0.028	55.0	51.6	78.0	5.74
H10-3	459	3650	0.581	0.028	55.0	51.6	78.0	6.78

*Arnold Engineering Development Center

They provide a good comparison of film cooling effectiveness since case H1-1 was run with 27.4 % film cooling while case H5-2 was run with only 9.73 % film cooling. Cases H6-2 and H9-2 have almost identical stagnation conditions, while being cooled with 9.34 % and 4.27 % film cooling respectively. The original wall temperature data for the five cases correlated are given in Tables II, III, IV, V, and VI.

Values for the backside cooling heat transfer coefficient and local values of the heat flux were calculated at the various thermocouple positions using the measured wall temperatures, the local dimensions of the coolant flow annulus, the coolant mass flow rate, and the physical properties of the coolant evaluated at the local film temperature. The Dittus-Boelter equation was used for calculation of the backside heat transfer coefficients.

Theoretical calculations of the backside surface temperature and wall heat flux distributions were made for the five cases named above. These are plotted, along with the measured temperatures and with heat flux curves calculated by smoothing the experimental temperature distributions, in Figures 7 through 16.

Comparison of Theoretical and Experimental Results. Attempts were made to perform the theoretical calculations described above using the eddy diffusivities based on wall shear stress calculated from both the Blasius equation and from the past increment value of the wall shear stress. In several cases both calculations were performed successfully, however in other cases the calculation using the wall

TABLE II
ORIGINAL TEMPERATURE DATA FOR GAS FILM CASE H1-1

Thermocouple Number	Averaged Temperature ($^{o}F.$)	Thermocouple Number	Averaged Temperature ($^{o}F.$)
1	88.00	13	193.33
2	122.60	14	159.59
3	—*	15	149.02
4	126.76	16	171.49
5	122.45	17	161.07
6	128.97	18	—
7	206.41	19	135.75
8	196.88	20	113.46
9	263.24	21	94.55
10	265.37	22	96.11
11	—	23	129.68
12	222.02	24	—

* A dash indicates a thermocouple which was not reading.

TABLE III
ORIGINAL TEMPERATURE DATA FOR GAS FILM CASE H2-2

Thermocouple Number	Averaged Temperature (^{o}F.)	Thermocouple Number	Averaged Temperature (^{o}F.)
1	147.63	13	301.16
2	197.99	14	229.16
3	——— *	15	197.80
4	207.48	16	152.25
5	196.11	17	220.70
6	203.00	18	———
7	382.93	19	175.19
8	341.27	20	117.73
9	424.68	21	104.17
10	406.02	22	105.47
11	———	23	126.51
12	344.21	24	———

* A dash indicates a thermocouple which was not reading

TABLE IV
ORIGINAL TEMPERATURE DATA FOR GAS FILM CASE H6-2

Thermocouple Number	Averaged Temperatures (°F.)	Thermocouple Number	Averaged Temperatures
1	136.67	13	301.60
2	190.64	14	128.71
3	—*	15	236.09
4	202.42	16	114.16
5	189.19	17	117.05
6	196.72	18	—
7	350.63	19	98.07
8	328.76	20	98.71
9	424.00	21	94.22
10	385.58	22	91.16
11	276.36	23	90.70
12	306.11	24	—

* A dash indicates a thermocouple which was not reading.

TABLE V
ORIGINAL TEMPERATURE DATA FOR GAS FILM CASE H5-2

Thermocouple Number	Averaged Temperature (°F.)	Thermocouple Number	Averaged Temperature (°F.)
1	——— *	13	269.84
2	152.15	14	136.44
3	101.18	15	289.31
4	166.60	16	113.87
5	157.74	17	136.55
6	163.68	18	———
7	260.71	19	96.68
8	240.69	20	104.22
9	323.00	21	97.40
10	316.40	22	99.07
11	242.53	23	96.05
12	274.65	24	———

* A dash indicates a thermocouple which was not reading.

TABLE VI
ORIGINAL TEMPERATURE DATA FOR GAS FILM CASE H9-2

Thermocouple Number	Averaged Temperature (°F.)	Thermocouple Number	Averaged Temperature (°F.)
1	——— *	13	238.65
2	201.50	14	91.89
3	———	15	116.64
4	209.25	16	93.32
5	202.23	17	———
6	212.55	18	100.51
7	359.61	19	97.30
8	301.13	20	108.55
9	430.54	21	104.45
10	291.20	22	108.93
11	169.00	23	115.15
12	163.20	24	———

* A dash indicates a thermocouple which was not reading.

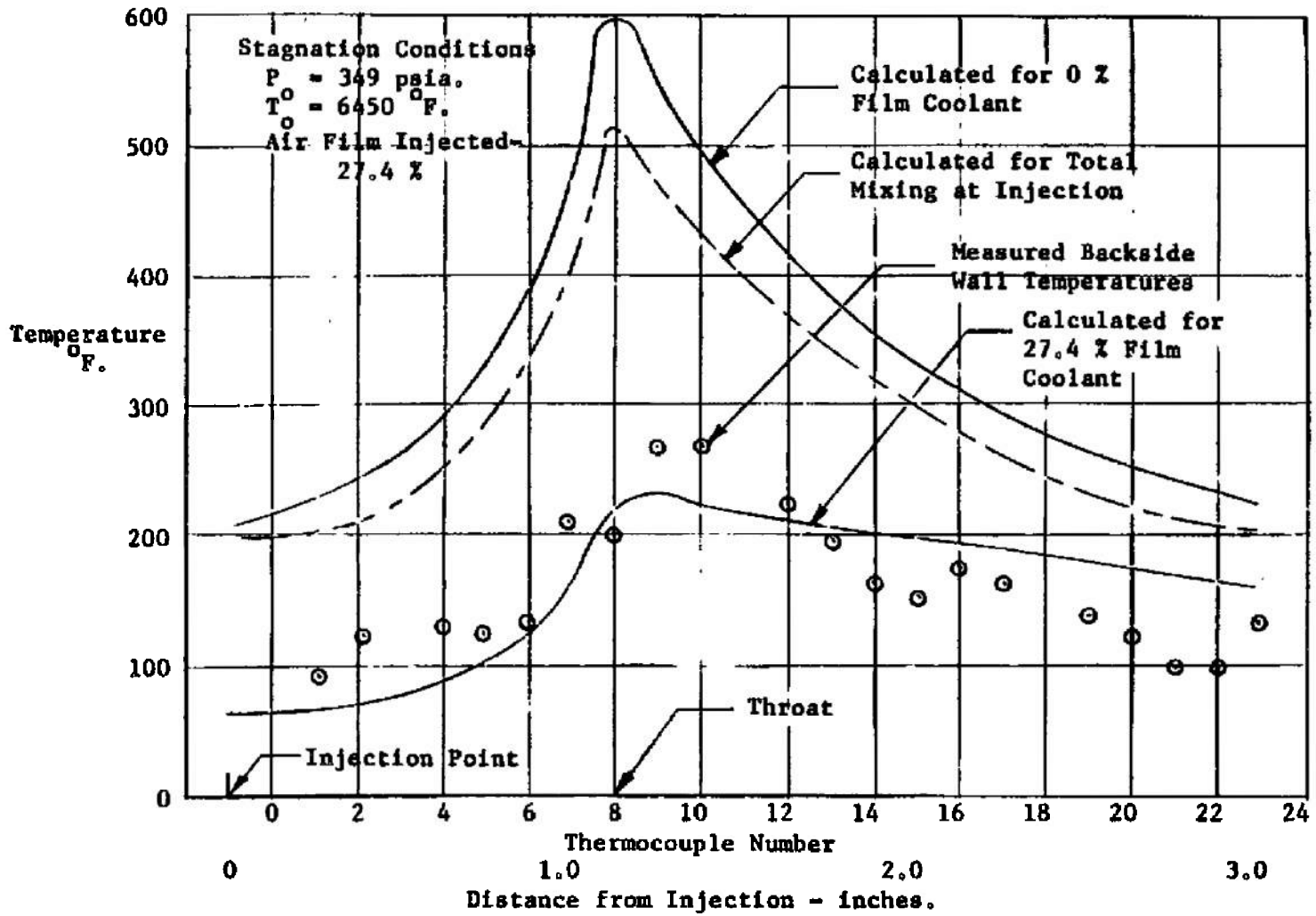

Fig. 7 Gas Film Temperature Correlation With Data for Case H1-1

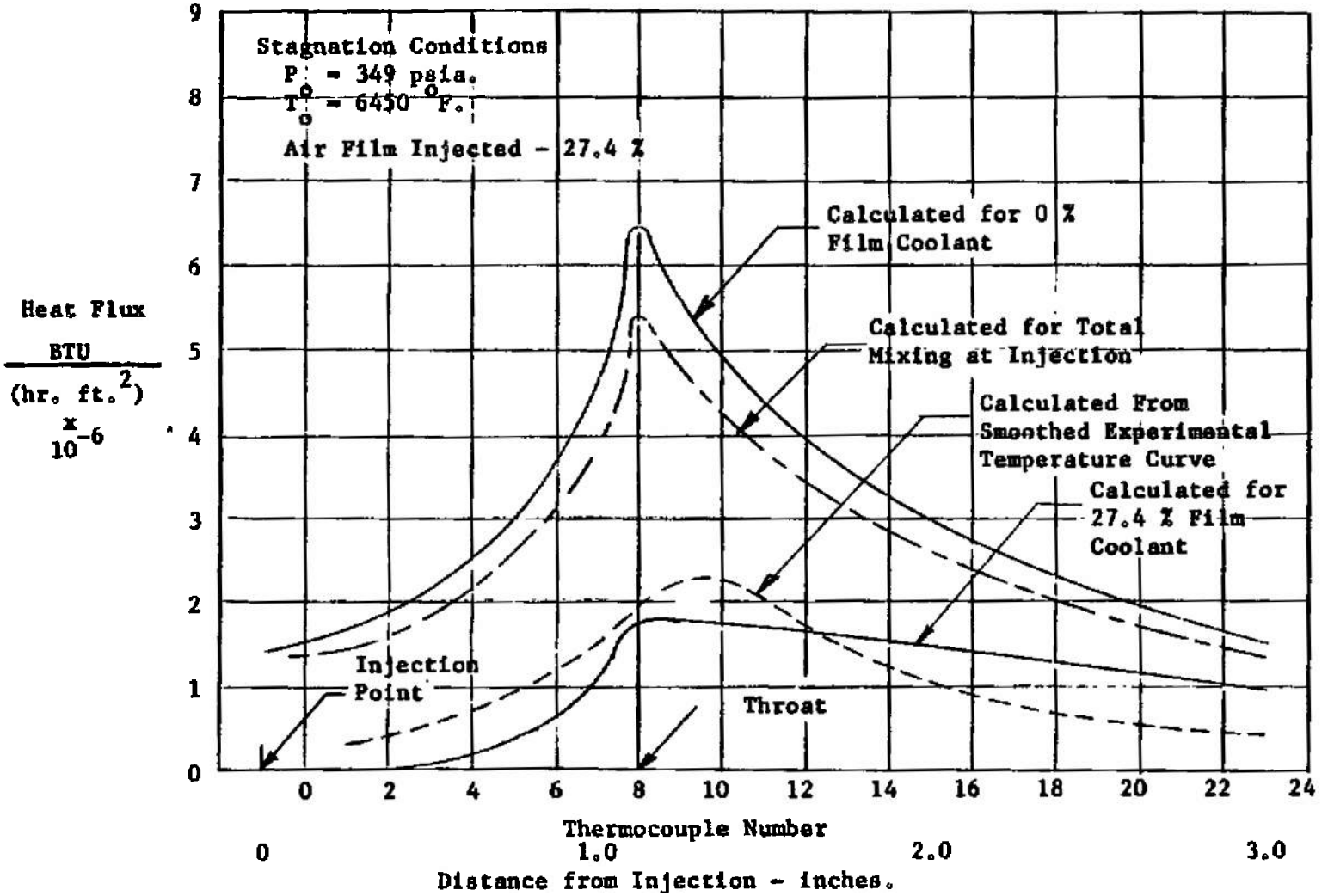

Fig. 8 Gas Film Heat Flux Correlation With Data for Case H1-1

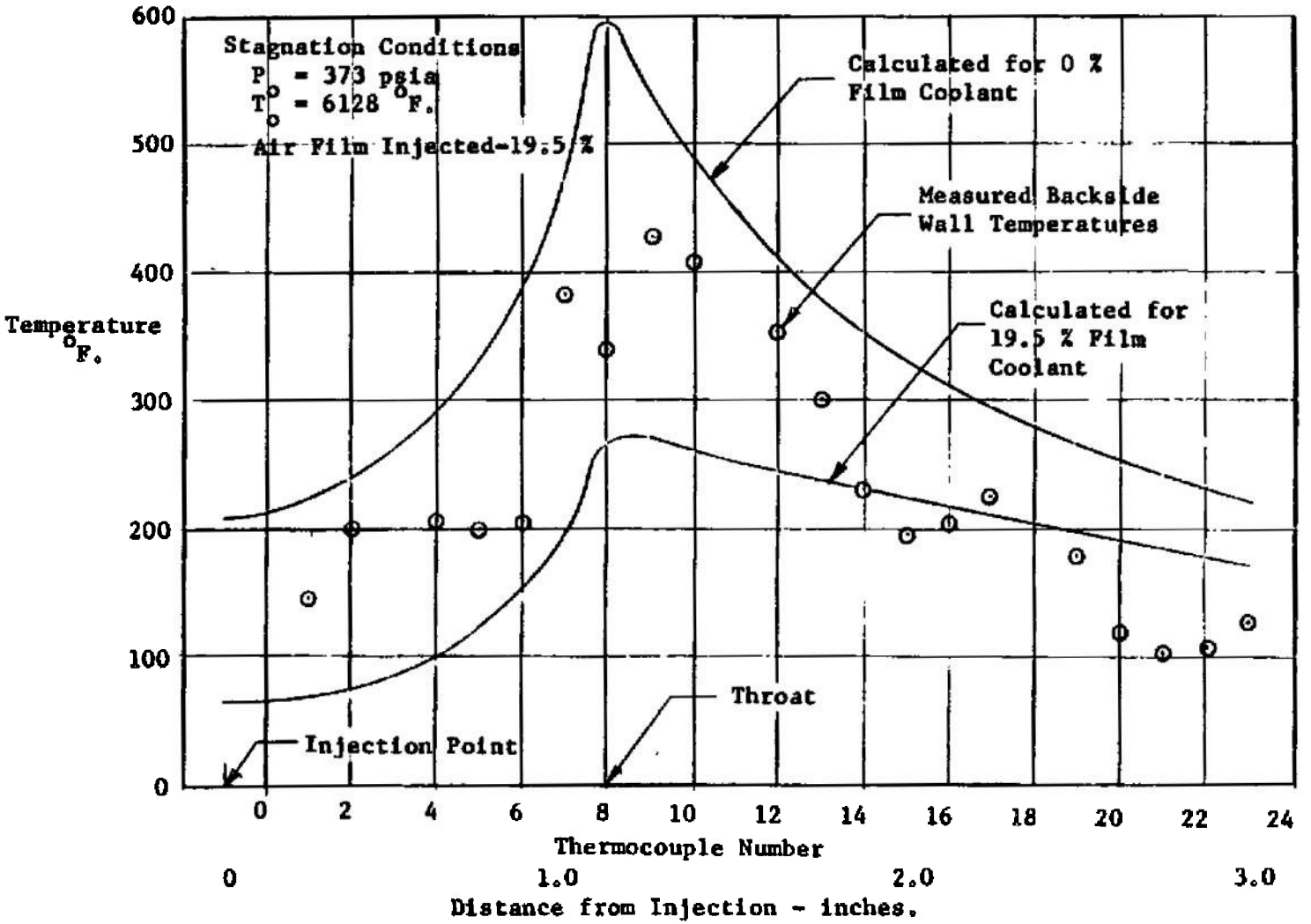

Fig. 9 Gas Film Temperature Correlation With Data for Case H2-2

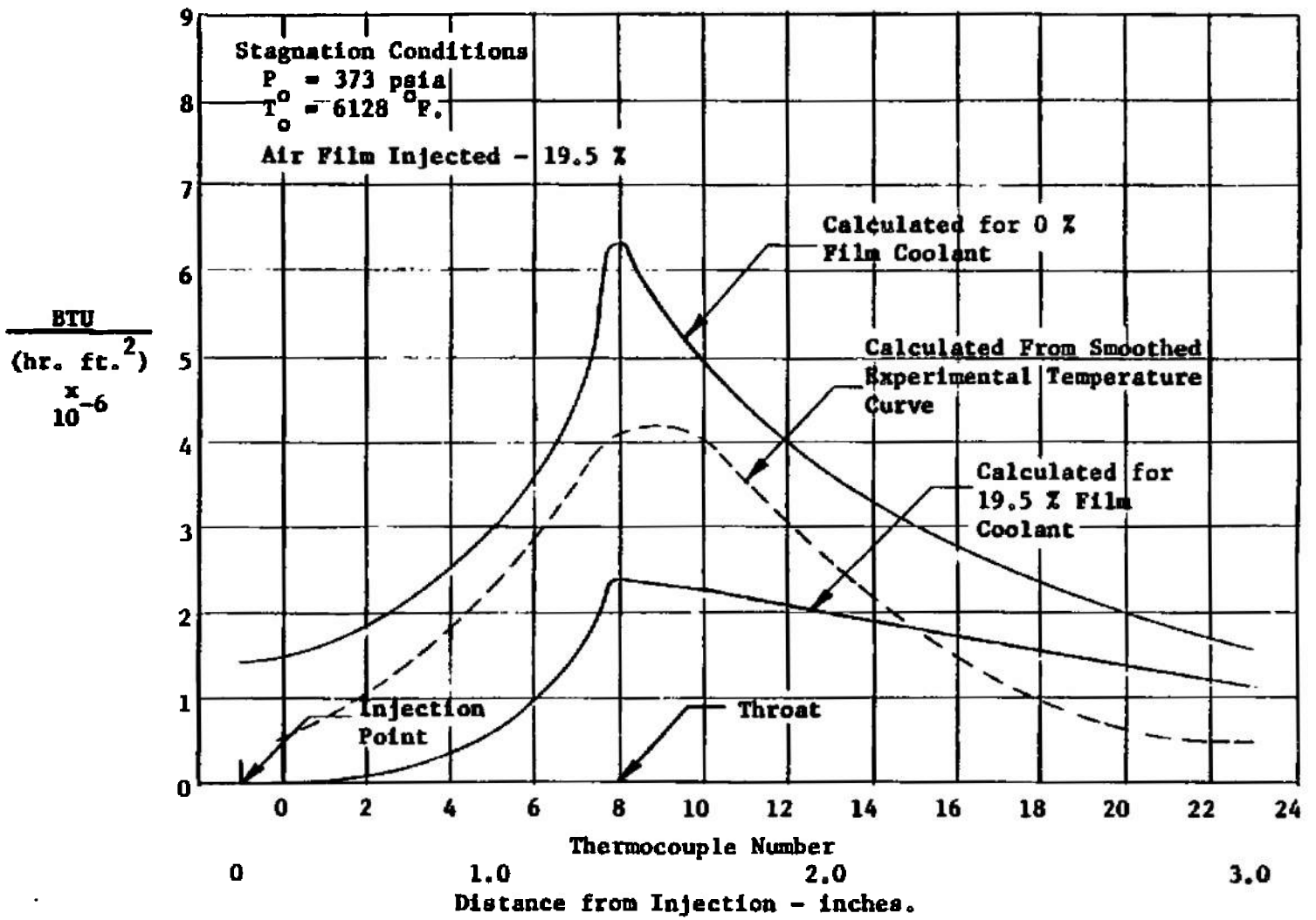

Fig. 10 Gas Film Heat Flux Correlation With Data for Case H2-2

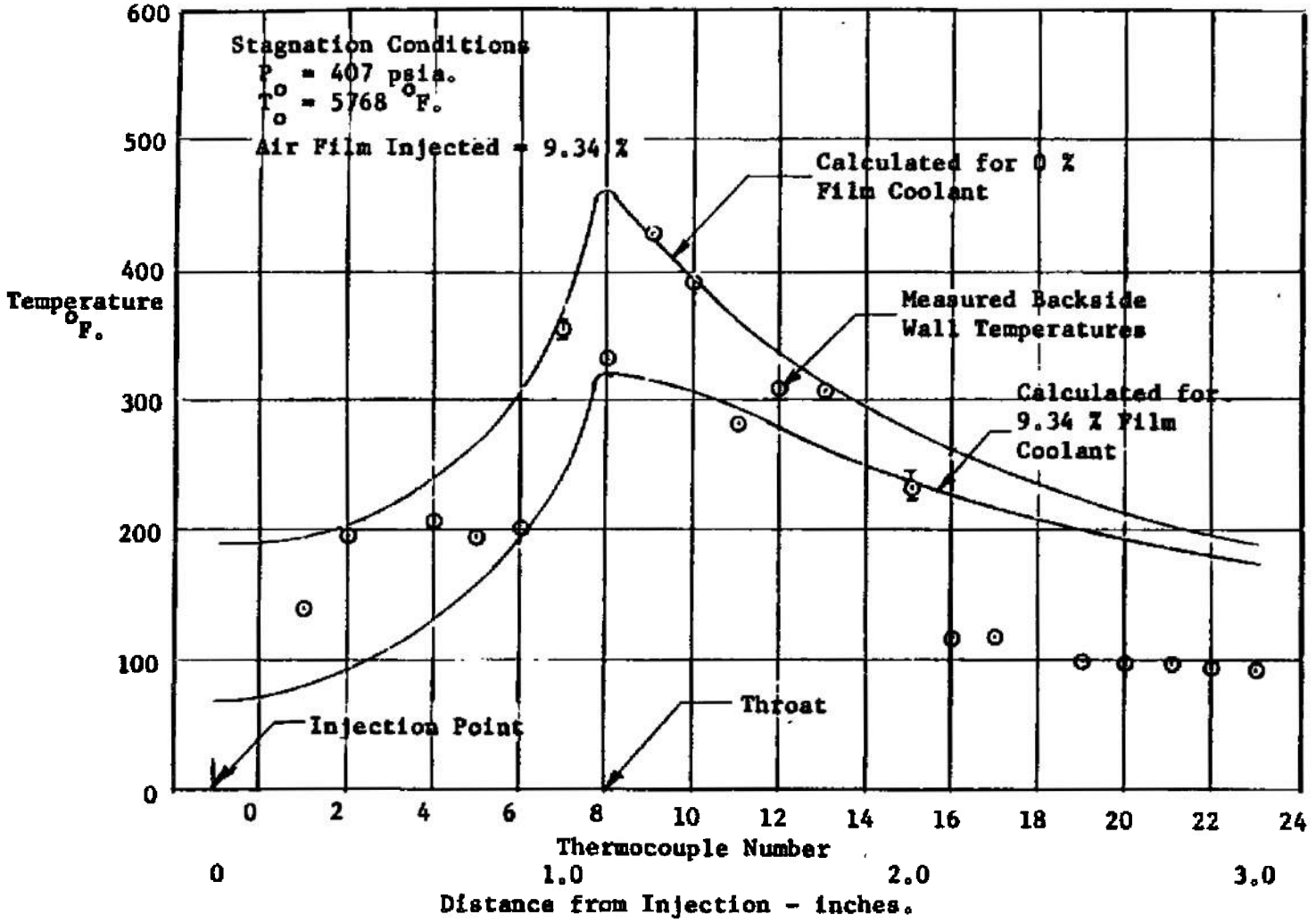

Fig. 11 Gas Film Temperature Correlation With Data for Case H6-2

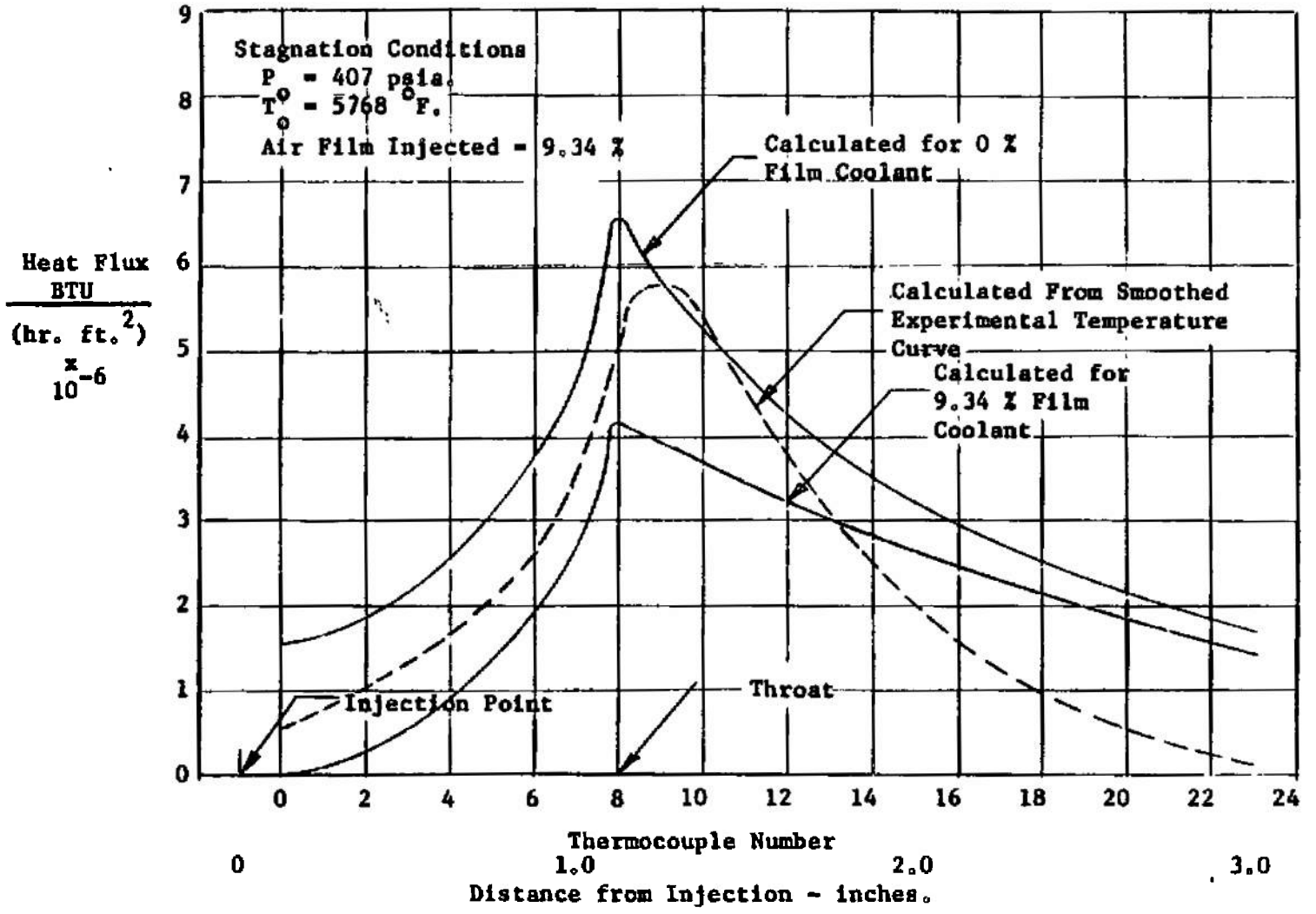

Fig. 12 Gas Film Heat Flux Correlation With Data for Case H6-2

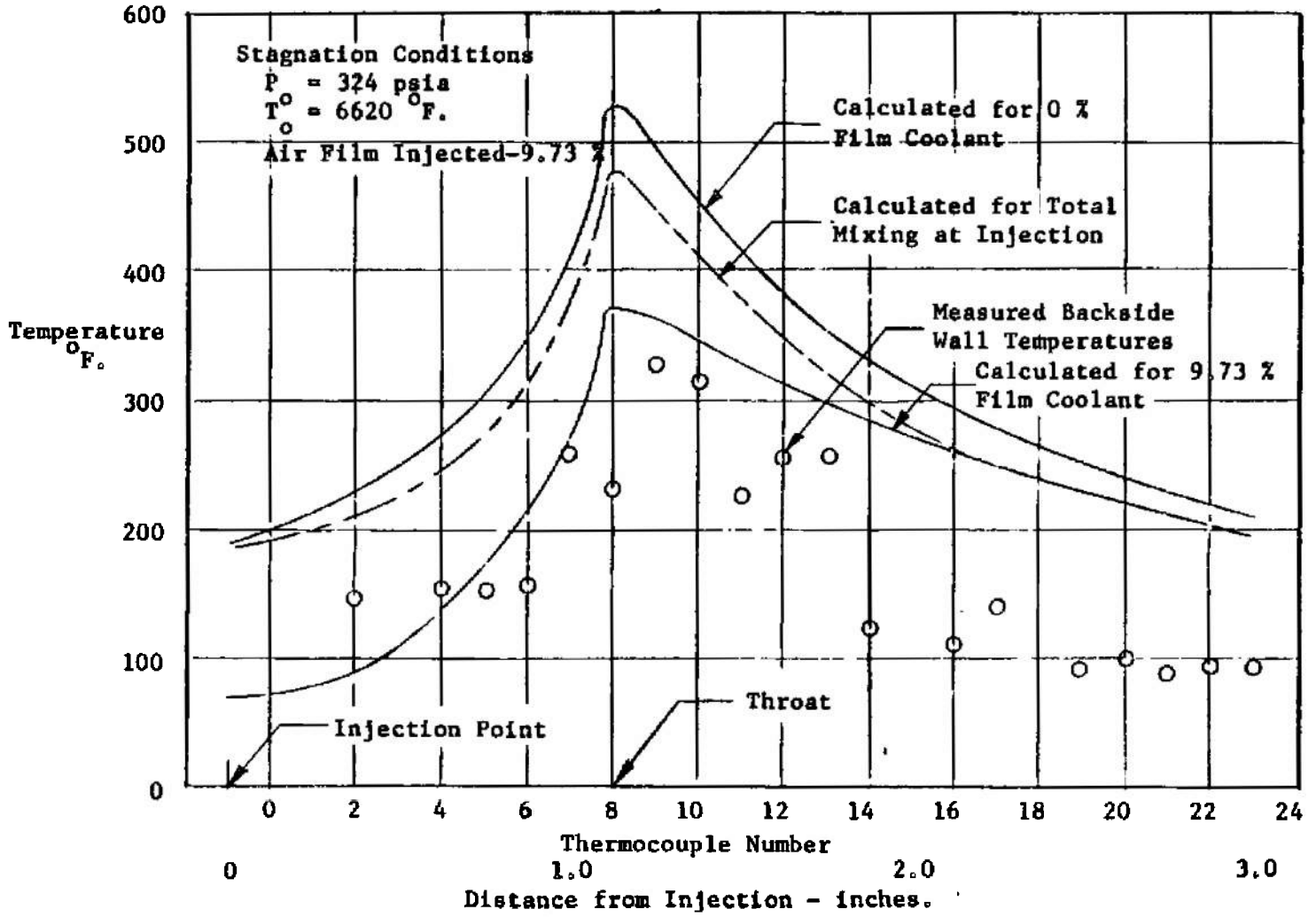

Fig. 13 Gas Film Temperature Correlation With Data for Case H5-2

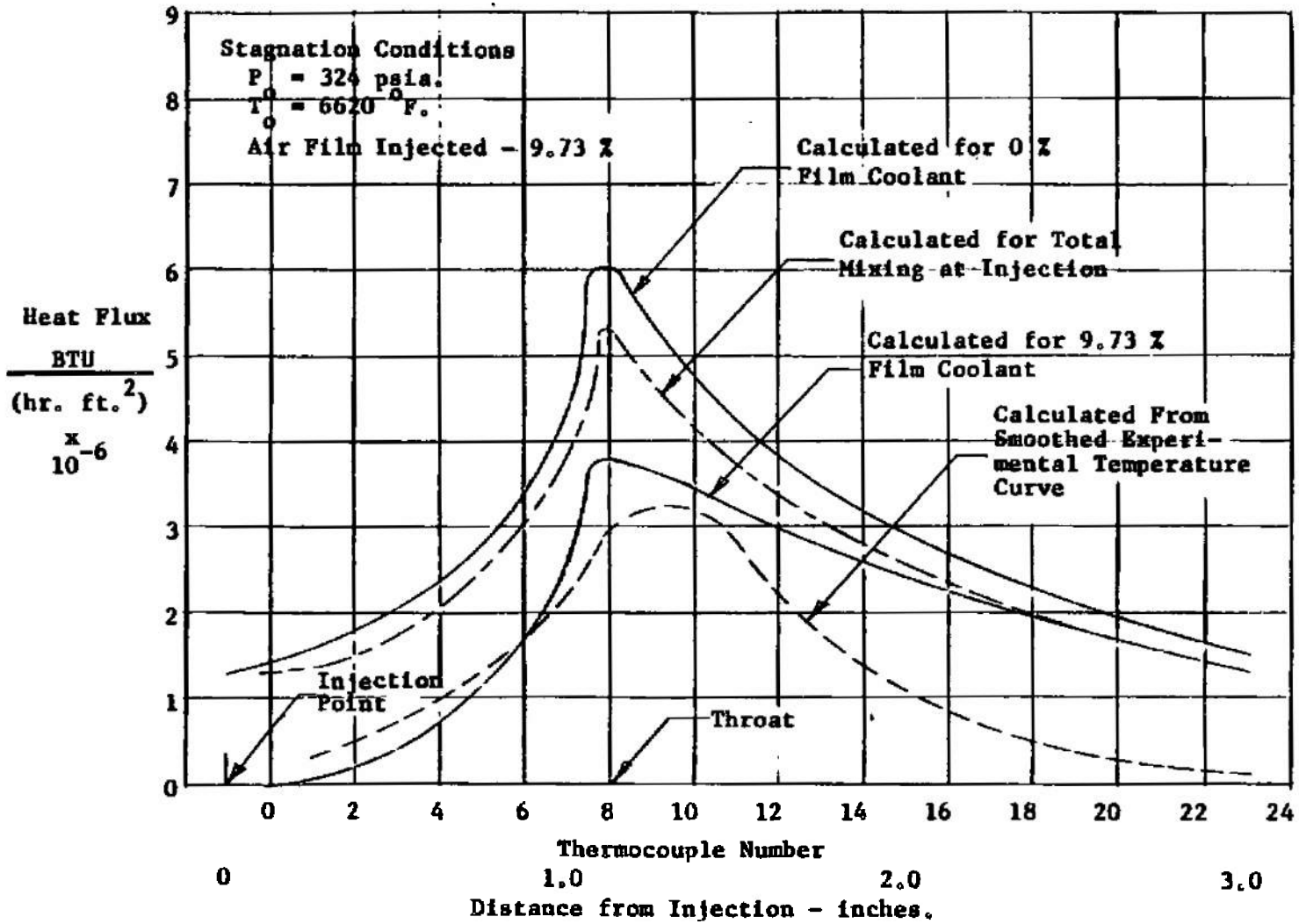

Fig. 14 Gas Film Heat Flux Correlation With Data for Case H5-2

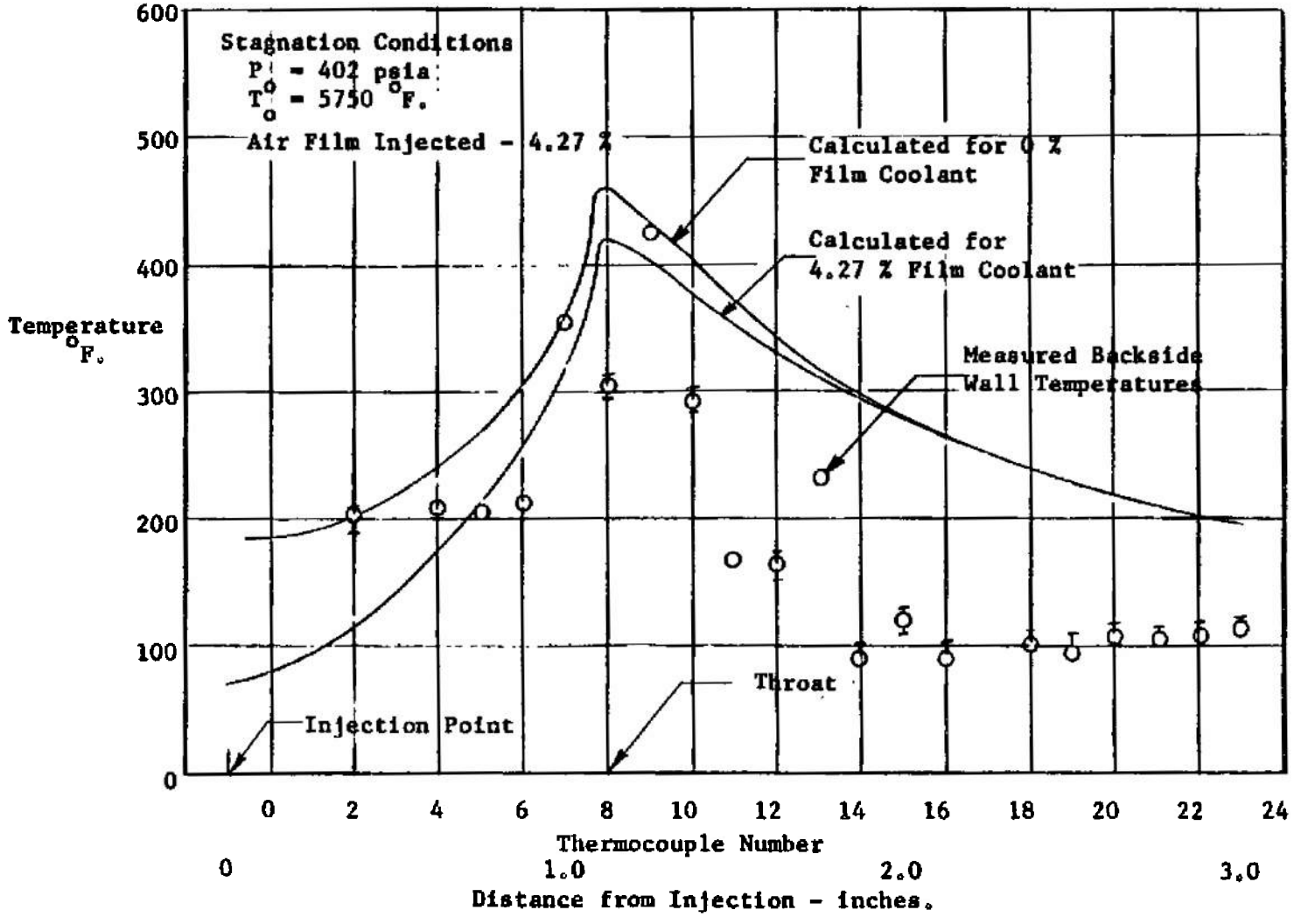

Fig. 15 Gas Film Temperature Correlation With Data for Case H9-2

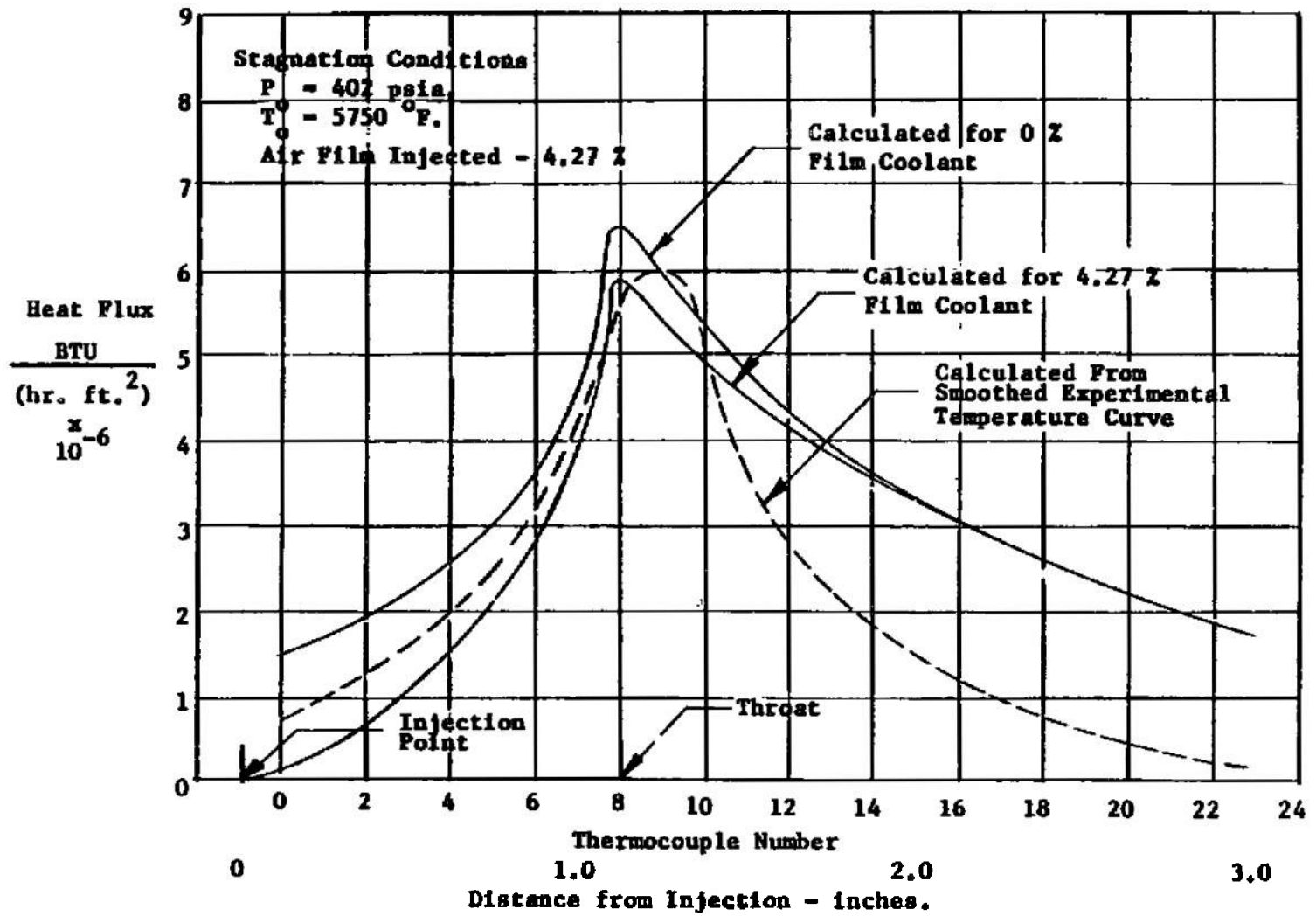

Fig. 16 Gas Film Heat Flux Correlation With Data for Case H9-2

shear stress from the past increment became unstable and either the iterative procedures for the velocity profile or the temperature profile would not converge. Reduction of the incremental distance achieved convergence for some of the cases which were initially unstable, however in cases with very low ratios of film coolant even the reduction to increment lengths of the order of 1/10,000 of the nozzle length did not bring about stability of the solutions. Calculations using the eddy diffusivity based on wall shear stress calculated at each increment from the Blasius equation, on the other hand, remained stable for reasonable incremental lengths for all cases. These results are the ones chosen for comparison with the experimental results. Mainstream and coolant fluid properties as functions of temperature were evaluated from the data presented graphically in Appendix E.

The analytical program written gives as output the local wall heat flux and the streamside nozzle surface temperature. The calculated heat flux was used with the wall thickness and thermal conductivity to calculate backside wall temperatures for correlation with the measured backside temperatures.

In addition to the data taken by the present investigator some recent data were available taken by Lieu (25) for air film cooling of a supersonic nozzle. It was decided to make correlations of the Lieu data for a case with stagnation pressure 315 psia. and stagnation temperature 1032 ^{o}R. The analytical and experimental results for

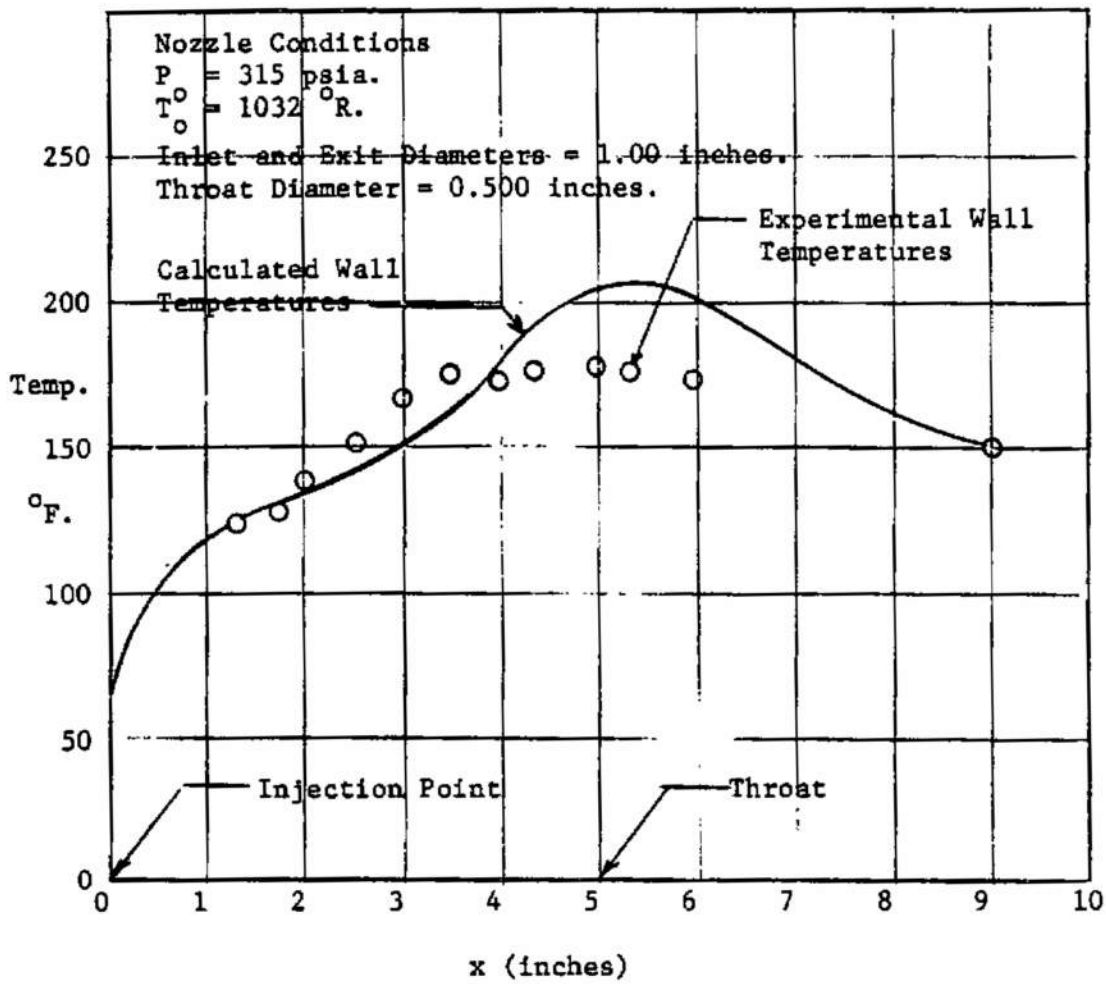

Fig. 17 Gas Film Temperature Correlation With Data From the Lieu Nozzle – 4.35% Injection Ratio

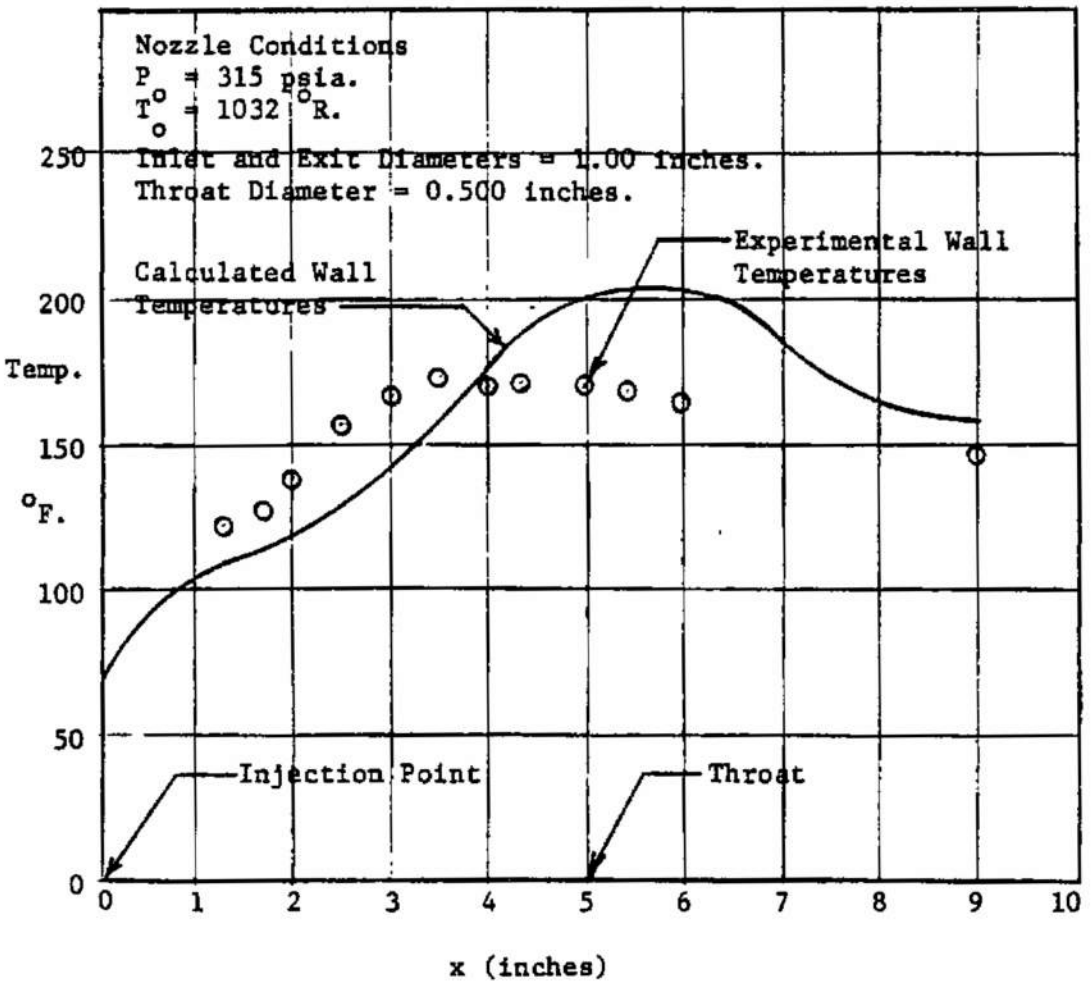

Fig. 18 Gas Film Temperature Correlation With Data From the Lieu Nozzle – 8.24% Injection Ratio

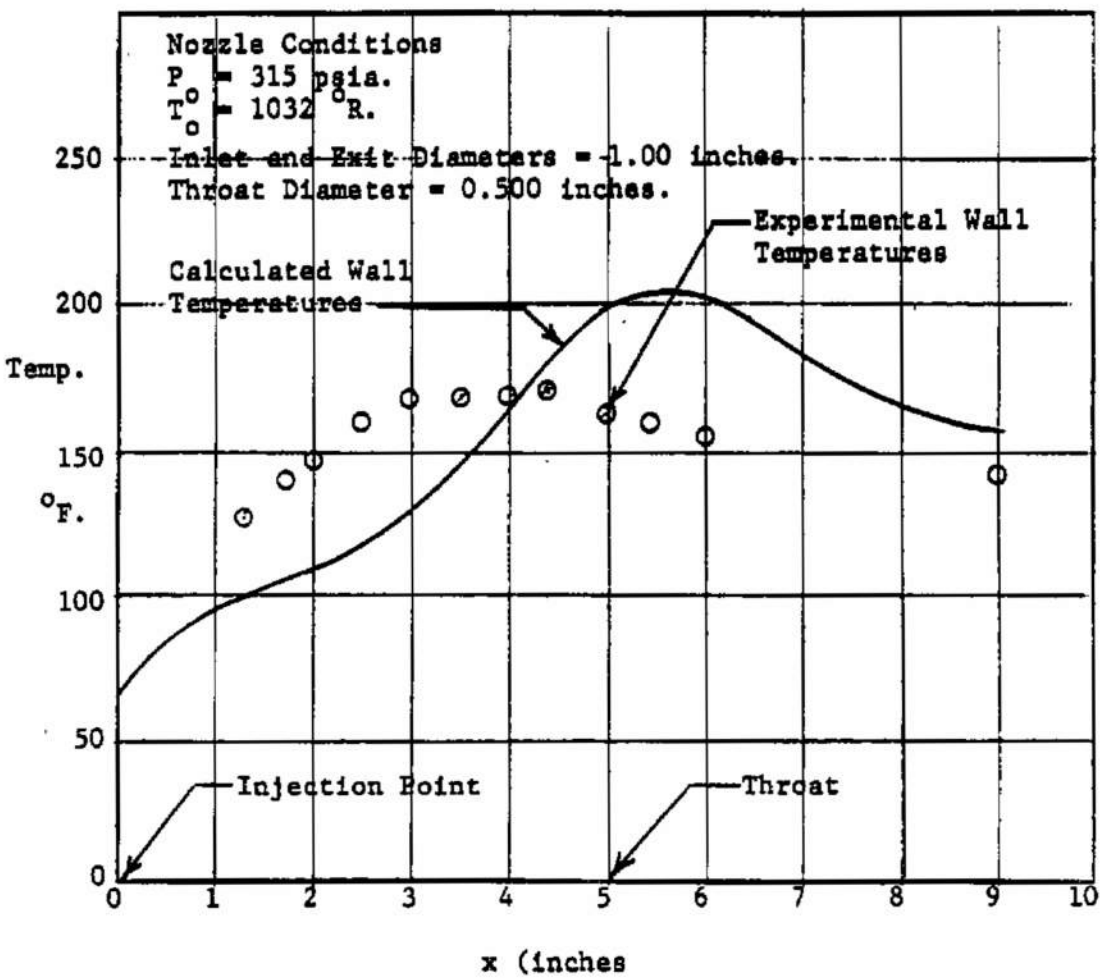

Fig. 19 Gas Film Temperature Correlation With Data From the Lieu Nozzle – 12.33% Injection Ratio

three different coolant injection rates are presented in Figures 17, 18, and 19.

As a check on the changes which would occur in the theoretically predicted wall temperatures and heat fluxes, if it were assumed that the gas film coolant were totally mixed with the free stream gas in a very short distance from the injection point, two additional theoretical calculations were made. Total mixing was assumed for Case H1-1, which had 27.4 % gas film coolant, and theoretical calculations were made for wall temperatures and heat fluxes. Case H2-2, which had 9.73 % gas film coolant, was also recalculated assuming total mixing at the injection point. These theoretically calculated curves are shown, along with the curves calculated for no film cooling and for full film cooling, in Figures 7, 8, 13, and 14.

Without discussing each of the Figures 7 through 16 in detail several general observations may be made. First, the theoretically predicted temperatures for no film cooling fall well above the measured temperatures for the larger ratios of gas film coolant, but as the amount of film coolant is decreased the theoretical curve approaches the measured temperatures until the correlation is very good for Case H9-2, with approximately 5 % film coolant. This indicates that the predicted temperatures for no film cooling using the present analysis should be reasonably accurate. As a further check on the theoretical model, with no film cooling, comparison was made to data published by the Jet Propulsion Laboratory (42) and the results are shown in Figure 20. This figure further demonstrates the validity of the theoretical model to predict temperature or heat flux profiles, at least through the throat. With the accuracy of

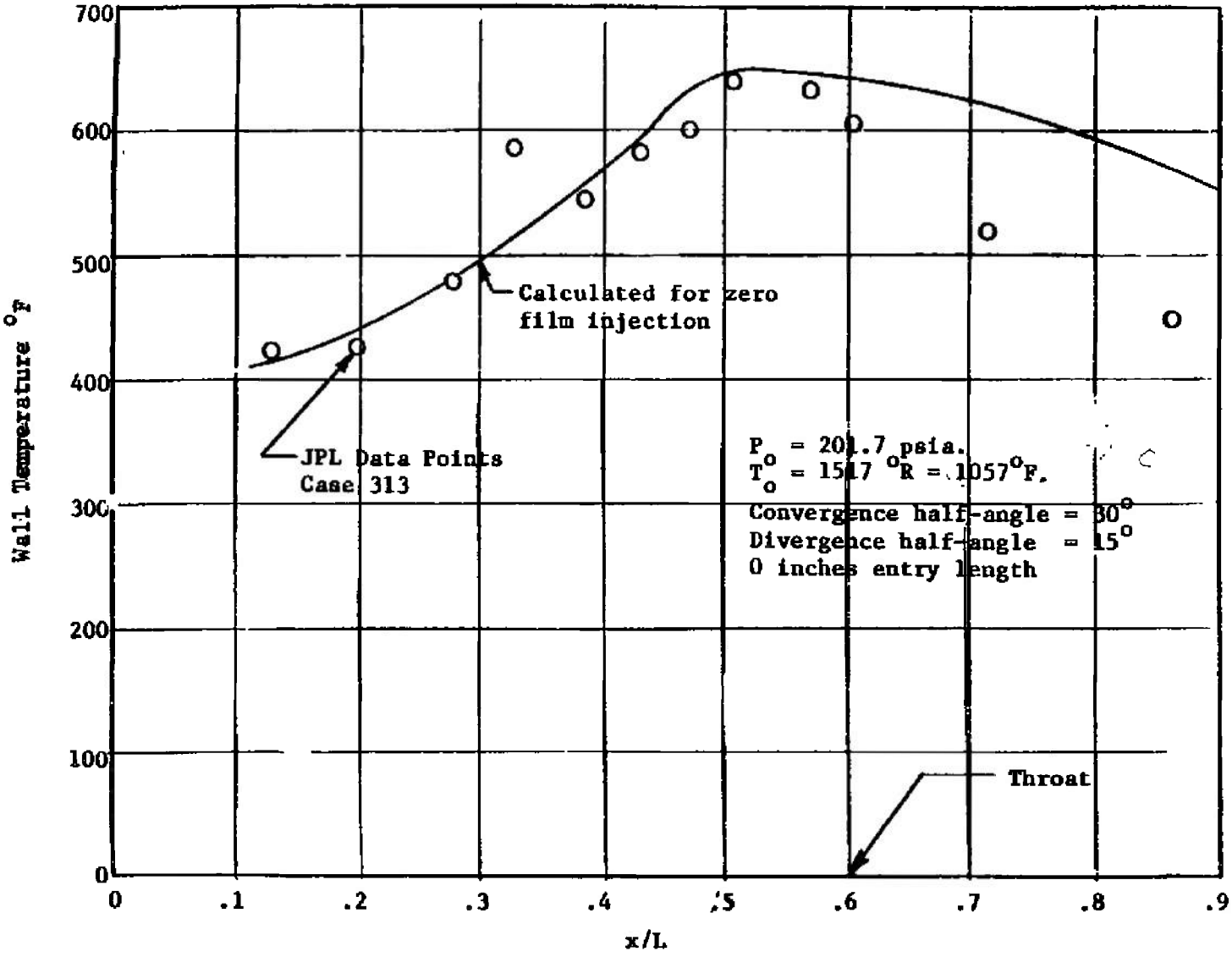

Fig. 20 Comparison of Theoretical Model with Data from Jet Propulsion Laboratory

the no film cooling calculations established, examination of the above named figures indicates that the gas film coolant does measurably lower the wall temperatures and heat fluxes, particularly in the converging section of the nozzle. Third, from Figures 7, 8, 13, and 14, which contain curves calculated assuming complete mixing of the coolant with the mainstream at injection, it may be seen that such predicted values fall well above the measured values of wall temperature and heat flux.

The effectiveness of the gas film for protecting the nozzle wall is further shown in Figure 21, which shows photographs of the converging section of the nozzle and the inside surface of the injection ring. These photographs were made without cleaning up the surfaces following the conclusion of the experimental program. The conical converging section of the nozzle is still relatively smooth and clean. There is a noticeable change very close to the throat, where the nozzle is somewhat roughened and discolored. The inside of the injection ring is badly eroded. In a previous nozzle operated without gas film cooling (27), the entire convergent portion was eroded during the experiments.

Figures 22 and 23 show a direct comparison of the wall heat flux for the two pairs of cases with very similar stagnation conditions. In Figure 22 the larger heat flux for the case with approximately 10 % cooling as compared with the case for approximately 30 % cooling is evident. In Figure 23, for cases with approximately 5 % and 10 % cooling there is very little difference, but an examination of the tabulated experimental temperatures for the two cases shows that the temperatures near the nozzle entrance for the 5 % cooling case were

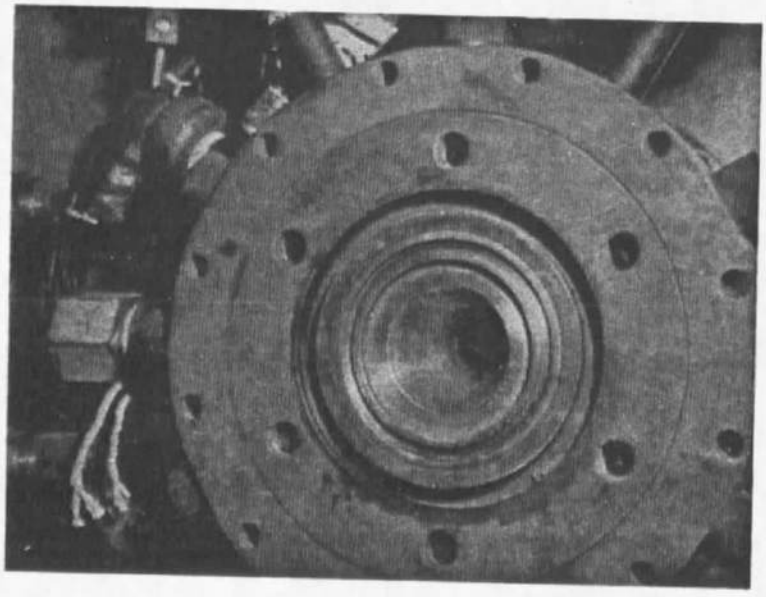

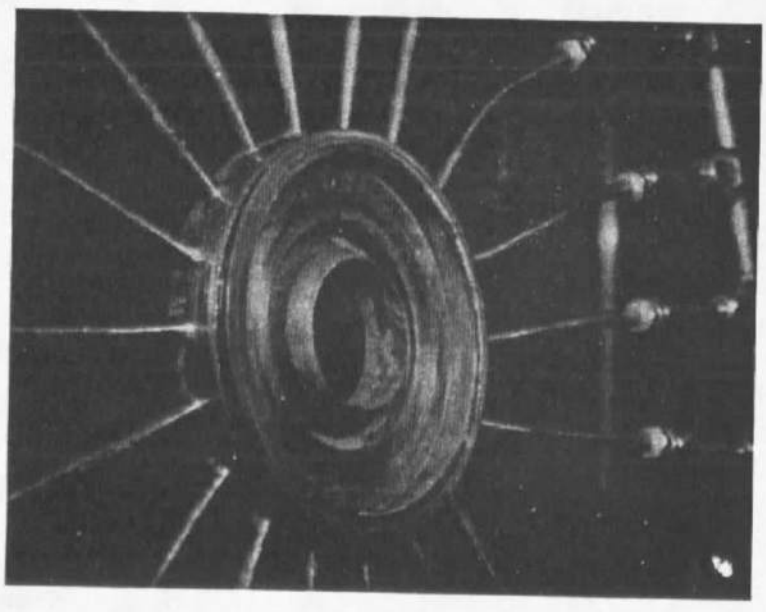

Fig. 21 Photograph of Nozzle Liner and Injection Ring after Termination of Experimentation

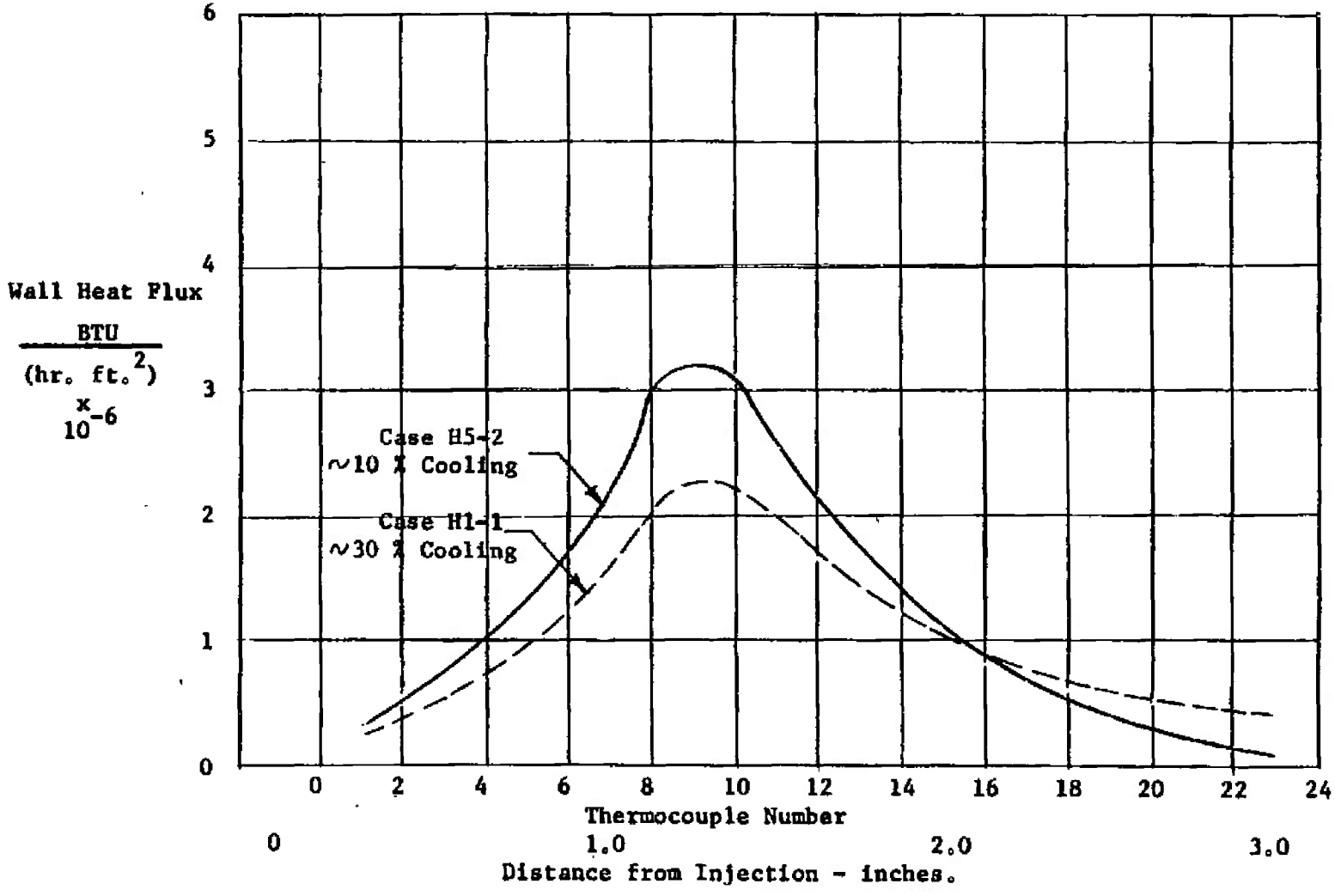

Fig. 22 Comparison of Heat Fluxes for Cases H1-1 and H5-2

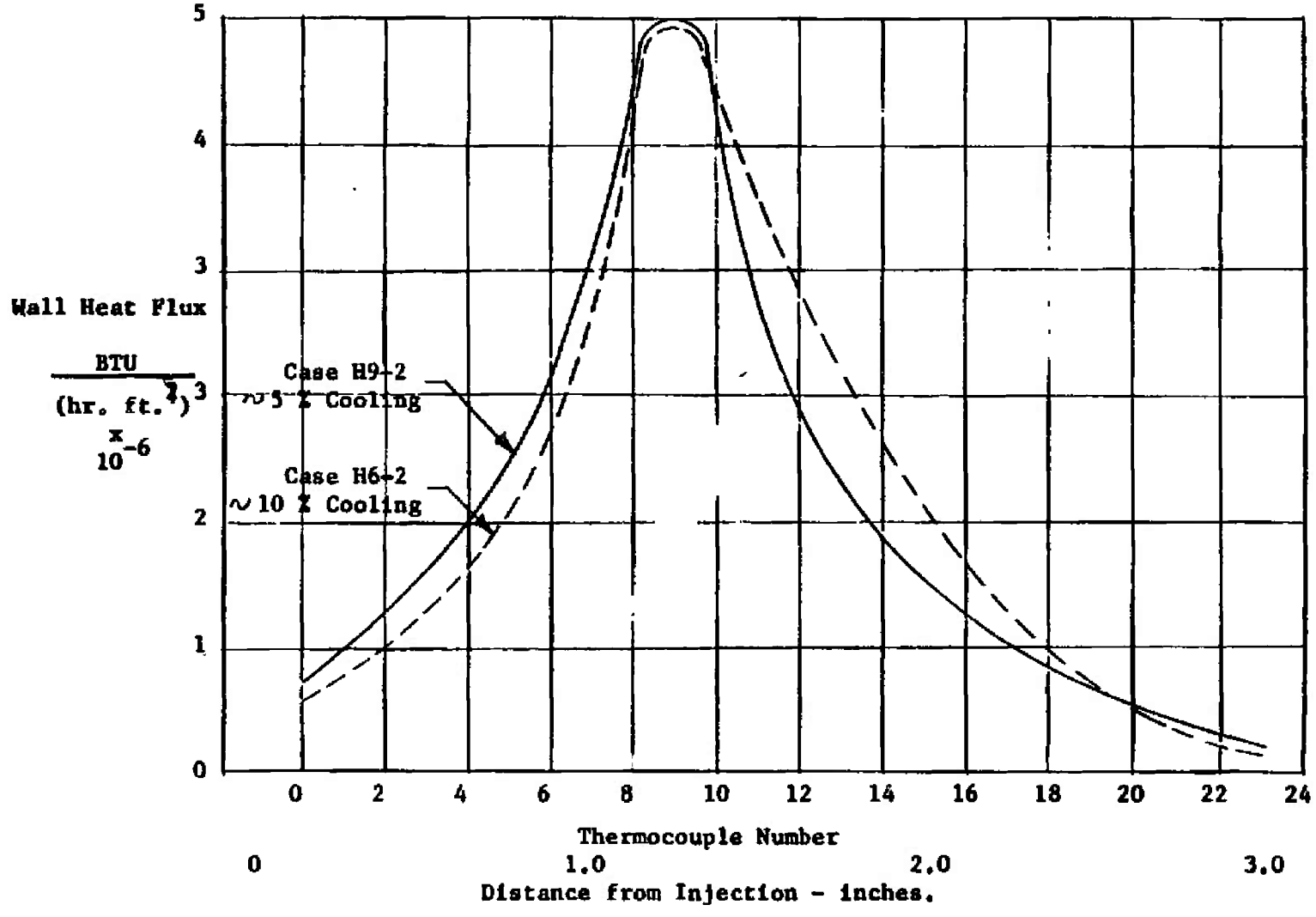

Fig. 23 Comparison of Heat Fluxes for Cases H6-2 and H9-2

slightly higher. Comparison of the backside coolant flow rates for the two cases from Table I, pages 33 and 34, shows that the 5 % case was more strongly cooled. Taken together this is an indication that the gas film coolant was effective in the converging section.

Study of the measured temperatures in Figures 7 through 16 shows a quick rise in temperature near the nozzle entrance, then a rather steady temperature until it rises rapidly toward the throat. The present investigator believes this is due to a certain amount of gross mixing at or near the injection point. This "mixed film" then forms the actual film coolant.

The temperature curves also reveal that as the nozzle was operated for longer periods of time the differential thermal expansion between the liner and the instrument rib caused the far downstream thermocouples to loosen from the wall and read low. This was caused by the freeing of the downstream end of the liner for expansion. Notice in this connection thermocouples 14 through 24 in Figures 11, 13, and 15. This also explains the poor correlation between the curves in Figure 22 for the section downstream from the throat.

Comparison of the calculated temperatures with the measured values in the case of the Lieu nozzle, Figures 17, 18, and 19 on pages 52, 53, and 54, respectively, show reasonably good correlation for the 4.35 % injection ratio but poorer correlation for the higher injection rates. The present investigator noted some apparent discrepancy between Lieu's data and the present data, however. For Lieu's nozzle the maximum temperature showed a definite shift upstream as the film cooling was increased. Both the analytical prediction and

the experimental data in the present investigation show maximum temperatures immediately downstream from the throat with very little shift in position as the injection ratio varies from ∿5% to ∿30%.

CHAPTER III
LIQUID FILM COOLING

I. THEORETICAL ANALYSIS

As was stated in Chapter I, Bartz's equation for the heat transfer coefficient in a nozzle without coolant injection is given in its final form as

$$h = \left(\frac{C}{D_*^{.2}}\right)\left(\frac{\mu^{.2} c_p}{Pr^{.6}}\right)\left(\frac{P_o g_c}{u_*}\right)\left(\frac{D_*}{r_c}\right)^{.1}\left(\frac{A_*}{A}\right)^{.9}\sigma \tag{28}$$

in which

$$\sigma = \frac{1}{\left[\frac{1}{2}\frac{T_w}{T_o}\left(1 + \frac{k-1}{2}M^2\right) + \frac{1}{2}\right]^{.8-\omega/5}\left[1 + \frac{k-1}{2}M^2\right]^{\omega/5}} \tag{29}$$

The main point of interest for the present investigation is that Bartz based his derivation on the Dittus-Boelter form of correlation for fully developed turbulent pipe flow, i.e.

$$Nu = C\,(Re)^m\,(Pr)^n \tag{30}$$

Emmons (13) developed a one dimensional analysis for cooling with an evaporating liquid film in fully developed turbulent pipe flow. It was based on the assumptions previously listed in Chapter I. He

started with the following basic equations for a turbulent incompressible boundary layer:

Continuity

$$\frac{\partial \bar{u}}{\partial x} + \frac{\partial \bar{v}}{\partial y} = 0 \tag{31}$$

Momentum

$$\bar{u} \frac{\partial \bar{u}}{\partial x} + \bar{v} \frac{\partial \bar{u}}{\partial y} = \frac{\partial}{\partial y} \left[(\nu + \epsilon_M) \frac{\partial \bar{u}}{\partial y} \right] \tag{32}$$

Energy

$$\bar{u} \frac{\partial \bar{T}}{\partial x} + \bar{v} \frac{\partial \bar{T}}{\partial y} = \frac{\partial}{\partial y} \left[(\alpha + \epsilon_H) \frac{\partial \bar{T}}{\partial y} \right] \tag{33}$$

Diffusion

$$\bar{u} \frac{\partial \bar{W}_a}{\partial x} + \bar{v} \frac{\partial \bar{W}_a}{\partial y} = \frac{\partial}{\partial y} \left[(\delta_a + \epsilon_D) \frac{\partial \bar{W}_a}{\partial y} \right] \tag{34}$$

The barred parameters in these equations represent time averaged quantities, for example:

$$\bar{u} = \lim_{\tau \to \infty} \frac{1}{\tau} \int_0^\tau u(t)\, dt \tag{35}$$

The bars are now dropped, with the understanding that these parameters are time averaged.

Emmons simplified Eqs. (31), (32), and (33) by assuming that terms including gradients in the x-direction are negligible compared with terms involving gradients in the y-direction. From the continuity equation this gave v = constant. Emmons evaluated this constant by assuming that the gas on the surface of the liquid was pure coolant vapor, thus

$$v = \frac{Q}{\gamma} \tag{36}$$

The momentum and energy equations were then

Momentum

$$\frac{Q}{\gamma}\frac{du}{dy} = \frac{d}{dy}\left[(\upsilon + \varepsilon_M)\frac{du}{dy}\right] \tag{37}$$

Energy

$$\frac{Q}{\gamma}\frac{dT}{dy} = \frac{d}{dy}\left[(\alpha + \varepsilon_H)\frac{dT}{dy}\right] \tag{38}$$

At this point Emmons introduced the expression for the eddy diffusivity of momentum as developed by Rannie (29) and modified by Turcotte for the case of wall injection (40).

$$\varepsilon_M = \upsilon \sinh^2\left(\frac{by^+}{13.89}\right) \tag{39}$$

Substituting from Eq. (39) into Eq. (37) and integrating assuming zero velocity at y = 0 gave

$$u = \frac{\tau_w \gamma}{\rho_w Q}\left[\exp\left(\frac{13.89\ Q}{by\sqrt{\tau_w/\rho_w}}\tanh\frac{by\sqrt{\tau_w/\rho_w}}{13.89\upsilon}\right) - 1\right] \tag{40}$$

From Turcotte's analysis (40)

$$\tau_w = \tau_{ni}\left[\exp\left(\frac{\beta 13.89\ Q}{by\sqrt{\tau_w/\rho_w}}\right)\right] \tag{41}$$

so

$$u = \frac{\tau_{ni}\, e^{-\beta Q}}{\rho_w Q}\left[\exp\left(\beta Q e^{\frac{\beta Q}{2}}\tanh\frac{e^{\frac{-\beta Q}{2}}}{\beta\upsilon\gamma}\right) - 1\right] \tag{42}$$

where

$$\beta = \frac{13.89}{b\gamma u^*} \tag{43}$$

and

$$u^* = \sqrt{\tau_{ni}/\rho_w} \tag{44}$$

Emmons then used an extended Reynolds analogy, with Pr = 1 and $\varepsilon_H = \varepsilon_M$ to get the temperature distribution as

$$\frac{T-T_s}{T_g-T_s} = \frac{\gamma \tau_{ni} e^{-\beta Q}}{\rho_w u_g Q} \left[\exp\left(\beta Q e^{\frac{\beta Q}{2}} \tanh \frac{\gamma e^{\frac{-\beta Q}{2}}}{\beta \gamma v}\right) - 1 \right] \tag{45}$$

Use of this temperature distribution gave the following equation for the Stanton Number

$$St = \frac{1}{2} f_{ni} \frac{u_m}{u_g} e^{-\beta Q} \tag{46}$$

Emmons then noted that for the case $u_m = u_g$ and Q = 0 this reduces to the result obtained by the simple Reynolds analogy. He then proceeded to use the heat transfer coefficient obtained from Eq. (45), specifically

$$h = \frac{k_H \tau_{ni}}{\mu u_g} e^{-\beta Q} \tag{47}$$

without further modification.

It was noted by the present investigator that the exponential term in Eqs. (46) and (47) could be looked upon as a simple correction term applied to the non-injection heat transfer coefficient to take into account the fluid injection, either by evaporation or by transpiration at the surface.

There are better correlating equations available for predicting the convective heat transfer coefficient without injection than that which comes from the simple Reynolds analogy. One of these is the Dittus-Boelter equation for fully developed turbulent pipe flow, the form of which was used by Bartz in his analysis (2). It was thus decided to program a stepwise finite difference analysis for digital computer solution using the Dittus-Boelter correlation at each step but substituting the coefficient "C" as determined by Bartz. The convective heat transfer coefficient thus determined would then be modified using Emmons' "exponential correction" factor. The program also provides for the direct use of experimentally determined heat transfer rates without injection and modifying these using Emmons' "exponential correction" factor.

Emmons' analysis assumed that the surface of the coolant film was at saturation temperature immediately upon injection. If the coolant has a high heat capacity and high saturation temperature this is not a good assumption, even for very high heat transfer rates. It was thus decided to forego this assumption and calculate the temperature profile of the liquid film starting at the injection point and taking into account the evaporation of the film while it is increasing in

temperature up to the saturation temperature.

In order to calculate the developing temperature profile it is necessary to assume, or calculate, the velocity profile. Since the ratio of the diffusivity of momentum to the diffusivity of heat, i.e., Pr is > 3 at room temperature for water, the main coolant liquid under consideration, it was decided to assume instantaneous development of the velocity profile upon injection. A condition of constant shear stress across the liquid film was also assumed. This latter assumption appears to be reasonable for such a thin film as that used for film cooling.

Consider a fluid layer as shown in Figure 24, with mass flow rate w. Now for constant properties and constant shear stress across this layer

$$u_{n+1} = u_n + \frac{\tau_w d_n}{\mu} \tag{48}$$

and

$$w = 2\pi r_n \rho d_n \left(\frac{u_{n+1} + u_n}{2}\right) \tag{49}$$

Combining Eqs. (48) and (49) and rearranging

$$\left(\frac{\rho\tau_w}{2\mu}\right) d_n^2 + (\rho u_n) d_n - \frac{w}{2\pi r_n} = 0 \tag{50}$$

and

$$d_n = \frac{-\rho u_n + \sqrt{(\rho u_n)^2 + \rho\tau_w w/\pi r_n \mu}}{\rho\tau_w/\mu} \tag{51}$$

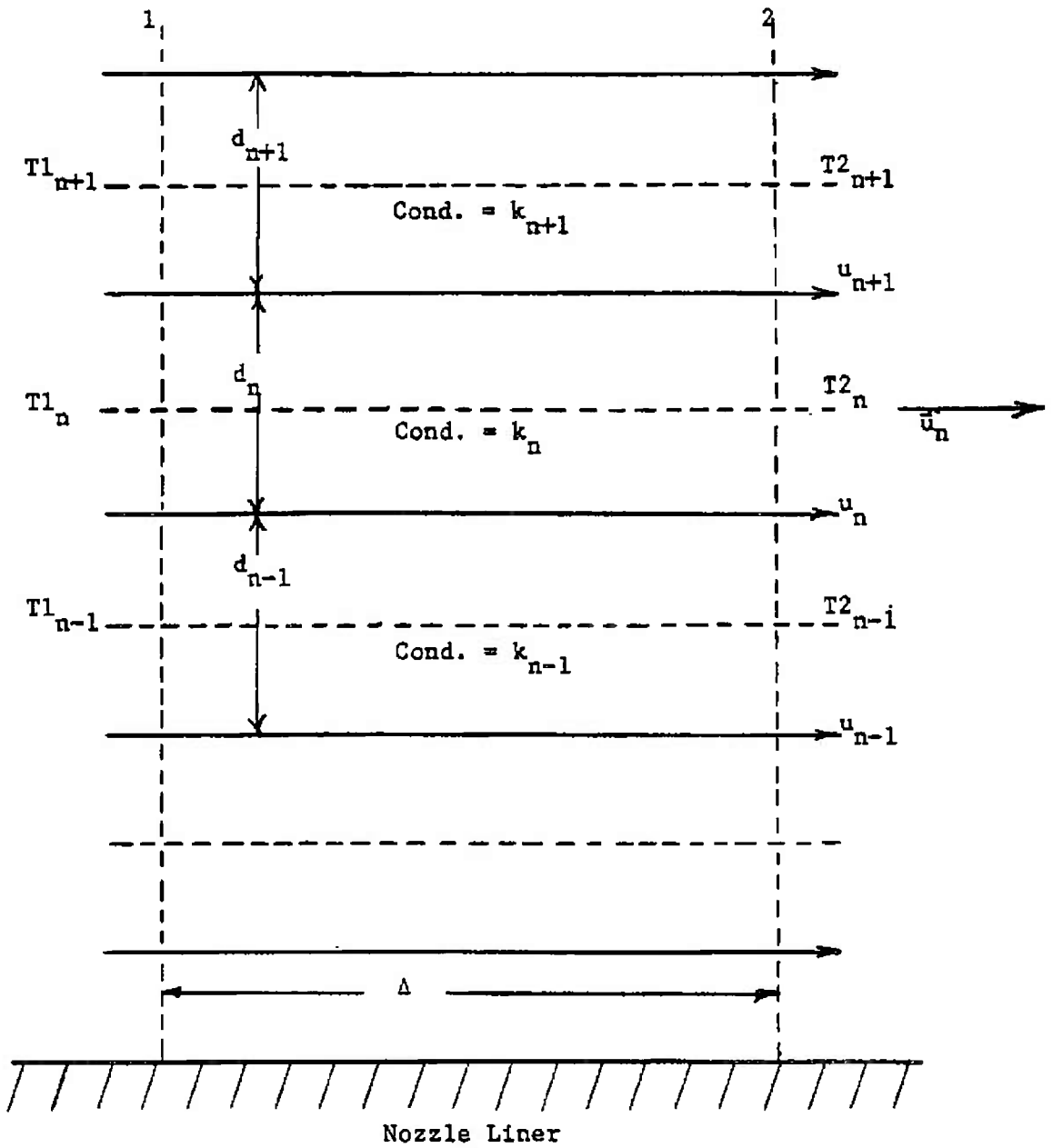

Fig. 24 Velocity and Temperature Notation for Liquid Film by Layers and Increments

The positive value on the radical is used since d_n must be positive. Starting with a known value of u_n and estimating initial values of ρ, μ, and τ_w Eq. (51) may be solved for d_n, then u_{n+1} calculated from Eq. (19). As better average values of temperatures become known from the iterative solution of the heat balance equations ρ and μ are corrected and the velocity profile recalculated. It is not necessary to re-evaluate the velocity profile for each temperature iteration as it produces only very slight effects. However, when the convergence criterion for the temperature iteration is satisfied, the velocity profile should be corrected and convergence checked again. This assures the use of values of ρ and μ which are temperature corrected.

The equations necessary for the temperature profile calculation are derived by taking a heat balance on the nth layer. The heat balance for steady state requires that:

$$\text{Net Heat Rate Convected In} + \text{Net Heat Rate Conducted In} = 0 \tag{52}$$

Referring to Figure 24, page 69.

$$\text{Net Heat Rate Convected In} = w_n c_n (T1_n - T2_n) \tag{53}$$

$$\text{Net Heat Rate Conducted In} = 2\pi r\Delta \left[\frac{\left(\frac{T1_{n+1} + T2_{n+1}}{2}\right) - \left(\frac{T1_n + T2_n}{2}\right)}{\frac{d_{n+1}}{2k_{n+1}} + \frac{d_n}{2k_n}} + \frac{\left(\frac{T1_{n-1} + T2_{n-1}}{2}\right) - \left(\frac{T1_n + T2_n}{2}\right)}{\frac{d_{n-1}}{2k_{n-1}} + \frac{d_n}{2k_n}} \right] \tag{54}$$

Let

$$\overline{T}_{n+1} = \frac{(T1_{n+1} + T2_{n+1})}{2} \tag{55}$$

and similarly for $\overline{T}_n$ and $\overline{T}_{n-1}$.

Also let

$$K_{n+1} = \frac{2\pi r_{n+1}}{\left(\frac{d_{n+1}}{2k_{n+1}} + \frac{d_n}{2k_n}\right)} \tag{56}$$

and similarly for K_n and K_{n-1}.

Now substituting from Eqs. (53), (54), (55), and (56) into (52)

$$w_n c_n (T1_n - T2_n) + \Delta K_{n+1}(\overline{T}_{n+1} - \overline{T}_n) + \Delta K_{n-1}(\overline{T}_{n-1} - \overline{T}_n) = 0 \tag{57}$$

Resubstituting from Eq. (55) for $\overline{T}_n$ and solving for $T2_n$

$$T2_n = \frac{T1_n\left[w_n c_n - \frac{\Delta}{2}(K_{n+1} + K_{n-1})\right] + \Delta(K_{n+1}T_{n+1} + K_{n-1}T_{n-1})}{w_n c_n + \frac{\Delta}{2}(K_{n+1} + K_{n-1})} \tag{58}$$

Now Eq. (58) applies for the interior layers of the film but other equations must be developed for the heat balance on the stream-side and wall-side layers. For the stream-side layer

$$w_s c_s (T1_s - T2_s) + \Delta K_{s-1}(\overline{T}_{s-1} - \overline{T}_s) + 2\pi r_s \Delta h (T_\infty - \overline{T}_s) - 2\pi r_s Q h_{fg} = 0 \tag{59}$$

and

$$T2_s = \frac{T1_s \left[w_s c_s - \frac{\Delta}{2}(K_{s-1} + 2\pi r_s h)\right] + (K_{s-1}\overline{T}_{s-1} + 2\pi r_s h T_\infty) - 2\pi r_s Q h_{fg}}{w_s c_s + \frac{\Delta}{2}(K_{s-1} + 2\, r_s h)} \tag{60}$$

For the wall-side layer

$$w_w c_w (T1_w - T2_w) + \Delta K_{w+1}(\overline{T}_{w+1} - \overline{T}_w) + \Delta K_b (T_b - T_w) = 0 \tag{61}$$

where

$$K_b = \frac{2\pi r_w}{\frac{d_w}{2k_w} + \frac{d_1}{k_1} + \frac{1}{h_b}} \tag{62}$$

Thus

$$T2_w = \frac{T1_w \left[w_w c_w - \frac{\Delta}{2}(K_{w+1} + K_b)\right] + \Delta(K_{w+1}\overline{T}_{w+1} + K_b T_b)}{w_w c_w + \frac{\Delta}{2}(K_{w+1} + K_b)} \tag{63}$$

Iterative calculation of Q is described starting in paragraph 2, page 77. The coefficient h is determined from the modified Dittus-Boelter equation which will subsequently be discussed in detail. The coefficient h_b is determined from the backside coolant flow conditions.

Since the backside coolant flow will be turbulent for practically all cases, a regular Dittus-Boelter calculation will normally be used.

Application of Eqs. (58), (60), and (63) across the film results in a set of nonlinear simultaneous algebraic equations. The nonlinearity comes from the dependence of c, d, and k on T. Since this dependence is relatively weak, however, the equations may be solved by the Gauss-Seidel iteration method with periodic corrections of c, d, and k for temperature change. This is done in the same manner as the periodic correction of ρ and μ in the velocity profile calculation. The temperature profile is first estimated. Substitution is then made into the explicit equations for $T2_w$, - - - -, $T2_s$ and the amount of change in $T2_n$ checked against some convergence criterion until it is satisfied for all the layers. Periodically c, d, and k are re-evaluated, with a final evaluation made as a check when $T2_n$ has converged.

Other methods could be used for the solution of Eqs. (58), (60), and (63). For example, by rearrangement they could be put into the matrix form:

$$\bar{\bar{A}}\,\bar{T} = \bar{B} \tag{64}$$

By estimating $\bar{T}$, $\bar{\bar{A}}$ could be calculated. Then

$$T = \bar{\bar{A}}^{-1}\,\bar{B}$$

$\bar{\bar{A}}$ could then be recalculated using the new values for $\bar{T}$ and the method repeated until $\bar{T}$ converges. The Gauss-Seidel iteration method was used because the coefficient matrix is sparsely populated and this method does not require manipulation of the zero elements.

The incremental film temperature calculation is continued as described above until $T2_s \geq T_{sat}$. Normally after some particular incremental calculation $T2_s > T_{sat}$. In order to determine the position where $T2_s = T_{sat}$ an interpolation is made. It was found that if the initial incremental steps are small a straight line interpolation here is sufficiently accurate without further iterative calculation of $T2_s$.

The evaporation rate Q must be calculated both in the region before $T2_s = T_{sat}$ and following this region. The only difference between the two calculations is that in the region before saturation temperature is reached the rate of evaporation is controlled by the available partial pressure of the film vapor and the mass transfer coefficient at the surface, whereas in the region following the rate of evaporation is controlled by the excess thermal energy deposited in the film by heat transfer from the mainstream. In both cases the heat transfer coefficient h must be corrected for the evaporation effect and the loss of liquid film due to evaporation must be calculated. Examination of these effects shows that they are coupled and thus require an iterative solution. The evaporation rate for a given evaporation enthalpy and temperature difference varies with h. On the other hand, the following equation for the heat transfer coefficient shows the dependence of h on the evaporation rate:

$$h = .0265 \frac{k_H}{D} (Re)^{.8} (Pr)^{.333} \left[\exp\left(\frac{-13.89\ Q}{b\gamma u^*} \right) \right] \qquad (65)$$

In Eq. (65) Q is the mass evaporation rate of the film coolant. In the region before saturation temperature is reached Q may be calculated directly using Eq. (69), page 75, and the vapor partial pressure.

For the region following the attainment of saturation temperature, hereafter called the boiling region, there is a simple relationship between Q and h.

$$Qh_{fg}A = hA\left(T_{Adw} - \frac{T1_s + T2_s}{2}\right) - Q_s \tag{66}$$

or

$$Q = \frac{h\left(T_{Adw} - \frac{T1_s + T2_s}{2}\right) - \frac{Q_s}{A}}{h_{fg}} \tag{67}$$

Substituting from Eq. (67) into Eq. (66)

$$h = \frac{.0265k_H}{D}(Re)^{.8}(Pr)^{.333}\left[\exp\frac{-13.89h\left(T_{Adw} - \frac{T1_s+T2_s}{2}\right)-13.89\frac{Q_s}{A}}{b\,h_{fg}\,u^*}\right] \tag{68}$$

In Emmons' analysis it was assumed that the fluid in the boundary layer over the liquid surface is pure coolant vapor and that the thermal conductivity k_H in Eq. (68) should be that of the pure coolant vapor evaluated at T_{sat}. It has been demonstrated (12) that constant property solutions for skin friction, Nusselt number and recovery factor may be used even when large variations in physical properties occur provided the properties are evaluated at a reference temperature T^* which is expressed explicitly as

$$T^* = T_g + 0.5(T_w - T_g) + 0.22(T_r - T_g) \tag{69}$$

It can be readily seen that T^* is the widely used film temperature (or average of T_w and T_g) plus a term to account for temperature recovery in high speed flow. This term seems to effect a good property correction even for dissociation effects. In the present solution fluid properties are evaluated at T^*.

If the thermal conductivity of the binary mixture differs greatly from that of the coolant vapor an effort should be made to evaluate k_H for the binary mixture. If the concentration of coolant vapor at the liquid film surface can be calculated the thermal conductivity for a gas mixture at half this concentration should be a better value to use than that of the pure coolant vapor. This conductivity should be evaluated at T^* as indicated above.

Examination of Eqs. (32), (33), and (34) shows that the same analogy may be made between mass transfer and momentum transfer as that which was made between heat transfer and momentum transfer. Experimental results indicate that by use of the proper form for the diffusivity of mass and use of the Schmitt number, Sc, in place of Pr, a coefficient of mass transfer for turbulent flow may be calculated as

$$h_M = \frac{.0265k_M}{D} (Re)^{.8} (Sc)^{.333} \tag{70}$$

It is therefore proposed that in accordance with the above mentioned analogy Eq. (70) be modified and written in the form of Eq. (68) as

$$h_M = \frac{.0265k_M}{D} (Re)^{.8} (Sc)^{.333} \left[\exp\left(\frac{-13,890}{bTu^*}\right)\right] \tag{71}$$

If the total coolant injection rate is only a small percentage of the main gas flow rate any concentration of coolant in the main stream may be neglected so for this case

$$Y_c = \frac{Q}{h_M} \tag{72}$$

Now

$$Y = Y_c + Y_s \tag{73}$$

Substituting Eqs. (72) and (73) into Eq. (71) gives

$$h_M = \frac{.0265k_M}{D}(Re)^{.8}(Sc)^{.333}\left[\exp\frac{-13,890}{bu^*\left(\frac{Q}{h_M}+\gamma_s\right)}\right] \tag{74}$$

The iterative procedure for determining h is then as follows:

1. Calculate k_M and Sc at T^*.
2. Calculate Q based on value of h for previous increment.
3. Starting with Q from step 2 iteratively calculate h_M using Eqs. (71), (72), (73), and (74).
4. Calculate h from Eq. (65).
5. Calculate Q from Eq. (67).
6. Calculate γ_c from Eq. (72).
7. Re-evaluate k_H based on γ_c from step 6.
8. Re-evaluate h using Eq. (68) and compare with h from step 4.
9. Repeat steps 3 through 7 until h converges.
10. Re-evaluate Q and compare with Q from step 2.
11. Repeat steps 3 through 10 until Q converges.

Two additional problems are encountered in the procedure outlined above. One of these is the determination of the thermal conductivity of a binary gas mixture at a given temperature and the other is the determination of the diffusivity of mass for the coolant vapor through the mainstream gas for a known pressure and temperature.

Thermal conductivities of gas mixtures may be estimated from

$$k_{mix} = \sum_1^n x_i k_i \tag{75}$$

where the x_i and k_i are mole fractions and thermal conductivities, respectively, of the pure gas species.

Given the diffusivity of mass for a binary gas mixture at one condition of pressure and temperature the diffusivity at other pressures and temperatures may be estimated from the following equation (93)

$$D_{AB} = \frac{C\,T^{3/2}}{P}\left[\frac{1}{M_A} + \frac{1}{M_B}\right] \tag{76}$$

thus where C is a constant;

$$(D_{AB})_{T_2,p_2} = (D_{AB})_{T,p}\left(\frac{T_2}{T}\right)^{3/2}\left(\frac{p}{p_2}\right) \tag{77}$$

In the present study Eq. (77) was used to predict mass diffusivities at the local reference temperature T^* and the local static pressure. Dependence of the diffusivity on concentration was neglected.

Now for the diffusion of mass

$$I_A = -D_{AB}\frac{d\rho_A}{dy} \tag{78}$$

where I_A is the mass current in lbm./ft.^{2}hr. and $d\rho_A/dy$ is the density gradient in lbm./ft.^{4}. In forced convection mass transfer the diffusivity D_{AB} plays the same role as that played by the thermal conductivity in conduction heat transfer. Eq. (71) may thus be rewritten as

$$h_M = \frac{.0265\ D_{AB}}{D} (Re)^{.8}(Sc)^{.333}\left[\exp\left(\frac{-13.89\ h_M}{bu^*}\right)\right] \tag{79}$$

In order to use the above equations at each axial position the mainstream velocity, temperature, and density must be calculated. Frozen flow through the nozzle is assumed with a specific heat ratio determined by the bulk mean temperature at the nozzle entry. The equation which relates the local diameter to throat diameter ratio, specific heat ratio, and Mach number is

$$\left(\frac{D}{D_t}\right)^2 = \frac{1}{M}\left[\frac{2}{k+1} + \left(\frac{k-1}{k+1}\right)M^2\right]^{\frac{k+1}{2(k-1)}} \tag{80}$$

Now (D/D_t) and k are known and M is to be calculated. Since Eq. (80) cannot be solved explicitly for M some iterative procedure must be used to solve for M.

To solve Eq. (80) for M the following rapidly converging iterative procedures were devised. Designate the Mach numbers in Eq. (80) differently by subscripts as follows:

$$\left(\frac{D}{D_t}\right)^2 = \frac{1}{M_a}\left[\frac{2}{k+1} + \left(\frac{k-1}{k+1}\right)M_b^2\right]^{\frac{k+1}{2(k-1)}} \tag{81}$$

Now for iteration in the subsonic portion of the nozzle, i. e., upstream from the throat, Eq. (81) is solved explicitly for M_a.

$$M_a = \frac{\left[\frac{2}{k+1} + \left(\frac{k-1}{k+1}\right)M_b^2\right]^{\frac{k+1}{2(k-1)}}}{\left(\frac{D}{D_t}\right)^2} \tag{82}$$

The iteration may be started by substituting any number from 0 to 1 into Eq. (82) for M_b. The value of M_a calculated is then substituted back in for M_b and the procedure repeated until the difference between M_a and M_b meets a specified criterion. For the <u>supersonic</u> portion of the nozzle, i. e., downstream from the throat, Eq. (81) is solved explicitly for M_b.

$$M_b = \left[\frac{\left(M_a\left(\frac{D}{D_t}\right)^2\right)^{\frac{2(k-1)}{k+1}} - \frac{2}{k+1}}{\left(\frac{k-1}{k+1}\right)}\right]^{\frac{1}{2}} \tag{83}$$

This iteration is started by substituting 1 or a number greater than 1 into Eq. (81) for M_a. After M_b is calculated it is substituted back in for M_a and the procedure repeated as described above.

With the Mach number calculated the local pressure, temperature and density for the main stream gas may be calculated.

The general calculational procedure for liquid film cooling proceeds as follows:

1. For the known axial position calculate the ratio D/D_t.
2. Using Eqs. (82) and (83) and the iterative procedure described calculate the Mach number.

3. Using the Mach number calculate the local (free stream) pressure, temperature and density.
4. Evaluating properties at the reference temperature calculate Re, Pr, Sc, and D_{AB}.
5. Calculate τ_{ni} and T_{sat} for the film.
6. Check to see if the film surface is up to T_{sat}. If not calculate the film velocity and temperature profiles correcting for evaporation effects and go to step (9). If the film surface is at or above T_{sat} go to step (7).
7. Set film surface temperature equal to T_{sat} and calculate film velocity and temperature profiles.
8. Calculate h iteratively correcting for the change in thermal conductivity due to mass transfer.
9. Subtract the amount of film coolant evaporated over the axial increment from the mass flow rate in the film surface layer. (Some fraction of the layer is set as a maximum amount to be evaporated per axial increment and the increment size reduced if this is exceeded).
10. Increment the axial position and return to step (1).

The above procedure has been programmed in Fortran IV language for digital computer execution and the program is included as Appendix B.

The above procedure may also be applied for calculation of coolant evaporation rates if experimental heat transfer values without film cooling are available. If the flow condition is turbulent, so that Turcotte's formula for ϵ_M, Eq. (39), is a good approximation

Emmons' exponential correction factor should be directly applicable. The procedure is as follows:

1,2,3,4,5. These steps are the same as for calculation of the heat load from stream variables.

6. Check to see if the film surface is up to T_{sat}. If not use the experimental heat load, q_x, and calculate film velocity and temperature profiles correcting for evaporation effects and go to step (9). If the film surface is at or above T_{sat} go to step (7).

7. Set the film surface temperature equal to T_{sat} and calculate the film velocity and temperature profiles.

8. Using

$$Q = \frac{q_{ex} - \frac{Q_s}{A}}{h_{fg}} \tag{84}$$

and

$$q = q_{ex} \frac{k_H}{(k_H)_{ni}} \left[\exp \left(\frac{-13.89\, Q}{b\gamma u^{*}} \right) \right] \tag{85}$$

calculate the heat load to the film, q, iteratively correcting for the change in thermal conductivity due to mass transfer.

9, 10. Same as for direct calculation from stream variables.

II. DISCUSSION OF ANALYTICAL RESULTS

The above analysis of liquid film cooling was programmed in Fortran IV language for execution on a digital computer. The program is included as Appendix B. Since experimental studies of this type cooling were not to be performed a test case was postulated in order to check out the analysis. In this test case the nozzle configuration, mainstream stagnation conditions, and the backside cooling heat transfer coefficient were similar to those for the experimental studies of gas film cooling. It was found that a finite distance is required for the liquid film to rise to saturation temperature, and that a significant fraction of the liquid evaporates during this interval. In the case chosen this amounted to approximately 30 per cent of the injected film mass flow rate. Figure 25 shows the increase of the film surface temperature and the backside wall temperature as the film progresses through the nozzle. The increased heat flux at the throat and the rapidly decreasing pressure cause the liquid at the surface to reach the saturation temperature just downstream from the throat for this particular case. The liquid surface then remains at the saturation temperature in the diverging portion of the nozzle as the pressure continues to drop, and the rate of film evaporation is controlled largely by the heat transfer rate available from the mainstream gas. The sample computer calculation for this case is given in Appendix F.

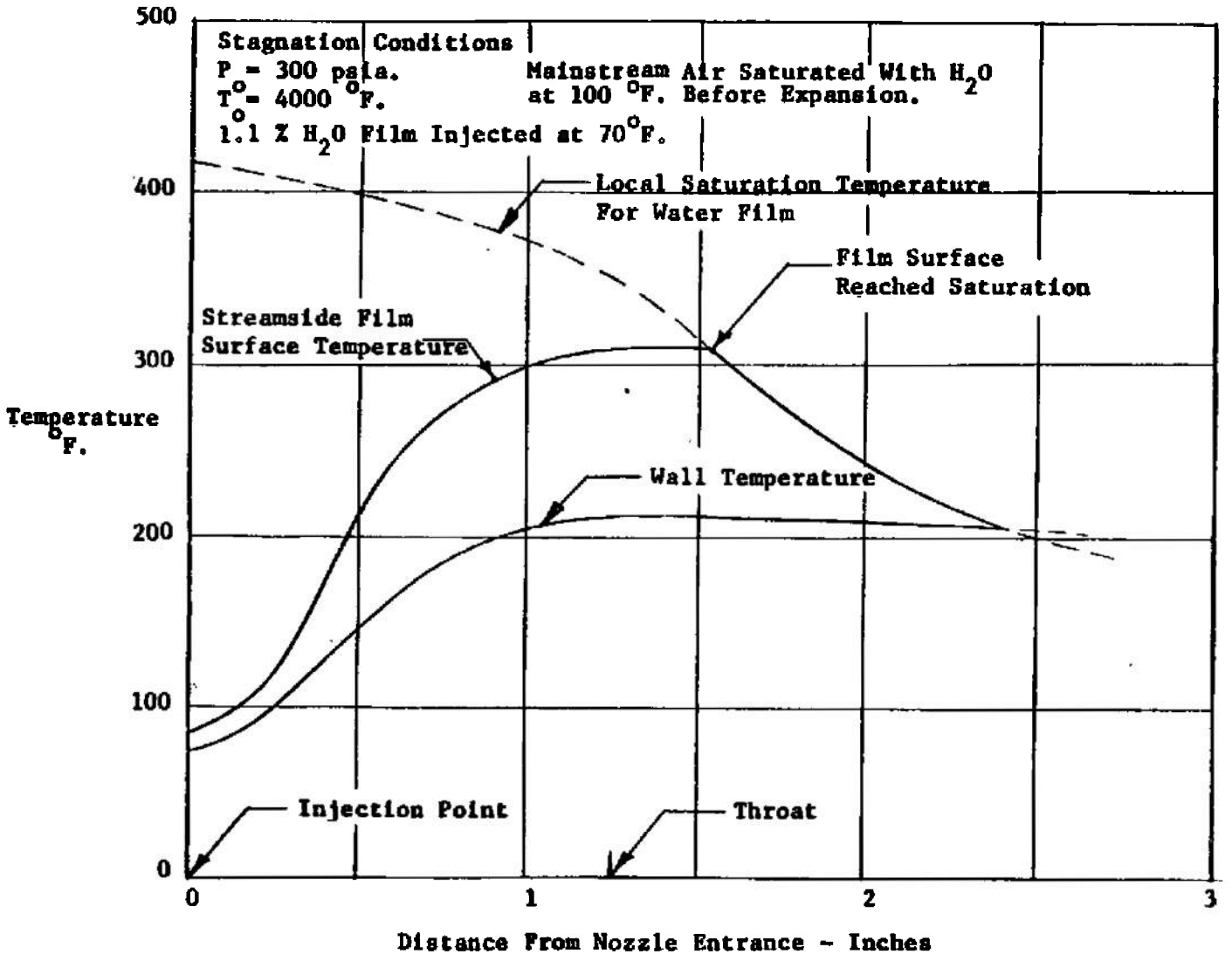

Fig. 25 Graph of Sample Liquid Film Calculation Results

CHAPTER IV
TRANSPIRATION COOLING

I. THEORETICAL ANALYSIS

Transpiration Based on Emmons' Liquid Film Analysis. A careful comparison of liquid film cooling with transpiration cooling shows that they differ in only two ways, namely, in transpiration cooling:

1. There is no liquid film to be transported or to absorb heat.
2. The coolant flow rate may be controlled locally independently of the heat transfer rate.

The basic analysis for liquid film cooling in the locations where boiling occurs may thus be utilized for transpiration cooling.

In the case of transpiration cooling with a liquid it is necessary for the liquid to be vaporized at the surface or before reaching the surface. The best procedure is to specify a local surface temperature which is equal to or greater than the local saturation temperature. The parameter to be calculated is the coolant mass flow rate per unit area required to maintain the surface at the specified temperature. This may be done iteratively using the following procedure:

1,2,3,4. Same as for liquid film cooling.

5. Calculate T_{sat} and set the surface temperature either equal to T_{sat} or to some specified temperature higher than T_{sat}.
6. Starting with the heat transfer rate without transpiration use this to calculate the required rate to hold

the surface at the set temperature.

7. Correct the heat transfer rate for transpiration effects using the procedure outlined for liquid film cooling. Recalculate the required transpiration rate. Repeat this step until either the change in heat transfer rate or the change in transpiration rate meets the set convergence criterion.

8. Increment the axial position and return to step (1).

The procedure is identical for gas transpiration cooling except the calculation of T_{sat} is not required. It has been programmed in Fortran IV language for execution on a digital computer. The program is included in Appendix D.

The same type of calculation may be made using heat transfer rates determined experimentally without transpiration cooling. The changes are the same as those for liquid film cooling except the calculation of film evaporation is not required.

Analysis Based on Gas Film Cooling. The analysis given for gas film cooling may be used for gas transpiration cooling provided it is assumed that the same model may be used in the calculation of eddy diffusivities for both types of cooling. This is done by specifying a very small axial increment for the calculation and a small amount of coolant fluid to be added at each increment. A new coolant stream layer is added whenever the second coolant layer from the nozzle wall contains twice as much fluid as it originally contained. The calculation is performed assuming an adiabatic wall.

II. TRANSPIRATION CALCULATION RESULTS

Since experimental studies of transpiration cooling were not to be performed test cases were postulated in order to check out the analyses.

The results of the calculation using the Liquid or Gas Transpiration Cooling Program are shown graphically in Figure 26. Note that as the calculation proceeds into the nozzle an increasing coolant flow rate is required to hold the nozzle wall at 500 ^{o}F. The calculation was continued only far enough to insure proper operation of the program and convergence of the iterative procedures. The sample computer calculation for this case is given in Appendix F.

The results of a transpiration calculation using the Gas Film Cooling Program are shown graphically in Figure 27. Note the shape of the wall temperature profile curve for a fixed injection rate at each increment. The maximum temperature occurs, as expected, very near the throat. The sample computer calculation for this case is given in Appendix F.

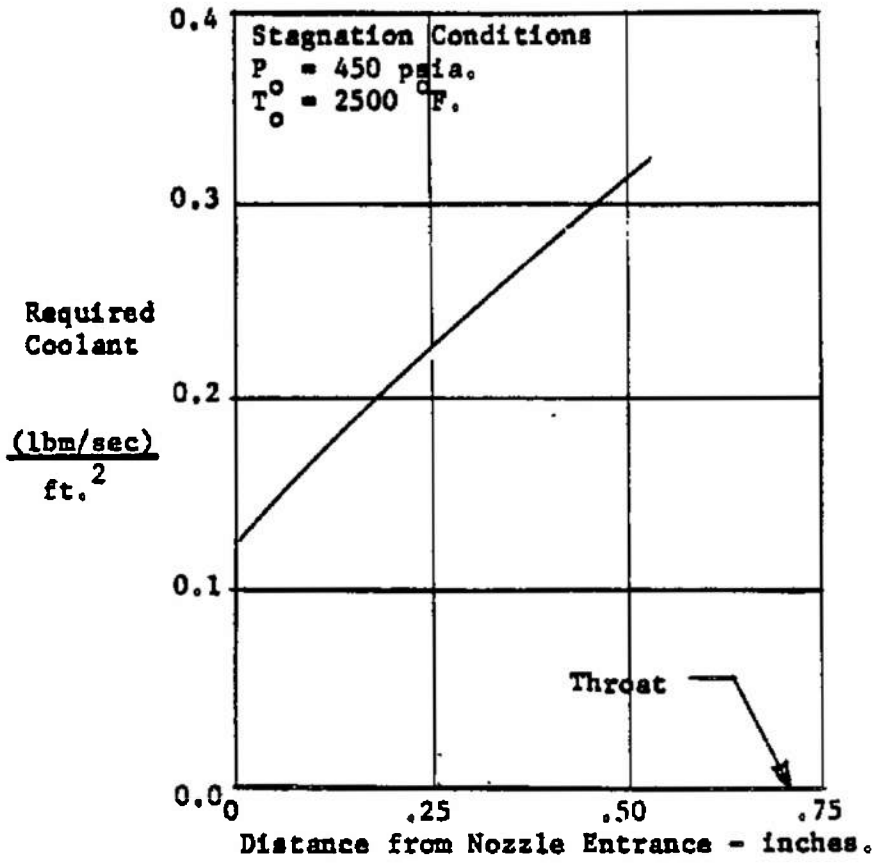

Fig. 26 Graph of Sample Transpiration Calculation Results Using Liquid or Gas Transpiration Cooling Program

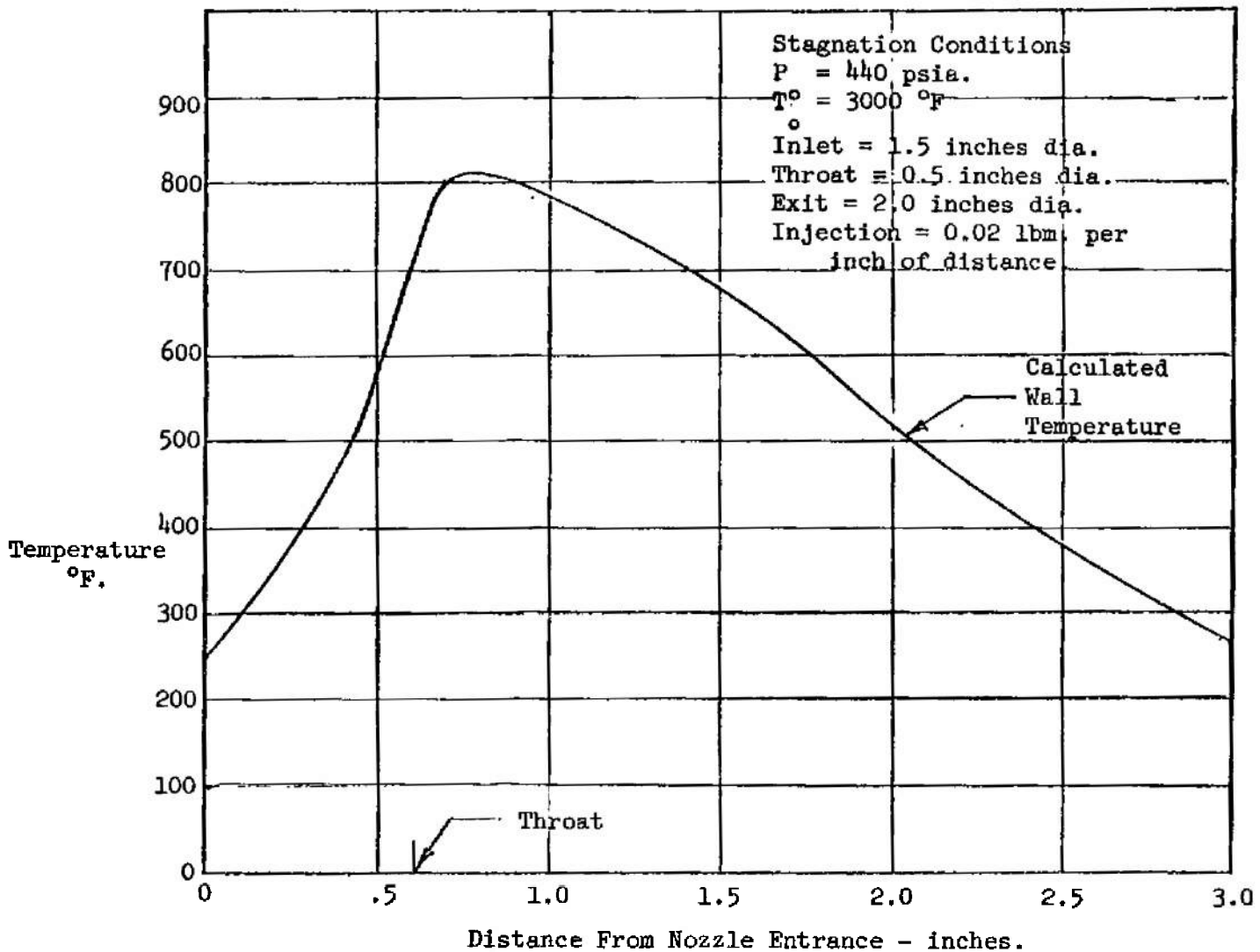

Fig. 27 Graph of Sample Transpiration Calculation Results Using Gas Film Cooling Program

CHAPTER V
CONCLUSIONS AND RECOMMENDATIONS

Based on the experimental results presented and the development of satisfactory calculational techniques to implement the analyses given in the present study, the following conclusions can be drawn:

1. Gas film cooling can be used to measurably lower the wall temperatures and the wall heat fluxes in the converging section and at the throat of a high-pressure high-temperature nozzle. For this nozzle a change of gas film coolant injection ratio from 5% to 10% produced a measurable decrease in the wall temperatures and the wall heat flux up to a point near the throat. Higher gas film cooling ratios, such as 30%, lower the temperature and heat flux in the converging section and at the throat appreciably and have a measurable effect extending into the supersonic expansion section. Some gross mixing occurs at the injection point, the exact amount being as yet some undetermined function of the injection geometry, the relative velocities of the main gas stream and the coolant stream at the injection point, and the entering velocity profiles and turbulence conditions.

2. A straightforward boundary layer type analysis has been developed and programmed which predicts with reasonable accuracy the nozzle wall temperatures and wall heat fluxes in the converging section and at the throat for gas film cooled nozzles. The calculated wall temperatures and heat fluxes using the full amount of film coolant injected in the experiment and the values calculated assuming no film

coolant bracketed the measured values of temperature and heat flux for all cases correlated. The analysis must be modified* in the supersonic portion of the nozzle if accurate prediction of wall temperatures and heat fluxes is required in this region.

3. Calculational techniques have been developed and programmed for predicting the effectiveness of liquid film cooling and liquid or gas transpiration cooling in nozzles. These techniques should be checked against experimental data before they are used for design purposes, however.

It is recommended that gas film cooling experiments in supersonic nozzles be performed with various injection geometries and mainstream to coolant flow velocity ratios in order to evaluate the amount of gross mixing which occurs at injection as some function of these parameters.

It is also recommended that liquid film cooling experiments be performed on a supersonic nozzle operating at high stagnation pressures and temperatures in order to evaluate the accuracy of predictions using the liquid film cooling analysis in the present investigation.

It is further recommended that nozzles fully cooled up to the throat by transpiration be constructed and tested experimentally in order to evaluate the accuracy of predictions using the analyses presented in the present investigation.

---

*A possible modification uses information as shown in Fig. 7-58 of Turbulence by J. O. Hinze, a text published by McGraw-Hill.

BIBLIOGRAPHY

BIBLIOGRAPHY

1. Baron, J. R. "The Binary-Mixture Boundary Layer Associated with Mass Transfer Cooling at High Speeds," Massachusetts Institute of Technology Naval Supersonic Laboratory, Technical Report 160, May, 1956.

2. Bartz, D. R. "A Simple Equation For Rapid Estimation of Rocket Nozzle Convective Heat Transfer Coefficients," Jet Propulsion, Vol. 27, No. 1, January, 1957.

3. Bartz, D. R. "An Approximate Solution of Compressible Turbulent Boundary Layer Development and Convective Heat Transfer in Convergent-Divergent Nozzles," Transactions of the American Society of Mechanical Engineers, November, 1955.

4. Bauer, E., and Zlotnick, M. "Transport Coefficients of Air to 8000 $^{\circ}$K.," Journal of the American Rocket Society, Vol. 29, No. 10, Part 1, October, 1959.

5. Bennett, C. O., and Myers, J. E. Momentum, Heat, and Mass Transfer. New York: McGraw-Hill Book Company, Inc., 1962.

6. Bernicker, R. P. "An Experiment With A Transpiration Cooled Nozzle," Massachusetts Institute of Technology Naval Supersonic Laboratory, Technical Report 447, July, 1960.

7. Bird, R. B., Stewart, W. E., and Lightfoot, E. N. Transport Phenomena. New York: John Wiley and Sons, Inc., 1960.

8. Boden, R. H. "Heat Transfer in Rocket Motors and the Application of Film and Sweat Cooling," Transactions of the American Society of Mechanical Engineers, Vol. 73, 1951.

9. Chin, J. H., et al. "Film Cooling With Multiple Slots and Louvers," Heat Transfer, Vol. 83, August, 1961.

10. Craven, C. W. "A Study of the Wall Cooling Due to Tangential Injection of a Fluid Around the Periphery of an Axially Symmetric Jet," Unpublished Master's Thesis, The University of Tennessee, March, 1963.

11. Crocco, L. "An Approximate Theory of Porous, Sweat, or Film Cooling With Reactive Fluids," Journal of the American Rocket Society, Vol. 22, November-December, 1952.

12. Eckert, E. R. G. "Engineering Relations for Heat Transfer and Friction in High-Velocity Laminar and Turbulent Boundary-Layer Flow Over Surfaces With Constant Pressure and Temperature," Transactions of the American Society of Mechanical Engineers, Vol. 78, 1956.

13. Emmons, D. L. "Effects of Selected Gas Stream Parameters and Coolant Physical Properties on Film Cooling of Rocket Motors," Purdue University Jet Propulsion Center, TM 62-5, August, 1962.

14. Eschenback, R. C., and Skinner, G. M. "Development of Stable, High Pressure Arc Air Heaters For a Hypersonic Wind Tunnel," Wright Air Development Division, Technical Report 61-100, July, 1961.

15. Grabau, M. "A Method of Forming Empirical Equations for the Thermodynamic Properties of Air From Ambient Temperatures to 15,000 K., With Applications." Arnold Engineering Development Center, AEDC-TN-59-102, August, 1959.

16. Graham, A. R., and Zucrow, M. J. "Film Cooling, Its Theory and Applications," Report No. TM-57-3, Contract N70NR39418, Purdue University, October, 1957.

17. Hatch, J. E., and Papell, S. S. "Use of a Theoretical Flow Model to Correlate Data for Film Cooling or Heating an Adiabatic Wall by Tangential Injection of Gases of Different Fluid Properties", NASA TN D-130, November, 1959.

18. Hartnett, J. C., Birkekak, R. C., and Eckert, E. R. C. "Velocity Distributions, Temperature Distributions, Effectiveness, and Heat Transfer for Air Injected through a Tangential Slot into a Turbulent Boundary Layer," Journal of Heat Transfer, Vol. 83, Series C, No. 3, August, 1961.

19. Hermann, R., Melnik, W. L., and Staukevics, J. O. "Research on Evaporative Film Cooling of a Mach Number 7 Contoured Wind Tunnel Nozzle in the Rosemont Aeronautical Laboratories Hypersonic Facility," Wright Air Development Division, Technical Report 60-251, May, 1960.

20. Hyman, S., et al. "Transpiration and Film Cooling for Solid Propellant Rocket Nozzles," United Nuclear Corporation, NDAA 2150-1, February, 1961.

21. Knuth, E. "The Mechanics of Film Cooling - Part 1," Jet Propulsion, Vol. 24, No. 6, November-December, 1954.

22. Knuth, E. "The Mechanics of Film Cooling - Part 2," Jet Propulsion, Vol. 25, No. 1, January, 1955.

23. Libby, P. A., and Pallone, A. A. "A Method For Analyzing the Heat Insulating Properties of the Laminar Compressible Boundary Layer," Journal of the Aeronautical Sciences, Vol. 21, No. 12, 1954.

24. Librizzi, J., and Cresci, R. J. "Transpiration Cooling of a Turbulent Boundary Layer in an Axisymmetric Nozzle," Wright-Patterson Air Force Base Aeronautical Research Laboratories, ARL 63-103, June, 1963.

25. Lieu, B. H. "Air-Film Cooling of a Supersonic Nozzle," United States Naval Ordnance Laboratory, White Oak, Maryland, Research Report No. 224, August, 1964.

26. Mayer, E., and Bartas, J. C. "Transpiration Cooling in Porous Metal Walls," Jet Propulsion, Vol. 24, No. 6, November-December, 1954.

27. Pasqua, P. F., et al. "Analytical Studies on Nozzle Throat Cooling." Arnold Engineering Development Center, Technical Documentary Report, AEDC-TDR-63-58, April, 1963.

28. Ragent, B., and Noble, C. E. "High Temperature Transport Coefficients of Selected Gases," Wright Patterson Air Force Base, Contract AF 33(616)-8338, April, 1962.

29. Rannie, W. D. "Heat Transfer in Turbulent Shear Flow," Journal of the Aeronautical Sciences, Vol. 25, No. 5, May, 1956.

30. Ranz, W. E. "Mass and Heat Transfer for Large Gradients of Concentration and Temperature," ORR Project No. 2340, Technical Report No. 1, March, 1962.

31. Rubesin, M. W. "An Analytical Estimation of the Effect of Transpiration Cooling on the Heat Transfer and Skin-friction Characteristics of a Compressible, Turbulent Boundary Layer," National Advisory Committee for Aeronautics, TN 3341, December, 1954.

32. Scala, S. M., and Baulknight, C. E. "Transport and Thermodynamic Properties in a Hypersonic Boundary Layer. Part 1 - Properties of the Pure Species," Journal of the American Rocket Society, Vol. 29, No. 1, January, 1959.

33. Schlichting, H. Boundary Layer Theory. New York: McGraw-Hill Book Company, Inc., 1960.

34. Seban, R. A., and Back, L. H. "Velocity and Temperature Profiles in Turbulent Boundary Layers With Tangetial Injection," Journal of Heat Transfer, Vol. 84, Series C., No. 1, February, 1962.

35. Seban, R. A., and Back, L. H. "Effectiveness for a Turbulent Boundary Layer With Tangential Injection and Variable Free Stream Velocity," Journal of Heat Transfer, Vol. 84, Series C, No. 3, March, 1962.

36. Shapiro, A. H. The Dynamics and Thermodynamics of Compressible Fluid Flow. Vol. 1. New York: The Ronald Press Co., 1954.

37. Stanton, R. G. Numerical Methods For Science and Engineering. Englewood Cliffs, New Jersey: Prentice-Hall, Inc., June, 1961.

38. Steward, J. D. "Transpiration Cooling: An Engineering Approach," General Electric, Technical Information Series No. R595D338, May, 1959.

39. Townsend, A. A. Structure of Turbulent Shear Flow. London, England: Cambridge University Press, 1956.

40. Turcotte, D. L. "A Sublayer Theory for Fluid Injection into the Incompressible Turbulent Boundary Layer," Journal of the Aerospace Sciences, Vol. 27, No. 9, September, 1960.

41. Wheeler, H. L., and Duwez, P. "Heat Transfer Through Sweat Cooled Porous Tubes," Jet Propulsion, Vol. 25, No. 10, October, 1955.

42. Back, L. H., Massier, P. F., Gier, H. C. "Convective Heat Transfer in a Convergent-Divergent Nozzle (Revision No. 1)", Technical Report No. 32-415, Jet Propulsion Laboratory, California Institute of Technology. Feb. 15, 1965.

APPENDIXES

APPENDIX A
NOTATION

A	nozzle cross sectional area or incremental heat transfer area
A_*	nozzle throat cross sectional area
$\bar{\bar{A}}$	two-dimensional coefficient matrix
$\bar{B}$	column matrix
b	Turcotte's constant to correct diffusivity for mass injection
C	constant
c_p	specific heat at constant pressure
c_*	sonic velocity at nozzle throat
c_w	heat capacity of fluid in layer at wall
D	nozzle inside diameter
D_{AB}	binary mass diffusivity
D_*	nozzle throat inside diameter
D_t	nozzle throat inside diameter
d_n	liquid coolant layer thickness
d_l	local nozzle liner thickness
f_{ni}	friction factor with no injection or evaporation
g_c	gravitational constant
h	convective heat transfer coefficient
h_{fg}	enthalpy of evaporation
h_M	coefficient of mass transfer
J	Joules constant = 778 ft lb/Btu
k	ratio of specific heats, c_p/c_v
k_l	nozzle liner thermal conductivity
k_H	thermal conductivity
k_M	"conductivity" of mass

M	Mach number
M_A	molecular weight of species A
M_B	molecular weight of species B
Nu	Nusselt's number
P_o	stagnation pressure
p_1	pressure at increment entrance
p_2	pressure at increment exit
Pr	Prandtl's number
Q	liquid film evaporation rate
Q_s	energy stored in increment of liquid film
Re	Reynold's number
r	radius
r_c	radius of curvature of nozzle throat
r_i	inside radius of nozzle
Sc	Schmidt number
St	Stanton's number
T	temperature
T_g	temperature of gas stream
T_o	stagnation temperature
T_r	recovery temperature
T_s	temperature at liquid film surface
T_{sat}	saturation temperature, coolant vapor
T_w	wall temperature
$\bar{T}$	column temperature matrix
T_{Adw}	adiabatic wall temperature
t	time
u	time averaged velocity in x-direction
u^*	friction velocity $\sqrt{\tau/\rho}$
u^+	dimensionless velocity u/u^*
u_*	gas stream velocity at throat

u_g	gas stream velocity
u_m	stream mean velocity
v	time averaged velocity in the y-direction
W_a	time averaged density of molecular species a
w	mass flow rate
w_w	mass flow rate of coolant layer at the wall
x	axis parallel to nozzle wall
y	axis perpendicular to nozzle wall
y^+	dimensionless y variable yu^*/υ

GREEK

α	molecular diffusivity of heat
Δ	increment length of liquid film cooling analysis
δ_a	molecular diffusivity of mass
ϵ	general diffusivity
ϵ_D	eddy diffusivity of mass
ϵ_H	eddy diffusivity of heat
ϵ_M	eddy diffusivity of momentum
γ	gas density at liquid-gas interface
γ_c	coolant gas partial density
γ_s	mainstream gas partial density
μ	coefficient of viscosity
υ	molecular diffusivity of momentum
ρ	density
ρ_w	density at wall or surface
τ_{ni}	wall shear stress without injection or evaporation
τ_w	wall shear stress
ψ	ratio of diffusivity of heat to diffusivity of momentum
ω	empirical exponent relating viscosity to temperature

APPENDIX B
LIQUID FILM COOLING PROGRAM

```
C     FIRST INPUT CARD 40 BLANKS FOR CASE TITLE.
C     SECOND INPUT CARD
C        F1---F5  COEFFS FOR FILM VISC.,LBM/FT.SEC.
C     THIRD INPUT CARD
C        E1---E5  COEFFS FOR FILM HT. CAP.,B/LBM.F.
C     FOURTH INPUT CARD
C        CN1---CN5  COEFFS FOR FILM COND.,B/HR.FT.F.
C     FIFTH INPUT CARD
C        G1---G5  COEFFS FOR STREAM VISC., LBM/FT.SEC.
C     SIXTH INPUT CARD
C        R1---R5  COEFFS FOR FILM DENS., LBM/CU.FT.
C     SEVENTH INPUT CARD
C        VK1---VK5  COEFFS FOR VAP.COND., B/HR.FT.F.
C     EIGHTH INPUT CARD
C        AK1---AK5  COEFFS FOR STREAM COND., B/HR.FT.F.
C     NINTH INPUT CARD
C        PR1---PR5  COEFFS FOR MAINSTREAM PRANDTL NO.
C     TENTH INPUT CARD
C        PZ = INLET GAS PRESSURE P-ZERO,LB./IN. SQ.
C        TZ = INLET GAS TEMP. T-ZERO, DEGREES F.
C        DT = THROAT DIAMETER D*, INCHES
C        QI=INITIAL COOLANT FLOW RATE,LBM/SEC.
C        TCI = INITIAL COOLANT TEMPERATURE, DEGREES F.
C     ELEVENTH INPUT CARD
C        GK = MAINSTREAM RATIO OF SPECIFIC HEATS.
C        RHZ = INITIAL MAINSTREAM DENSITY, LBM./CU.FT.
C        B = TURCOTTES CONSTANT FOR WALL SHEAR CALCULATION.
C        RG = GAS CONSTANT R AT THROAT CONDITIONS
C         PPZ = INITIAL PARTIAL PRESSURE OF COOLANT, PSI.
C     TWELFTH INPUT CARD
C        WCON = NOZZLE LINER THERMAL CONDUCTIVITY,B/HR.FT.F.
C        WTMOL= MOLECULAR WEIGHT OF THE FILM LIQUID
C        TCOM = CONVERGENCE CRITERION ON TF ITERATION
C        TBN = CRITERION FOR THERMAL BOUNDARY LAYER, DEG. F.
C        DIF = VAPOR-AIR DIFFUSION COEFF., FT.SQ./SEC.
C     THIRTEENTH INPUT CARD
C        DX= DISTANCE INCREMENT, INCHES.
C        SM1= DISTANCE TO NOZZLE THROAT, INCHES
C        QDIV=MAX. FRACTION OF LAYER EVAP. PER SECTION
C        RGC = COOLANT VAPOR GAS CONST. R
C     FOURTEENTH INPUT CARD
C        M2 = MAXIMUM NUMBER OF INCREMENTS.
C        KS = NO. OF TABLE ENTRIES FOR D AND S.
C        N = NUMBER OF FILM LAYERS
C        KPG = NUMBER OF TABLE ENTRIES FOR TSAT,HF, AND HG.
C     NEXT KS CARDS
```

```
C          S--IN., D--IN., WTHCK--IN., HW--B/HR.SQ.FT.F.
C       NEXT KPG CARDS
C          ON EACH CARD IN ORDER AS FOLLOWS--
C          PG--PSIA,  TSAT--DEG. F.,  HF--BTU/LB,  HG--BTU/LB.
C       OUTPUT DESCRIPTION
C          S = DISTANCE ALONG WALL FROM INJECTION, INCHES.
C          Q/A = WALL HEAT LOAD, B/HR.SQ.FT.
C          TB = LOCAL OUTSIDE WALL TEMP.,DEG.F.
C          NBOIL = NUMBER TO SHOW BOILING CONDITION
C             0 = NO BOILING
C             1 = BOILING
C          H = MAINSTREAM CONVECTION COEFF., B/HR.SQ.FT.DEG.F.
C          EXP9 = EXPONENTIAL ATTENUATION FACTOR
C          TF2(NI) = TEMP. OF INSIDE COOLANT LAYER, DEG.F.
C          NI = NUMBER OF INSIDE COOLANT LAYER
  100   FORMAT (1H ,5(E12.3))
  101   FORMAT (1H ,5(I5))
  102   FORMAT (1X,34HPRESSURE EXCEEDS CRITICAL PRESSURE)
  103   FORMAT (5X,4HQRAT,14X,2HQI,15X,5HGFLOW)
  104   FORMAT (1X,F12.8,5X,F12.8,5X,F12.8)
  105   FORMAT (5(E12.3))
  106   FORMAT (1H1,6HOUTPUT)
  107   FORMAT (1H1,34HH. C. ROLAND * LIQUID FILM COOLING)
  108   FORMAT (1H0,10HINPUT DATA)
  109   FORMAT (5(I5))
  110   FORMAT (3(E12.3),3(I4))
  111   FORMAT (1X,40H
  112   FORMAT (1X,3E12.3,3I5)
  113   FORMAT (15HFILM EVAPORATED)
  114   FORMAT (3(F10.5))
  115   FORMAT (1X,3(F10.5))
  116   FORMAT (7X,1HS,12X,3HQ/A,9X,2HTB,5X,5HNBOIL)
  117   FORMAT (1X,25HMAX. DISTANCE IS EXCEEDED)
  118   FORMAT (7X,1HH,12X,4HEXP9,5X,7HTF2(NI),4X,2HNI)
        DIMENSION TF2(21),V(21),FMU(21),RHF(21),TF(21),CF(21),
       1TL(21),CPF(21),RT(21),STAB(40),DTAB(40),WTAB(40),
       2RL(21),QX(21),PGT(40),TSATT(40),HFT(40),HGT(40),
       3HWTAB(40),CT1(21),CT2(21),CT3(21),CT4(21),CT5(21)
 1      S=0.000000001
        READ 111
        READ 105, F1, F2, F3, F4, F5
        READ 105, E1, E2, E3, E4, E5
        READ 105, CN1,CN2,CN3,CN4,CN5
        READ 105, G1, G2, G3, G4, G5
        READ 105, R1, R2, R3, R4, R5
        READ 105, VK1,VK2,VK3,VK4,VK5
        READ 105, AK1,AK2,AK3,AK4,AK5
        READ 105, PR1,PR2,PR3,PR4,PR5
        READ 105, PZ, TZ, DT, Q1  , TCI
        READ 105, GK, RHZ, B, RG , PPZ
```

```
      READ 105, WCON, WTMOL, TCOM, TBN, DIF
      READ 105, DX, SM1, QDIV, RGC
      READ 109, M2, KS, N, NTYPE, KPG
      DO 150 J=1,KS
150   READ 105, STAB(J), DTAB(J), WTAB(J), HWTAB(J)
      DO 200 J=1,KPG
200   READ 105, PGT(J), TSATT(J), HFT(J), HGT(J)
      PUNCH 107
      PUNCH 111
      PUNCH 108
      PUNCH 100,F1,F2,F3,F4,F5
      PUNCH 100, E1, E2, E3, E4, E5
      PUNCH 100,CN1,CN2,CN3,CN4,CN5
      PUNCH 100, G1, G2, G3, G4, G5
      PUNCH 100,R1,R2,R3,R4,R5
      PUNCH 100, VK1,VK2,VK3,VK4,VK5
      PUNCH 100, AK1,AK2,AK3,AK4,AK5
      PUNCH 100,PR1,PR2,PR3,PR4,PR5
      PUNCH 100, PZ, TZ, DT, QI  , TCI
      PUNCH 100, GK, RHZ, B, RG , PPZ
      PUNCH 100,WCON, WTMOL, TCOM, TBN, DIF
      PUNCH 100, DX, SM1, QDIV, RGC
      PUNCH 101, M2, KS, N, NTYPE, KPG
      DO 230 J=1,KS
230   PUNCH 100, STAB(J), DTAB(J), WTAB(J), HWTAB(J)
      DO 195 J=1,KPG
195   PUNCH 100, PGT(J), TSATT(J), HFT(J), HGT(J)
169   EXP2=GK/(GK-1.)
      EXP3=1./(GK-1.)
      EXP4=2./(GK+1.)
      EXP5=(GK-1.)/(GK+1.)
      EXP6=.5/EXP5
      EXP7=2.*EXP5
      EXP9=1.
      DXF=DX/12.
      FN=N
      M=N+1
      QL=QI/FN
      QL2=QL*QDIV
      TSURF=TCI
      NBOIL=0
      NI=1
167   DO 240 J=1,M
      TF(J)=TCI
      TF2(J)=TCI
      QX(J)=QL
      RL(J)=0.
      CT1(J)=0.
      CT2(J)=0.
240   V(J)=0.
```

```
      S=S+DX/2.
      QTOT=0.
      DO 500 I=1,M2
      IF (S-STAB(KS)) 43,9,550
9     D=DTAB(KS)
      WTHCK=WTAB(KS)/12.
      HW=HWTAB(KS)
      GO TO 11
43    DO 6 J=1,KS
      IF (S-STAB(J)) 7,8,6
7     D=DTAB(J-1)+(S-STAB(J-1))*(DTAB(J)-DTAB(J-1))/
     1(STAB(J)-STAB(J-1))
      W=WTAB(J-1)+(S-STAB(J-1))*(WTAB(J)-WTAB(J-1))/
     1(STAB(J)-STAB(J-1))
      WTHCK=W/12.
      HW=HWTAB(J-1)+(S-STAB(J-1))*(HWTAB(J)-HWTAB(J-1))/
     1(STAB(J)-STAB(J-1))
      GO TO 11
8     D=DTAB(J)
      WTHCK=WTAB(J)/12.
      HW=HWTAB(J)
      GO TO 11
6     CONTINUE
11    DRAT=D/DT
      D=D*.083333
      VRAT1=1.
      IF (S-SM1) 12,12,13
12    VM=((EXP4+EXP5*(VRAT1**2))**EXP6)/(DRAT**2)
      GO TO 14
13    VM=SQRT(((VRAT1*(DRAT**2))**EXP7-EXP4)/EXP5)
14    VCRIT=.002*VM
      VCOM=ABS(VM-VRAT1)
      IF (VCOM-VCRIT) 16,16,15
15    VRAT1=VM
      IF (S-SM1) 12,12,13
16    PAR=1.+((GK-1.)/2.)*(VM**2)
      TG=(TZ+460.)/PAR
      TGS=TG-460.
      RHG=RHZ/(PAR**EXP3)
      VG=VM*((GK*32.2*RG*TG)**.5)
      IF (S-SM1) 30,30,31
30    TGM=(TG+TSURF+460.)/2.+.22*.445*TG*(GK-1.)*(VM**2)
      TGM=TGM-460.
      TG=TG*(1.+.445*(GK-1.)*(VM**2))
      TG=TG-460.
      GO TO 32
31    TGM=(TG+TSURF+460.)/2.+.22*.430*TG*(GK-1.)*(VM**2)
      TGM=TGM-460.
      TG=TG*(1.+.430*(GK-1.)*(VM**2))
      TG=TG-460.
```

```
32    PG=PZ/(PAR**EXP2)
26    IF (PG-PGT(KPG)) 84,499,499
84    CONTINUE
      DO 19 J=1,KPG
      IF (PG-PGT(J)) 18,17,19
17    TSAT=TSATT(J)
      HFS=HFT(J)
      HG=HGT(J)
      GO TO 20
18    PRAT=(PG-PGT(J-1))/(PGT(J)-PGT(J-1))
      TSAT=TSATT(J-1)+PRAT*(TSATT(J)-TSATT(J-1))
      HFS=HFT(J-1)+PRAT*(HFT(J)-HFT(J-1))
      HG=HGT(J-1)+PRAT*(HGT(J)-HGT(J-1))
      GO TO 20
19    CONTINUE
20    CONTINUE
      DO 680 J=1,KPG
      IF (TF2(NI)-TSATT(J)) 681,682,680
682   PPRES = PGT(J)
      HFGP=HGT(J)-HFT(J)
      GO TO 683
681   TRAT=(TF2(NI)-TSATT(J-1))/(TSATT(J)-TSATT(J-1))
      HFSP=HFT(J-1)+TRAT*(HFT(J)-HFT(J-1))
      HGP=HGT(J-1)+TRAT*(HGT(J)-HGT(J-1))
      HFGP=HGP-HFSP
      GO TO 683
680   CONTINUE
683   CONTINUE
      AK=AK1+AK2*TGM+AK3*TGM**2+AK4*TGM**3+AK5*TGM**4
      GMU = G1+G2*TGM+G3*TGM**2+G4*TGM**3+G5*TGM**4
      PRG=PR1+PR2*TGM+PR3*TGM**2+PR4*TGM**3+PR5*TGM**4
      VK=VK1+VK2*TGM+VK3*TGM**2+VK4*TGM**3+VK5*TGM**4
      CON=AK
      RHV=144.*PG*WTMOL/(1545.*(TSAT+460.))
      REG=(RHG*VG*D)/GMU
      DA=3.142*D*DXF
      DMF=DIF*(((TGM+460.)/530.)**1.5)*(14.7/PG)
      SCN=GMU/(RHG*DMF)
      IF (I-1) 21,21,22
21    GFLOW=      RHG*VG*.785*(D**2)
      QRAT=QI/GFLOW
      PUNCH 106
      PUNCH 103
      PUNCH 104, QRAT, QI, GFLOW
22    TW1=.0265*(RHG/32.2)*(VG**2)/(REG**.2)
      H=.0265*CON*(REG**.8)*(PRG**.333)*EXP9/D
      RHST=QTOT/(.785*D**2*VG)
      PPST=RHST*RGC*(TG+460.)/144.
      IF (NBOIL) 690,690,25
690   QEV5=H*(TG-TF2(NI))/(HFGP*3600.)
```

```
      QEV=QEV5
      HMASS=H*DMF/CON
      RHOS=QEV5/HMASS
      PPRES=PPST+RHOS*RGC*TF2(NI)/144.
      DO 940 J=1,KPG
      IF (PPRES -PGT(J)) 941,941,940
941   PRAT=(PPRES-PGT(J-1))/(PGT(J)-PGT(J-1))
      TF2(NI)=TSATT(J-1)+PRAT*(TSATT(J)-TSATT(J-1))
      GO TO 942
940   CONTINUE
942   QTOT=QTOT+QEV*DA
      PRINT 105, PPST, RHST, QTOT, PPRES
      QX(NI)=QX(NI)-QEV*DA
      IF (QX(NI)) 990,990,25
990   MI=NI+1
      QX(MI)=QX(MI)+QX(NI)
      NI=NI+1
25    NCT=1
      NCT3=0
141   NCT2=0
      TW=TW1
      LX=M-NI
      DO 62 J=1,LX
      L=M-J
      TM=(TF(L)+TF2(L))/2.
      C2=TM
      C3=TM**2
      C4=C2*C3
      C5=C3*C3
      C6=C3*C4
      FMU(L)=F1/C3+F2/C2+F3+F4*C2+F5*C3
      FMU(L)=FMU(L)/32.2
      RHF(L)=R1+R2*C2+R3*C3+R4*C4+R5*C5
      CF(L)=CN1+CN2*C2+CN3*C3+CN4*C4+CN5*C5
      CPF(L)=E1+E2*C2+E3*C3+E4*C4+E5*C5
      AV=1.571*D*RHF(L)*TW/FMU(L)
      BV=3.142*D*V(L+1)*RHF(L)
      CV=-QX(L)
      TL(L)=(-BV+SQRT((BV**2)-4.*AV*CV))/(2.*AV)
      V(L)=V(L+1)+TL(L)*TW/FMU(L)
      IF (L-N) 63,64,64
64    RL(L)=TL(N)/(2.*CF(N)*DA)+WTHCK/(WCON*DA)+1./(HW*DA)
      GO TO 62
63    RL(L)=TL(L)/(2.*CF(L)*DA)+TL(L+1)/(2.*CF(L+1)*DA)
62    CONTINUE
82    NCT=1
      DO 80 J=NI,N
      J1=J-1
      J2=J+1
      IF (NBOIL) 405,405,407
```

```
407   TF2(NI)=TSAT
      GO TO 80
405   IF (J-NI) 96,96,70
96    TF2(NI)=TSET
      GO TO 80
70    IF (NCT2-1) 700,701,701
700   CT1(J)=1./(QX(J)*7200.*CPF(J)*RL(J1))
      CT2(J)=1./(QX(J)*7200.*CPF(J)*RL(J))
      CT3(J)=1.+CT1(J)+CT2(J)
      CT4(J)=CT1(J)/CT3(J)
      CT5(J)=CT2(J)/CT3(J)
701   TFCOM=TF2(J)
      TF2(J)=TF(J)/CT3(J)+CT4(J)*(TF2(J1)+TF(J1)-TF(J))
     1+CT5(J)*(TF2(J2)+TF(J2)-TF(J))
74    TCT=ABS(TF2(J)-TFCOM)
      IF (TCT-TCOM) 80,80,76
76    NCT=NCT+1
80    CONTINUE
      NCT2=NCT2+1
      IF (NCT2-10) 89,141,141
89    IF (NCT-1) 81,81,82
81    IF (NCT3) 87,87,92
87    NCT3=1
      GO TO 141
92    IF (NBOIL) 408,408,409
409   QST=0.
      DO 410 J=NI,N
410   QST=QST+QX(J)*CPF(J)*(TF2(J)-TF(J))
      QWT=(TF(N)+TF2(N)-2.*TCI)/(7200.*RL(N))
      TW=TW1*EXP9
      UST=(TW*32.2/RHV)**.5
      HM1=.0265*DMF*(REG**.8)*(SCN**.333)*EXP9/D
      QEV1=((H*(TG-TSAT)/3600.)-QST/DA-QWT/DA)/(HG-HFS)
422   GMAS=(PG*144.-QEV1*RGC*(TSAT+460.)/HM1)/(RG*
     1(TSAT+460.))
      EXP9=EXP(-13.89*QEV1/(B*UST*(QEV1/HM1+GMAS)))
      HM=.0265*DMF*(REG**.8)*(SCN**.333)*EXP9/D
      IF ( ABS(HM-HM1)-.02*HM) 420,420,421
421   HM1=HM
      TW=TW1*EXP9
      UST=(TW*32.2/RHV)**.5
      GO TO 422
420   CONTINUE
436   H1=.0265*CON*(REG**.8)*(PRG**.333)*EXP9/D
      QEV=((H1*(TG-TSAT)/3600.)-QST/DA-QWT/DA)/(HG-HFS)
      GMA=QEV/HM
      PV=GMA*1545.*(TSAT+460.)/(144.*WTMOL)
      IF (PV-PG) 430,431,431
431   PV=PG
      GV=PV*144./(RGC*(TSAT+460.))
```

```
      GVM=GV/2.
      PVM=GVM*RGC*(TGM+460.)/144.
      PSM=PG-PVM
      GSM=PSM*144./(RG*(TGM+460.))
      GVM=GVM*RGC/1545.
      GSM=GSM*RG/1545.
      XC=GVM/(GVM+GSM)
      XS=GSM/(GVM+GSM)
      CON=XC*VK+XS*AK
      H=.0265*CON*(REG**.8)*(PRG**.333)*EXP9/D
      QEV=((H *(TG-TSAT)/3600.)-QST/DA-QWT/DA)/(HG-HFS)
      GO TO 432
430   GVM=GMA/2.
      PVM=GVM*RGC*(TGM+460.)/144.
      PSM=PG-PVM
      GSM=PSM*144./(RG*(TGM+460.))
      GVM=GVM*RGC/1545.
      GSM=GSM*RG/1545.
      XC=GVM/(GVM+GSM)
      XS=GSM/(GVM+GSM)
      CON2=XC*VK+XS*AK
      H=H1*CON2/CON
      IF (ABS(H-H1)-.02*H) 432,432,434
434   CON=CON2
      GO TO 436
432   IF (ABS(QEV-QEV1)-.02*QEV) 495,495,494
494   QEV1=QEV
      GO TO 422
495   QT=QEV*(3.14*D*DXF)
      IF (QT-QL2) 440,440,441
441   S=S-(1.-QL2/QT)*DX
      DX=QL2*DX/QT
      DXF=DX/12.
      DO 443 J=NI,N
443   TF2(J)=TF(J)+(QL2/QT)*(TF2(J)-TF(J))
      QT=QL2
440   IF (QT-QX(NI)) 446,447,448
446   QX(NI)=QX(NI)-QT
      GO TO 300
447   QX(NI)=0.
      NI=NI+1
      IF (NI-N) 300,300,575
448   QEX=QT-QX(NI)
      QX(NI)=0.
      NI=NI+1
      QX(NI)=QX(NI)-QEX
      IF (NI-N) 300,300,575
408   IF (TF2(NI)-TSAT) 300,302,302
302   RAT=(TSAT-TF(NI))/(TF2(NI)-TF(NI))
      NBOIL=1
```

```
      DO 305 J=NI,N
305   TF2(J)=TF(J)+RAT*(TF2(J)-TF(J))
      S=S-DX+RAT*DX
300   TM=(TF2(N)+TF(N))/2.
      QA=(TM-TCI)/(RL(N)*DA)
      TB=TCI+QA/HW
      PUNCH 116
      PUNCH 112, S, QA, TB, NBOIL
      PUNCH 118
      PUNCH 112, H, EXP9,TF2(NI),NI
      S=S+DX
450   DO 455 J=NI,N
      TDIF=TF2(J)-TF(J)
      TF(J)=TF2(J)
455   TF2(J)=TF(J)+TDIF
500   CONTINUE
      GO TO 1
499   PUNCH 102
      GO TO 1
575   PUNCH 113
      GO TO 1
550   PUNCH 117
      GO TO 1
      END
```

APPENDIX C
GAS FILM COOLING COMPUTER PROGRAM

```
C      FIRST INPUT CARD 40 BLANKS FOR CASE TITLE.
C      SECOND DATA INPUT CARD
C         PZ = INLET GAS PRESSURE, LB./SQ.IN.
C         TZ = INLET GAS TEMPERATURE, DEGREES F.
C         DT = THROAT INSIDE DIAMETER, INCHES.
C         N = NUMBER OF COOLANT LAYERS
C         M = INITIAL NUMBER OF STREAM LAYERS
C         NSH = NO. TO SPECIFY TYPE WALL SHEAR CALCULATION.
C            0 = WALL SHEAR FROM BLASIUS EQUATION.
C            1 = WALL SHEAR FROM PREVIOUS INCREMENT PROFILE.
C      THIRD DATA INPUT CARD
C         GK = GAS CONSTANT, CP/CV
C         RHZ = INITIAL GAS DENSITY, LBM./CU.FT.
C         QRAT1 = INJECTION RATIO AT ENTRANCE
C         QRAT2 = SECOND INJECTION RATIO
C         QRAT3 = THIRD INJECTION RATIO
C      FOURTH DATA INPUT CARD
C         RG = GAS CONSTANT R
C         WCON = LINER THERMAL CONDUCTIVITY,B/HR.FT.DEG.F.
C         PR = PRANDTL NO. OF COOLANT GAS.
C         M2 = MAX. NO. OF INCREMENTS
C         KS = NO. OF TABLE ENTRIES FOR D AND WTHCK FROM S.
C         NT = NO. TO DESIGNATE TYPE WALL COOLING
C            0 = BACKSIDE COOLED
C            1 = ADIABATIC WALL
C      FIFTH DATA INPUT CARD
C         DX = DISTANCE INCREMENT, INCHES
C         EHM = RATIO OF THERMAL TO MOMENTUM DIFFUSIVITIES
C         SM1 = DISTANCE TO NOZZLE THROAT, INCHES
C         NTYPE = CASE TYPE
C            0 = SINGLE INJECTION
C            1 = MULTIPLE INJECTION
C            2 = INJECTION AT EACH INCREMENT
C         NI1 = INCREMENT NO. FOR SECOND INJECTION
C         NI2 = INCREMENT NUMBER FOR THIRD INJECTION
C      SIXTH DATA INPUT CARD
C         RGC = COOLANT GAS CONSTANT R.
C         GAP = COOLANT INPUT SLOT WIDTH, INCHES
C         VCRIT = CONVERGENCE CRITERION ON ITERATIONS
C         QINJ = INJECTION RATIO AT ENTRANCE
C         VINJ = INJECTION VELOCITY
C      SEVENTH DATA INPUT CARD
C         TCI = INITIAL COOLANT TEMPERATURE, DEGREES F,
C         DXPT = DISTANCE BETWEEN PRINTOUTS, INCHES
C      EIGHTH DATA INPUT CARD
```

```
C          AK1---AK5  COEFFS FOR AK (MOLECULAR),B/HR.FT.DEG.F.
C       NINTH DATA INPUT CARD
C          G1---G5  COOLANT GMU COEFFS(MOLECULAR),LBM/HR.FT.
C       TENTH DATA INPUT CARD
C          V1---V5  STREAM GMU COEFFS(MOLECULAR),LBM/HR.FT.
C       ELEVENTH DATA INPUT CARD
C          CS1---CS5  COEFFS FOR CPS, B/LBM.DEG.F.
C       TWELFTH DATA INPUT CARD
C          CC1---CC5  COEFFS FOR CPC, B/LBM.DEG.F.
C       THIRTEENTH DATA INPUT CARD
C          NPT = CONTROL NUMBER FOR PRINTOUT
C              0 = VELOCITY AND TEMPERATURE PROFILES PRINTED
C              1 = NO PROFILE PRINTOUT
C       NEXT KS INPUT CARDS.
C          S--IN.,  D--IN.,  WTHCK--IN.,  HW--B./HR.SQ.FT.F.
C       NEXT N INPUT CARDS
C          VC1---FT./SEC.   TC1---DEG. F.
C       NEXT M INPUT CARDS
C          VS1---FT./SEC.   TS1---DEG. F.
C       OUTPUT DESCRIPTION
C          QINJ = COOLANT INJECTION RATE,LBM/SEC.
C          GFLOW = MAINSTREAM FLOW RATE, LBM/SEC.
C          S = DISTANCE ALONG LINER, INCHES.
C          TSURF = LINER SURFACE TEMPERATURE, DEG.F.
C          Q/A = HEAT TRANSFER RATE TO LINER, B/HR.SQIN.
C          DISP.THCK. = DISPLACEMENT THICKNESS AT S, INCHES.
       DIMENSION STAB(60),DTAB(60),WTAB(60),TC1(60),TS1(20),
      1TC2(60),TS2(20),DC(60),DS(20),QS(20),QC(60),VS1(20),
      2VS2(20),VC1(60),VC2(60),RHS(20),RHC(60),EDS(20),
      3EDC(60),DIC(60),DIS(20),CPC(60),CPS(20),AC(60),BC(60),
      4AS(20),BS(20),EC(60),ES(20),FC(60),FS(20),PC(60),
      5PS(20),DYC(60),DYS(20),YC(60),YS(20),HWTAB(60)
  100  FORMAT (5X,4HQINJ,16X,5HGFLOW)
  101  FORMAT (5X,1HS,9X,5HTSURF,9X,3HQ/A,6X,10HDISP.THCK.)
  102  FORMAT (5(E12.3))
  103  FORMAT (1H0,10HINPUT DATA)
  104  FORMAT (3E12.3,3I5)
  105  FORMAT (F12.5,8X,F12.5)
  106  FORMAT (1H1,6HOUTPUT)
  107  FORMAT (1H1,31HH. C. ROLAND * GAS FILM COOLING)
  108  FORMAT (1X,19HADIABATIC WALL CASE)
  109  FORMAT (1X,20HBACKSIDE COOLED CASE)
  110  FORMAT(1X,40H
  111  FORMAT (1H ,5(E12.3))
  112  FORMAT (1X,3E12.3,3I5)
  113  FORMAT (1X,30HWALL SHEAR FROM PAST INCREMENT)
  114  FORMAT (1X,32HWALL SHEAR FROM BLASIUS EQUATION)
  115  FORMAT (3F10.5)
  116  FORMAT (1H ,3F10.5)
```

```
117   FORMAT (1X,25HMAX. DISTANCE IS EXCEEDED)
118   FORMAT (1X,16HSINGLE INJECTION)
119   FORMAT (1X,18HMULTIPLE INJECTION)
120   FORMAT (1X,27HINJECTION AT EACH INCREMENT)
621   FORMAT (1X,6(E12.3))
140   FORMAT (1X,35HTRANSPIRATION WITH BACKSIDE COOLING)
640   FORMAT (I5)
647   FORMAT (1X,I5)
990   FORMAT (1X,22HQI IS LESS THAN 2QC(N))
998   FORMAT (1H ,I5,5X,E12.3)
1     S=.0000000001
      SPT=0.0
      READ    110
      READ    104, PZ, TZ, DT, N, M, NSH
      READ    102, GK, RHZ, QRAT1, QRAT2, QRAT3
      READ    104, RG, WCON, PR, M2, KS, NT
      READ 104, DX, EHM, SM1, NTYPE, NI1, NI2
      READ    102, RGC, GAP, VCRIT, QINJ, VINJ
      READ    102, TCI, DXPT
      READ    102, AK1, AK2, AK3, AK4, AK5
      READ    102, G1, G2, G3, G4, G5
      READ    102, V1, V2, V3, V4, V5
      READ    102, CS1, CS2, CS3, CS4, CS5
      READ    102, CC1, CC2, CC3, CC4, CC5
      READ 640, NPT
      PRINT 107
      PUNCH 107
      PRINT  110
      PUNCH 110
      IF (NSH) 572,572,573
572   PRINT 114
      PUNCH 114
      GO TO 574
573   PRINT 113
      PUNCH 113
574   IF (NT) 570,570,575
570   PRINT 109
      PUNCH 109
      GO TO 580
575   PRINT 108
      PUNCH 108
580   IF (NTYPE-1) 820,825,830
820   PRINT 118
      PUNCH 118
      GO TO 850
825   PRINT 119
      PUNCH 119
      GO TO 850
830   IF (NT) 150,150,151
```

```
151   PRINT 120
      PUNCH 120
850   PRINT 103
      PUNCH 103
      PRINT  112, PZ, TZ, DT, N, M, NSH
      PRINT  111, GK, RHZ, QRAT1, QRAT2, QRAT3
      PRINT  112, RG, WCON,-PR, M2, KS, NT
      PRINT  112, DX, EHM, SM1, NTYPE, NI1, NI2
      PRINT  111, RGC, GAP, VCRIT, QINJ, VINJ
      PRINT  111, TCI, DXPT
      PRINT  111, AK1, AK2, AK3, AK4, AK5
      PRINT  111, G1, G2, G3, G4, G5
      PRINT  111, V1, V2, V3, V4, V5
      PRINT  111, CS1, CS2, CS3, CS4, CS5
      PRINT  111, CC1, CC2, CC3, CC4, CC5
      PRINT  647, NPT
      PUNCH  112, PZ, TZ, DT, N, M, NSH
      PUNCH  111, GK, RHZ, QRAT1, QRAT2, QRAT3
      PUNCH  112, RG, WCON, PR, M2, KS, NT
      PUNCH  112, DX, EHM, SM1, NTYPE, NI1, NI2
      PUNCH  111, RGC, GAP, VCRIT, QINJ, VINJ
      PUNCH  111, TCI, DXPT
      PUNCH  111, AK1, AK2, AK3, AK4, AK5
      PUNCH  111, G1, G2, G3, G4, G5
      PUNCH  111, V1, V2, V3, V4, V5
      PUNCH  111, CS1, CS2, CS3, CS4, CS5
      PUNCH  111, CC1, CC2, CC3, CC4, CC5
      PUNCH  647, NPT
      DO 4 J=1,KS
2     READ 102, STAB(J), DTAB(J), WTAB(J), HWTAB(J)
      PUNCH 111, STAB(J), DTAB(J), WTAB(J), HWTAB(J)
4     PRINT 111, STAB(J), DTAB(J), WTAB(J), HWTAB(J)
      DO 904 J=1,N
902   READ 102, VC1(J), TC1(J)
      PUNCH 111, VC1(J), TC1(J)
904   PRINT 111, VC1(J), TC1(J)
      DO 905 J=1,M
903   READ 102, VS1(J), TS1(J)
      PUNCH 111, VS1(J), TS1(J)
905   PRINT 111, VS1(J), TS1(J)
      GK1=GK-1.
      GK2=GK+1.
      EXP2=GK/GK1
      EXP3=1./GK1
      EXP4=2./GK2
      EXP5=GK1/GK2
      EXP6=.5/EXP5
      EXP7=2.*EXP5
      CINJ=CC1+CC2*TCI+CC3*TCI**2+CC4*TCI**3+CC5*TCI**4
```

```
      TCRIT=VCRIT
      ML=M-1
      DO 500 I=1,M2
      NI=I
 65   DI=DX
      IF (S-STAB(KS)) 5,5,550
 5    DO 6 J=1,2
      IF (S-STAB(KS)) 43,9,550
 9    D=DTAB(KS)
      WTHCK=WTAB(KS)*.083333
      HW=HWTAB(KS)
      GO TO 11
 43   DO 26 K=1,KS
      K1=K-1
      IF (S-STAB(K)) 17,18,26
 17   D=DTAB(K1)+(S-STAB(K1))*(DTAB(K)-DTAB(K1))/(STAB(K)-
     1STAB(K1))
      WTHCK=(WTAB(K1)+(S-STAB(K1))*(WTAB(K)-WTAB(K1))/
     1(STAB(K)-STAB(K1)))*.083333
      HW=HWTAB(K1)+(S-STAB(K1))*(HWTAB(K)-HWTAB(K1))/
     1(STAB(K)-STAB(K1))
      GO TO 11
 18   D=DTAB(K)
      WTHCK=WTAB(K)*.083333
      HW=HWTAB(K)
      GO TO 11
 26   CONTINUE
 11   DRAT=D/DT
      D=D*.083333
      VRAT1=1.
      IF (S-SM1) 12,12,13
 12   VM=((EXP4+EXP5*(VRAT1**2))**EXP6)/(DRAT**2)
      GO TO 14
 13   VM=SQRT(((VRAT1*(DRAT**2))**EXP7-EXP4)/EXP5)
 14   VCOMP=.002*VM
      VCOM=ABS(VM-VRAT1)
      IF (VCOM-VCOMP) 16,16,15
 15   VRAT1=VM
      IF (S-SM1) 12,12,13
 16   PAR=1.+.5*GK1*(VM**2)
      TG=(TZ+460.)/PAR
      TGS=TG
      RHG=RHZ/(PAR**EXP3)
      VG=VM*((GK*32.2*RG*TG)**.5)
      IF (S-SM1) 30,30,31
 30   TGM=(TG+TC1(N)+460.)*.5+.22*.445*TG*GK1* VM**2)
      TG=TG*(1.+.445*GK1*(VM**2))
      GO TO 32
 31   TGM=(TG+TC1(N)+460.)*.5+.22*.430*TG*GK1*(VM**2)
```

```
      TG=TG*(1.+.430*GK1*(VM**2))
32    PG=PZ/(PAR**EXP2)
      IF (J-1) 7,7,8
7     PG1=PG
      TG1=TG-460.
      TGS1=TGS-460.
      TGM1=TGM-460.
      VG1=VG
      RHG1=RHG
      D1=D
      WTHCK1=WTHCK
      IF (NTYPE-1) 940,943,635
943   IF (NI-NI1) 940,941,942
941   S=S+DI/5.
      SI=S-DI/10.
      GO TO 6
942   IF (NI-NI1-5) 941,941,944
944   IF (NI-NI2) 635,941,946
946   IF (NI-NI2-5) 941,941,635
940   IF (NI-5) 630,630,635
630   S=S+DI/5.
      SI=S-DI/10.
      GO TO 6
635   S=S+D1
      SI=S-D1/2.
      GO TO 6
8     PG2=PG
      TG2=TG-460.
      TGS2=TGS-460.
      TGM2=TGM-460.
      VG2=VG
      RHG2=RHG
      D2=D
      WTHCK2=WTHCK
6     CONTINUE
      IF (NI-1) 71,71,72
71    GFLOW=RHG2*VG2*.785*(D2**2)
      QI=QRAT1*GFLOW
      PRINT 106
      PRINT 100
      PRINT 105, QI, GFLOW
      PUNCH 106
      PUNCH 100
      PUNCH 105, QI, GFLOW
      PUNCH 101
      IF (NPT) 72,72,672
672   PRINT 101
72    RHG=(RHG1+RHG2)/2.
      PG=(PG1+PG2)/2.
```

```
      TG=(TG1+TG2)/2.
      VG=(VG1+VG2)/2.
      TGM=(TGM1+TGM2)/2.
      RHINJ=PG*144./(RGC*(TCI+460.))
      D=(D1+D2)/2.
      WTHCK=(WTHCK1+WTHCK2)/2.
      RHGC=PG*144./(RGC*(TGM+460.))
      GNUS = (V1/TGM+V2+V3*TGM)/(3600.*RHGC)
      QI=QRAT1*GFLOW
      REG=VG*D/GNUS
      IF (NI-1) 610,610,605
605   IF (NSH) 610,610,615
610   TSS=.053*RHG*(VG**2)/(64.4*REG**.2)
      GO TO 620
615   TSS=2.*EDC(N)*VC2(N)*RHC(N)/(32.2*DC(N))
620   USTS=SQRT(TSS*32.2/RHGC)
      DO 10 J=1,M
      IF (NI-1). 35,35,36
35    RHS(J)=PG*144./(RG*(TS1(J)+460.))
      CPS(J)=CS1+CS2*TS1(J)+CS3*TS1(J)**2+CS4*TS1(J)**3+
     1CS5*TS1(J)**4
      TS2(J)=TS1(J)
      VS2(J)=VS1(J)
      GO TO 10
36    TDIF=TS2(J)-TS1(J)
      TS1(J)=TS2(J)
      TS2(J)=TS1(J)+TDIF
      CPS(J)=CS1+CS2*TS1(J)+CS3*TS1(J)**2+CS4*TS1(J)**3+
     1CS5*TS1(J)**4
      RHS(J)=PG*144./(RG*(TS1(J)+460.))
      VDIF=VS2(J)-VS1(J)
      VS1(J)=VS2(J)
      VS2(J)=VS1(J)+VDIF
10    CONTINUE
      TS1(M)=TGS1
      TS2(M)=TGS2
      VS2(M)=VG2
      DO 33 J=1,N
      IF (NI-1) 81,81,93
81    RHC(J)=PG*144./(RGC*(TC1(J)+460.))
      CPC(J)=CC1+CC2*TC1(J)+CC3*TC1(J)**2+CC4*TC1(J)**3+
     1CC5*TC1(J)**4
      TC2(J)=TC1(J)
      VC2(J)=VC1(J)
      GO TO 33
93    TDIF=TC2(J)-TC1(J)
      TC1(J)=TC2(J)
      TC2(J)=TC1(J)+TDIF
```

```
      CPC(J)=CC1+CC2*TC1(J)+CC3*TC1(J)**2+CC4*TC1(J)**3+
     1CC5*TC1(J)**4
      RHC(J)=PG*144./(RGC*(TC1(J)+460.))
      VDIF=VC2(J)-VC1(J)
      VC1(J)=VC2(J)
      VC2(J)=VC1(J)+VDIF
33    CONTINUE
      NL=N-1
      FNL=NL
      IF (NI-1) 19,19,760
19    VC1(N)=5.*USTS
      DIC(N)=D
      DC(N)=10.*GNUS/USTS
      YC(N)=DC(N)/2.
      QC(N)=RHC(N)*3.142*DIC(N)*DC(N)*VC1(N)
      IF (QI-2.*QC(N)) 910,911,911
911   QL=(QI-QC(N))/FNL
      DO 50 J=1,NL
50    QC(J)=QL
      DO 21 J=1,M
21    QS(J)=2.*QC(1)
      GO TO 53
760   DC(N)=10.*GNUS/USTS
      YC(N)=DC(N)/2.
      DIC(N)=D
      QCOM=RHC(N)*3.142*DIC(N)*DC(N)*VC1(N)
      IF (NTYPE-1) 20,921,777
921   IF (NI-NI1) 20,777,926
777   QINJ=GFLOW*QRAT2
      GO TO 924
926   IF (NI-NI2) 20,778,20
778   QINJ=GFLOW*QRAT3
924   IF (QINJ-QCOM) 983,927,927
983   QEX=QINJ+QC(N)-QCOM
      IF (QEX) 986,987,987
986   CPST=(QC(N)*CPC(N)+QINJ*CINJ-QEX*CPC(NL))/QCOM
      RHC(N)=(QC(N)*RHC(N)+QINJ*RHINJ-QEX*RHC(NL))/QCOM
      VC1(N)=(QC(N)*VC1(N)+QINJ*VINJ-QEX*VC1(NL))/QCOM
      TC1(N)=(QC(N)*TC1(N)*CPC(N)+QINJ*CINJ*TCI-
     1QEX*TC1(NL)*CPC(NL))/(QCOM*CPST)
      CPC(N)=CPST
      GO TO 988
987   QST=QC(NL)+QEX
      CPST=(QEX*CPC(N)+QC(NL)*CPC(NL))/QST
      RHC(NL)=(QEX*RHC(N)+QC(NL)*RHC(NL))/QST
      VC1(NL)=(QEX*VC1(N)+QC(NL)*VC1(NL))/QST
      TC1(NL)=(QEX*CPC(N)*TC1(N)+QC(NL)*CPC(NL)*TC1(NL))/
     1(QST*CPC(NL))
      CPC(NL)=CPST
```

```
      CPC(N)=(QINJ*CINJ+(QC(N)-QEX)*CPC(N))/QCOM
      RHC(N)=(QINJ*RHINJ+(QC(N)-QEX)*RHC(N))/QCOM
      VC1(N)=(QINJ*VINJ+(QC(N)-QEX)*VC1(N))/QCOM
      TC1(N)=(QINJ*CINJ*TCI+(QC(N)-QEX)*CPC(N)*TC1(N))/
     1(QCOM*CPC(N))
  988 QC(NL)=QC(NL)+QEX
      QC(N)=QCOM
      IF (QC(NL)/QC(1)-2.) 53,861,861
  861 M5=N+1
      TC1(M5)=TC1(N)
      TC2(M5)=TC2(N)
      VC1(M5)=VC1(N)
      VC2(M5)=VC2(N)
      QC(M5)=QC(N)
      CPC(M5)=CPC(N)
      RHC(M5)=RHC(N)
      DIC(M5)=D
      DC(M5)=DC(N)
      QC(NL)=QC(NL)/2.
      TC1(N)=TC1(NL)
      TC2(N)=TC2(NL)
      VC1(N)=VC1(NL)
      VC2(N)=VC2(NL)
      QC(N)=QC(NL)
      CPC(N)=CPC(NL)
      RHC(N)=RHC(NL)
      N=M5
      NL=N-1
      GO TO 53
  928 QST=QC(NL)+QC(N)+QEX
      CPST=QC(NL)*CPC(NL)+QC(N)*CPC(N)+QEX*CINJ
      TC1(NL)=(QC(NL)*CPC(NL)*TC1(NL)+QC(N)*CPC(N)*TC1(N)+
     1QEX*CINJ*TCI)/CPST
      TC2(NL)=TC1(NL)
      VC1(NL)=(QC(NL)*VC1(NL)+QC(N)*VC1(N)+QEX*VINJ)/QST
      VC2(NL)=VC1(NL)
      CPC(NL)=CPST/QST
      RHC(NL)=(QC(NL)*RHC(NL)+QC(N)*RHC(N)+QEX*RHINJ)/QST
      QC(NL)=QST
      IF (QC(NL)/QC(1)-2.) 795,851,851
  851 QC(NL)=QC(NL)/2.
      TC1(N)=TC1(NL)
      TC2(N)=TC2(NL)
      VC1(N)=VC1(NL)
      VC2(N)=VC2(NL)
      QC(N)=QC(NL)
      CPC(N)=CPC(NL)
      RHC(N)=RHC(NL)
      M5=N+1
```

```
      DIC(M5)=D
      DC(M5)=DC(N)
      N=M5
      NL=N-1
795   QC(N)=QCOM
      TC1(N)=TCI
      TC2(N)=TCI
      RHC(N)=RHINJ
      CPC(N)=CINJ
      VC1(N)=VINJ
      VC2(N)=VINJ
      GO TO 53
927   QEX=QINJ-QCOM
      NXL=QEX/QC(1)
      FNXL=NXL
      IF (NXL) 928,928,123
123   QST=QC(NL)+QC(N)
      CPST=(QC(NL)*CPC(NL)+QC(N)*CPC(N))/QST
      RHC(NL)=(QC(NL)*RHC(NL)+QC(N)*RHC(N))/QST
      TC1(NL)=(QC(NL)*CPC(NL)*TC1(NL)+QC(N)*CPC(N)*TC1(N))/
     1(QST*CPST)
      VC1(NL)=(QC(NL)*VC1(NL)+QC(N)*VC1(N))/QST
      QC(NL)=QST
      CPC(NL)=CPST
      M5=N+NXL
      DO 85 J=N,M5
      QC(J)=QEX/FNXL
      RHC(J)=RHINJ
      TC1(J)=TCI
      TC2(J)=TCI
      VC1(J)=VINJ
      VC2(J)=VINJ
      CPC(J)=CINJ
85    CONTINUE
      QC(M5)=QCOM
      DC(M5)=DC(N)
      DIC(M5)=D
      N=M5
      NL=N-1
      GO TO 53
20    QC(NL)=QC(NL)+QC(N)-QCOM
      QC(N)=QCOM
53    EDC(N)=(G1+G2*TC1(N)+G3*TC1(N)**2+G4*TC1(N)**3+G5*
     1TC1(N)**4)/(3600.*RHC(N))
      DO 24 J=1,NL
      JL=N-J
      JL1=JL+1
      DIC(JL)=DIC(JL1)-2.*DC(JL1)
      DC(JL)=QC(JL)/(RHC(JL)*3.142*DIC(JL)*VC1(JL))
```

```
      YC(JL)=YC(JL1)+DC(JL1)/2.+DC(JL)/2.
 24   EDC(JL)=.4*USTS*YC(JL)
 810  DO 75 J=1,M
      J1=J-1
      IF (J1) 22,22,23
 22   DIS(J)=DIC(1)-2.*DC(1)
      DS(J)=QS(J)/(RHS(J)*3.142*DIS(J)*VS1(J))
      YS(J)=YC(1)+DC(1)/2.+DS(J)/2.
      GO TO 75
 23   DIS(J)=DIS(J1)-2.*DS(J1)
      DS(J)=QS(J)/(RHS(J)*3.142*DIS(J)*VS1(J))
      YS(J)=YS(J1)+DS(J1)/2.+DS(J)/2.
 75   EDS(J)=.4*USTS*YS(J)
 812  NIT=0
 63   NCT=0
      DO 34 J=1,N
      J1=J-1
      J2=J+1
      VCOM=VC2(J)
      IF (NIT) 51,51,52
 51   PC(J)=3.142*DIC(J)*DC(J)*(PG1-PG2)*72.*(1.+(D2/D1)**2)
 52   IF (J1 ) 37,37,38
 37   IF (NIT) 61,61,62
 61   AC(J)=3.142*(DI/12.)*DIS(J)/(32.2*(DS(J)/(RHS(J)*
     1EDS(J))+DC(J)/(RHC(J)*EDC(J))))
      BC(J)=3.142*(DI/12.)*DIC(J)/(32.2*(DC(J1/(RHC(J)*
     1EDC(J))+DC(J2)/(RHC(J2)*EDC(J2))))
 62   VC2(J)=(QC(J)*VC1(J)/32.2+AC(J)*(VS1(J)+VS2(J)-VC1(J))
     1+BC(J)*(VC1(J2)+VC2(J2)-VC1(J))+PC(J))/(QC(J)/32.2
     2+AC(J)+BC(J))
      IF (VC2(J)-VG2) 300,300,301
 301  VC2(J)=VG2
 300  IF (ABS(VC2(J)-VCOM)-VCRIT*VC2(J)) 34,34,39
 38   IF (J-N) 41,42,42
 41   IF (NIT).171,171,172
 171  AC(J)=.2618*DI*DIC(J1)/(32.2*(DC(J1)/(RHC(J1)*EDS(J1))
     1+DC(J)/(RHC(J)*EDC(J))))
      BC(J)=3.142*(DI/12.)*DIC(J)/(32.2*(DC(J)/(RHC(J)*
     1EDC(J))+DC(J2)/(RHC(J2)*EDC(J2))))
 172  VC2(J)=(QC(J)*VC1(J)/32.2+AC(J)*(VC1(J1)+VC2(J1)-
     1VC1(J))+BC(J)*(VC1(J2)+VC2(J2)-VC1(J))+PC(J))/
     2(QC(J)/32.2+AC(J)+BC(J))
      IF (VC2(J)-VG2) 302,302,303
 303  VC2(J)=VG2
 302  IF (ABS(VC2(J)-VCOM)-VCRIT*VC2(J)) 34,34,39
 42   IF (NIT) 181,181,182
 181  AC(J)=.2618*DI*DIC(J1)/(32.2*(DC(J1)/(RHC(J1)*EDC(J1))
     1+DC(J)/(RHC(J)*EDC(J))))
      BC(J)=3.142*(DI/12.)*DIC(J)/(32.2*(DC(J)/(RHC(J)*
```

```
     1EDC(J))))
182   VC2(J)=(QC(J)*VC1(J)/32.2+AC(J)*(VC1(J1)+VC2(J1)-
     1VC1(J))-BC(J)*VC1(J)+PC(J))/(QC(J)/32.2+AC(J)+BC(J))
      IF (VC2(J)-VG2) 304,304,305
305   VC2(J)=VG2
304   IF (ABS(VC2(J)-VCOM)-VCRIT*VC2(J)) 34,34,39
39    NCT=NCT+1
34    CONTINUE
816   DO 70 J=1,ML
      J1=J-1
      J2=J+1
      VCOM=VS2(J)
      IF (NIT) 91,91,92
91    PS(J)=3.142*DIS(J)*DS(J)*(PG1-PG2)*72.*(1.+(D2/D1)**2)
92    IF (J1 ) 88,88,89
88    IF (NIT) 121,121,122
121   AS(J)=.2618*DI*DIS(J2)/(32.2*(DS(J2)/(RHS(J2)*EDS(J2))
     1+DS(J)/(RHS(J)*EDS(J))))
      BS(J)=3.142*(DI/12.)*DIS(J)/(32.2*(DS(J)/(RHS(J)*
     1EDS(J))+DC(J)/(RHC(J)*EDC(J))))
122   VS2(J)=(QS(J)*VS1(J)/32.2+AS(J)*(VS1(J2 )+VS2(J2 )-
     1VS1(J))+BS(J)*(VC1(J)+VC2(J)-VS1(J))+PS(J))/(QS(J)/
     232.2+AS(J)+BS(J))
      IF (VS2(J)-VG2) 306,306,307
307   VS2(J)=VG2
306   IF (ABS(VS2(J)-VCOM)-VCRIT*VS2(J)) 70,70,69
89    IF (NIT) 131,131,132
131   AS(J)=.2618*DI*DIS(J2)/(32.2*(DS(J2)/(RHS(J2)*EDS(J2))
     1    +DS(J)/(RHS(J)*EDS(J))))
      BS(J)=3.142*(DI/12.)*DIS(J)/(32.2*(DS(J)/(RHS(J)*
     1EDS(J))+DS(J1)/(RHS(J1)*EDS(J1))))
132   VS2(J)=(QS(J)*VS1(J)/32.2+AS(J)*(VS1(J2 )+VS2(J2 )-
     1VS1(J))+BS(J)*(VS1(J1)+VS2(J1)-VS1(J))+PS(J))/
     2(QS(J)/32.2+AS(J)+BS(J))
      IF (VS2(J)-VG2) 308,308,309
309   VS2(J)=VG2
308   IF (ABS(VS2(J)-VCOM)-VCRIT*VS2(J)) 70,70,69
69    NCT=NCT+1
70    CONTINUE
818   NIT=NCT
      IF (NCT) 80,80,63
80    CONTINUE
      NIT=0
213   NCT=0
      DO 205 J=1,N
      J1=J-1
      J2=J+1
      TCOM=TC2(J)
      IF (J1 ) 215,215,220
```

```
215   IF (NIT) 216,216,217
216   AC(J)=.2618*DI*DIS(J)/(DS(J)/(RHS(J)*EHM*EDS(J)*
     1CPS(J))+DC(J)/(RHC(J)*EHM*EDC(J)*CPC(J)))
      BC(J)=3.142*(DI/12.)*DIC(J)/(DC(J)/(RHC(J)*EHM*EDC(J)*
     1CPC(J))+DC(J2)/(RHC(J2)*EHM*EDC(J2)*CPC(J2)))
      EC(J)=QC(J)*(VC1(J)**2-VC2(J)**2)/(2.*778.*32.2)
      FC(J)=(.2618*DI*DIC(J)*DC(J)*RHC(J)*EDC(J)/(4.*778.*
     132.2))*((VS1(J)+VS2(J)-VC1(J2)-VC2(J2))/(DC(J)+
     2DC(J2)/2.+DS(J)/2.))**2
217   TC2(J)=(TC1(J)*(QC(J)*CPC(J)-AC(J)-BC(J))+AC(J)*
     1(TS1(J)+TS2(J))+BC(J)*(TC1(J2)+TC2(J2))+EC(J)+FC(J))
     2/(QC(J)*CPC(J)+AC(J)+BC(J))
      IF (ABS(TC2(J)-TCOM)-TCRIT*TC2(J)) 205,205,235
220   IF (J-N) 221,222,222
221   IF (NIT) 223,223,224
223   AC(J)=.2618*DI*DIC(J1 )/(DC(J1 )/(RHC(J1 )*EHM*EDC(J1)
     1*CPC(J1 ))+DC(J)/(RHC(J)*EHM*EDC(J)*CPC(J)))
      BC(J)=3.142*(DI/12.)*DIC(J)/(DC(J)/(RHC(J)*EHM*EDC(J)*
     1CPC(J))+DC(J2)/(RHC(J2)*EHM*EDC(J2)*CPC(J2)))
      EC(J)=QC(J)*(VC1(J)**2-VC2(J)**2)/(2.*778.*32.2)
      FC(J)=(.2618*DI*DIC(J)*DC(J)*RHC(J)*EDC(J)/(4.*778.*
     132.2))*((VC1(J1)+VC2(J1)-VC1(J2)-VC2(J2))/(DC(J)
     2+DC(J2)/2.+DC(J1)/2.))**2
224   TC2(J)=(TC1(J)*(QC(J)*CPC(J)-AC(J)-BC(J))+AC(J)*
     1(TC1(J1)+TC2(J1))+BC(J)*(TC1(J2)+TC2(J2))+EC(J)+FC(J))
     2/(QC(J)*CPC(J)+AC(J)+BC(J))
      IF (ABS(TC2(J)-TCOM)-TCRIT*TC2(J)) 205,205,235
222   IF (NIT) 225,225,226
225   AC(J)=.2618*DI*DIC(J1)/(DC(J1)/(RHC(J1)*EHM*EDC(J1)
     1    *CPC(J1))+DC(J)*PR/(RHC(J)*EDC(J)*CPC(J)))
      IF (NT) 450,450,455
450   BC(J)=.2618*DI*DIC(J)/(DC(J)*PR/(RHC(J)*EDC(J)*CPC(J))
     1+3600.*WTHCK/WCON+3600./HW)
      GO TO 460
455   BC(J)=0.
460   EC(J)=QC(J)*(VC1(J)**2-VC2(J)**2)/(2.*778.*32.2)
      FC(J)=(.2618*DI*DIC(J)*DC(J)*RHC(J)*EDC(J)/(4.*778.*
     132.2))*((VC1(J)+VC2(J))/(DC(J)/2.))**2
226   TC2(J)=(TC1(J)*(QC(J)*CPC(J)-AC(J)-BC(J))+AC(J)*
     1(TC1(J1)+TC2(J1))+BC(J)*(2.*TC1)+EC(J)+FC(J))/
     2(QC(J)*CPC(J)+AC(J)+BC(J))
      IF (ABS(TC2(J)-TCOM)-TCRIT*TC2(J)) 205,205,235
235   NCT=NCT+1
205   CONTINUE
821   DO 280 J=1,ML
      J1=J-1
      J2=J+1
      TCOM=TS2(J)
      IF (J1 ) 241,241,242
```

```
241   IF (NIT) 243,243,244
243   AS(J)=.2618*DI*DIS(J2 )/(DS(J2 )/(RHS(J2 )*EHM*EDS(J2)
     1*CPS(J2))+DS(J)/(RHS(J)*EHM*EDS(J)*CPS(J)))
      BS(J)=3.142*(DI/12.)*DIS(J)/(DS(J)/(RHS(J)*EHM*EDS(J)*
     1CPS(J))+DC(J)/(RHC(J)*EHM*EDC(J)*CPC(J)))
      ES(J)=QS(J)*(VS1(J)**2-VS2(J)**2)/(2.*778.*32.2)
      FS(J)=(.2168*DI*DIS(J)*DS(J)*RHS(J)*EDS(J)/(4.*778.*
     132.2))*((VS1(J2)+VS2(J2)-VC1(J)-VC2(J))/(DS(J)+DS(J2)
     2/2.+DC(J)/2.))**2
244   TS2(J)=(TS1(J)*(QS(J)*CPS(J)-AS(J)-BS(J))+AS(J)*
     1(TS1(J2)+TS2(J2))+BS(J)*(TC1(J)+TC2(J))+ES(J)+FS(J))/
     2(QS(J)*CPS(J)+AS(J)+BS(J))
      IF (ABS(TS2(J)-TCOM)-TCRIT*TS2(J)) 280,280,279
242   IF (NIT) 247,247,248
247   AS(J)=.2618*DI*DIS(J2 )/(DS(J2 )/(RHS(J2 )*EHM*EDS(J2)
     1*CPS(J2))+DS(J)/(RHS(J)*EHM*EDS(J)*CPS(J)))
      BS(J)=3.142*(DI/12.)*DIS(J)/(DS(J)/(RHS(J)*EHM*EDS(J)*
     1CPS(J))+DS(J1)/(RHS(J1)*EHM*EDS(J1)*CPS(J1)))
      ES(J)=QS(J)*(VS1(J)**2-VS2(J)**2)/(2.*778.*32.2)
      FS(J)=(.2168*DI*DIS(J)*DS(J)*RHS(J)*EDS(J)/(4.*778.*
     132.2))*((VS1(J2)+VS2(J2)-VS1(J1)-VS2(J1))/(DS(J)+
     2DS(J2)/2.+DS(J1)/2.))**2
248   TS2(J)=(TS1(J)*(QS(J)*CPS(J)-AS(J)-BS(J))+AS(J)*
     1(TS1(J2)+TS2(J2))+BS(J)*(TS1(J1)+TS2(J1))+ES(J)+FS(J))
     2/(QS(J)*CPS(J)+AS(J)+BS(J))
      IF (ABS(TS2(J)-TCOM)-TCRIT*TS2(J)) 280,280,279
279   NCT=NCT+1
280   CONTINUE
826   NIT=NCT
      IF (NCT) 290,290,213
290   CONTINUE
      TAV=.5*(TC1(N)+TC2(N))
      IF (NT) 410,410,420
410   CON1=PR*DC(N)/(EDC(N)*CPC(N)*RHC(N)*7200.)
      CON2=WTHCK/WCON
      CON3=1./HW
      QA=(TAV-TC1)/((CON1+CON2+CON3)*144.)
      TSURF=TC1+QA*(CON2+CON3)*144.
      GO TO 426
420   TSURF=TAV
      QA=0.
426   NL=N-1
      DYC(N)=6.*DC(N)
      DO 660 J=1,NL
      JL=N-J
      JL1=JL+1
660   DYC(JL)=DYC(JL1)+6.*DC(JL1)+6.*DC(JL)
      DO 670 J=1,M
      J1=J-1
```

```
      IF (J1) 675,675,680
675   DYS(J)=DYC(1)+6.*DC(1)+6.*DS(1)
      GO TO 670
680   DYS(J)=DYS(J1)+6.*DS(J1)+6.*DS(J)
670   CONTINUE
      DSPTK=DYC(1)+6.*DC(1)
      DO 720 J=1,M
720   DSPTK=DSPTK+(1.-RHS(J)*VS2(J)/(RHG2*VG2))*DIS(J)*12.*
     1DS(J)/DIS(1)
      IF (NPT) 641,641,642
641   IF (SI-SPT) 500,501,501
501   PRINT 621, TC2
      PRINT 621, VC2
      PRINT 621, QC
      PRINT 101
642   IF (SI-SPT) 500,502,502
502   PRINT 102, SI, TSURF, QA, DSPTK
      PUNCH 102, SI, TSURF, QA, DSPTK
      SPT=SPT+DXPT
500   CONTINUE
550   PRINT 117
      GO TO 995
910   PRINT 990
      GO TO 995
150   PRINT 140
995   GO TO 1
      END
```

APPENDIX D
TRANSPIRATION COOLING COMPUTER PROGRAM

```
C     FIRST INPUT CARD 40 BLANKS FOR CASE TITLE.
C     SECOND INPUT CARD
C        G1---G5  COEFFS FOR STREAM VISC.,LBM/FT.SEC.
C     THIRD INPUT CARD
C        VK1---VK5  COEFFS FOR VAP.COND.,B/HR.FT.F.
C     FOURTH INPUT CARD
C        AK1---AK5  COEFFS FOR STREAM COND.,B/HR.FT.F.
C     FIFTH INPUT CARD
C        PR1---PR5  COEFFS FOR STREAM PRANDTL NO.
C     SIXTH INPUT CARD
C        PZ = INLET GAS PRESSURE P-ZERO,LB/IN.SQ.
C        TZ = INLET GAS TEMP.T-ZERO,DEG.F.
C        DT = THROAT DIAMETER D*, INCHES.
C        TSURF = SPECIFIED SURFACE TEMP
C        CPL = HEAT CAPACITY OF TRANSP. LIQ.,B/LBM.F.
C     SEVENTH INPUT CARD
C        GK = MAINSTREAM RATIO OF SPECIFIC HEATS
C        RHZ = INITIAL MAINSTREAM DENSITY,LBM/CU.FT.
C        B = TURCOTTES CONSTANT FOR WALL SHEAR CALC.
C        RG = STREAM GAS CONSTANT R.
C        CPV = HEAT CAPACITY OF TRANSP.GAS OR VAP.,B/LBM.F.
C     EIGHTH INPUT CARD
C        WTMOL = COOLANT MOLECULAR WEIGHT.
C        DIF = COOLANT-AIR DIFFUSION COEFF.,FT.SQ./SEC.
C        DX = DISTANCE INCREMENT, INCHES.
C        SM1 = DISTANCE TO NOZZLE THROAT, INCHES.
C     NINTH INPUT CARD
C        M2 = MAXIMUM NUMBER OF INCREMENTS.
C        KS = NO. OF TABLE ENTRIES FOR D AND S.
C        KPG = NO. OF TABLE ENTRIES FOR TSAT,HF,HG.
C        NTYPE = CASE TYPE NUMBER
C           0 = GAS TRANSPIRATION
C           1 = LIQUID TRANSPIRATION
C     NEXT KS CARDS
C        ON EACH CARD IN ORDER AS FOLLOWS
C        S--INCHES, D--INCHES, WTHCK--INCHES.
C     NEXT KPG CARDS
C        ON EACH CARD IN ORDER AS FOLLOWS
C        PG--PSIA, TSAT--DEG.F., HF--BTU/LB, HG--BTU/LB.
C     OUTPUT DESCRIPTION
C        S = DISTANCE ALONG WALL FROM INJECTION, INCHES.
C        QEV = INJECTION RATE REQUIRED,(LBM/SEC)/SQ.FT.
C        QTOT = TOTAL INJECTION TO S, LBM/SEC.
C        QRAT = RATIO OF QTOT/(GAS FLOW) TO S.
C        TG = MAINSTREAM STATIC TEMPERATURE, DEG. F.
C        PG = LOCAL STATIC PRESSURE, PSIA.
```

```
C         EXP9 = EXPONECTIAL ATTENUATION FACTOR.
  100  FORMAT (1H ,5(E12.3))
  101  FORMAT (1H ,5(I5))
  102  FORMAT (1X,34HPRESSURE EXCEEDS CRITICAL PRESSURE)
  103  FORMAT (1X,20HLIQUID COOLANT TABLE)
  104  FORMAT (1X,12HNOZZLE TABLE)
  105  FORMAT (5(E12.3))
  106  FORMAT (1H1,6HOUTPUT)
  107  FORMAT(1H1,39HH. C. ROLAND*LIQ. AND GAS TRANSPIRATION)
  108  FORMAT (1H0,10HINPUT DATA)
  109  FORMAT (5(I5))
  110  FORMAT (3(E12.3), 3(I5))
  111  FORMAT (1X,40H                                          )
  112  FORMAT (1X,34HINCOMPATIBLE--TSURF LESS THAN TSAT)
  113  FORMAT (7X,1HS,11X,3HQEV,9X,4HQTOT,8X,4HQRAT)
  114  FORMAT (1H0,5X,5HGFLOW)
  115  FORMAT (7X,2HTG,10X,2HPG,9X,4HEXP9)
  117  FORMAT (1X,25HMAX. DISTANCE IS EXCEEDED)
       DIMENSION STAB(40),DTAB(40),WTAB(40),PGT(40),TSATT(40),
      1HFT(40),HGT(40)
    1  S=0.0000000001
       READ 111
       READ   105, G1, G2, G3, G4, G5
       READ   105, VK1, VK2, VK3, VK4, VK5
       READ   105, AK1, AK2, AK3, AK4, AK5
       READ   105, PR1, PR2, PR3, PR4, PR5
       READ   105, PZ,TZ,DT,TSURF,CPL
       READ   105, GK, RHZ, B, RG, CPV
       READ   105, WTMOL, DIF, DX, SM1
       READ   109, M2, KS, KPG ,NTYPE
       DO 200 J=1,KS
  200  READ 105, STAB(J), DTAB(J), WTAB(J)
       DO 201 J=1,KPG
  201  READ 105, PGT(J), TSATT(J), HFT(J), HGT(J)
       PUNCH 107
       PUNCH 111
       PUNCH 108
       PUNCH  100, G1, G2, G3, G4, G5
       PUNCH  100, VK1, VK2, VK3, VK4, VK5
       PUNCH 100, AK1, AK2, AK3, AK4, AK5
       PUNCH 100, PR1, PR2, PR3, PR4, PR5
       PUNCH 100, PZ, TZ, DT, TSURF,CPL
       PUNCH  100, GK, RHZ, B, RG ,CPV
       PUNCH  100, WTMOL, DIF, DX, SM1
       PUNCH  101, M2, KS, KPG ,NTYPE
       PUNCH 104
       DO 202 J=1,KS
  202  PUNCH 100, STAB(J), DTAB(J), WTAB(J)
       PUNCH 103
       DO 203 J=1,KPG
```

```
203   PUNCH 100, PGT(J), TSATT(J), HFT(J), HGT(J)
      PUNCH 106
      EXP2=GK/(GK-1.)
      EXP3=1./(GK-1.)
      EXP4=2./(GK+1.)
      EXP5=(GK-1.)/(GK+1.)
      EXP6=.5/EXP5
      EXP7=2.*EXP5
      EXP9=1.
      S=S+DX/2.
      DXF=DX/12.
      QTOT=0.
      DO 500 I=1,M2
      IF (S-STAB(KS)) 43,9,550
9     D=DTAB(KS)
      WTHCK=WTAB(KS)/12.
      GO TO 11
43    DO 6 J=1,KS
      J1=J-1
      IF (S-STAB(J)) 7,8,6
7     D=DTAB(J1)+(S-STAB(J1))*(DTAB(J)-DTAB(J1))/
     1(STAB(J)-STAB(J1))
      W=WTAB(J1)+(S-STAB(J1))*(WTAB(J)-WTAB(J1))/
     1(STAB(J)-STAB(J1))
      WTHCK=W/12.
      GO TO 11
8     D=DTAB(J)
      WTHCK=WTAB(J)/12.
      GO TO 11
6     CONTINUE
11    DRAT=D/DT
      D=D*.08333
      VRAT1=1.
      IF (S-SM1) 12,12,13
12    VM=((EXP4+EXP5*(VRAT1**2))**EXP6)/(DRAT**2)
      GO TO 14
13    VM=SQRT(((VRAT1*(DRAT**2))**EXP7-EXP4)/EXP5)
14    VCRIT=.002*VM
      VCOM=ABS(VM-VRAT1)
      IF(VCOM-VCRIT) 16,16,15
15    VRAT1=VM
      IF (S-SM1) 12,12,13
16    PAR=1.+((GK-1.)/2.)*(VM**2)
      TG=(TZ+460.)/PAR
      TGS=TG-460.
      RHG=RHZ/(PAR**EXP3)
      VG=VM*((GK*32.2*RG*TG)**.5)
      IF (S-SM1) 30,30,31
30    TGM=(TG+TSURF+460.)/2.+.22*.445*TG*(GK-1.)*(VM**2)
```

```
      TGM=TGM-460.
      TG=TG*(1.+.445*(GK-1.)*(VM**2))
      TG=TG-460.
      GO TO 32
31    TGM=(TG+TSURF+460.)/2.+.22*.430*TG*(GK-1.)*(VM**2)
      TGM=TGM-460.
      TG=TG*(1.+430.*(GK-1.)*(VM**2))
      TG=TG-460.
32    PG=PZ/(PAR**EXP2)
26    IF (PG-PGT(KPG)) 84,499,499
84    CONTINUE
      DO 19 J=1,KPG
      IF (PG-PGT(J)) 18,17,19
17    TSAT = TSATT(J)
      HFS=HFT(J)
      HG=HGT(J)
      GO TO 20
18    PRAT=(PG-PGT(J-1))/(PGT(J)-PGT(J-1))
      TSAT=TSATT(J-1)+PRAT*(TSATT(J)-TSATT(J-1))
      HFS=HFT(J-1)+PRAT*(HFT(J)-HFT(J-1))
      HG=HGT(J-1)+PRAT*(HGT(J)-HGT(J-1))
      GO TO 20
19    CONTINUE
20    CONTINUE
      IF (NTYPE) 700,700,701
701   IF (TSURF-TSAT) 720,700,700
700   AK=AK1+AK2*TGM+AK3*TGM**2+AK4*TGM**3+AK5*TGM**4
      GMU=G1+G2*TGM+G3*TGM**2+G4*TGM**3+G5*TGM**4
      PRG=PR1+PR2*TGM+PR3*TGM**2+PR4*TGM**3+PR5*TGM**4
      VK=VK1+VK2*TGM+VK3*TGM**2+VK4*TGM**3+VK5*TGM**4
      CON=AK
      D=(DT*DRAT)/12.
      RHV=144.*PG*WTMOL/(1545.*(TSURF+460.))
      REG=(RHG*VG*D)/GMU
      DMF=DIF*(((TGM+460.)/530.)**1.5)*(14.7/PG)
      SCN=GMU/(RHG*DMF)
      IF (I-1) 21,21,22
21    GFLOW=RHG*VG*.785*(D**2)
      PUNCH 114
      PUNCH 100, GFLOW
22    TW1=.0265*(RHG/32.2)*(VG**2)/(REG**.2)
      H=.0265*CON*(REG**.8)*(PRG**.333)*EXP9/D
      TW=TW1*EXP9
      UST=(TW*32.2/RHV)**.5
      HM1=.0265*DMF*(REG**.8)*(SCN**.333)*EXP9/D
      IF (NTYPE) 470,470,471
470   QEV1=(H*(TG-TSURF)/3600.)/(CPV*(TSURF-TCI))
      GO TO 422
471   QEV1=(H*(TG-TSURF)/3600.)/(CPL*(TSAT-TCI)+CPV*
```

```
     1(TSURF-TSAT))
422   GMAS=(PG*144.-QEV1*RGC*(TSURF+460.)/HM1)/(RG*
     1(TSURF+460.))
      EXP9=EXP(-13.89*QEV1/(B*UST*(QEV1/HM1+GMAS)))
      HM=.0265*DMF*(REG**.8)*(SCN**.333)*EXP9/D
      IF (ABS(HM-HM1)-.02*HM) 420,420,421
421   HM1=HM
      TW=TW1*EXP9
      UST=(TW*32.2/RHV)**.5
      GO TO 422
420   CONTINUE
436   H1=.0265*CON*(REG**.8)*(PRG**.333)*EXP9/D
      IF (NTYPE) 450,450,451
450   QEV1=(H1*(TG-TSURF)/3600.)/(CPV*(TSURF-TCI))
      GO TO 452
451   QEV1=(H1*(TG-TSURF)/3600.)/(CPL*(TSAT-TCI)+CPV*(TSURF
     1-TSAT))
452   GMA=QEV1/HM
      PV=GMA*1545.*(TSURF+460.)/(144.*WTMOL)
      IF (PV-PG) 430,431,431
431   PV=PG
      GV=PV*144.*WTMOL/(1545.*(TSAT+460.))
      GVM=GV/2.
      PVM=GVM*1545.*(TGM+460.)/(144.*WTMOL)
      PSM=PG-PVM
      GSM=PSM*144./(RG*(TGM+460.))
      GVM=GVM/WTMOL
      GSM=GSM*RG/1545.
      XC=GVM/(GVM+GSM)
      XS=GSM/(GVM+GSM)
      CON2=XC*VK+XS*AK
      H1=H1*CON2/CON
      GO TO 433
430   GVM=GMA/2.
      PVM=GVM*1545.*(TGM+460.)/(144.*WTMOL)
      PSM=PG-PVM
      GSM=PSM*144./(RG*(TGM+460.))
      GVM=GVM/WTMOL
      GSM=GSM*RG/1545.
      XC=GVM/(GVM+GSM)
      XS=GSM/(GVM+GSM)
      CON2=XC*VK+XS*AK
      H1=H1*CON2/CON
433   IF (NTYPE) 460,460,461
460   QEV=(H1*(TG-TSURF)/3600.)/(CPV*(TSURF-TCI))
      GO TO 462
461   QEV=(H1*(TG-TSURF)/3600.)/(CPL*(TSAT-TCI)+CPV*(TSURF
     1-TSAT))
462   IF (ABS(QEV-QEV1)-.02*QEV) 465,465,464
```

```
464   QEV1=QEV
      GO TO 422
465   CONTINUE
      QTOT=QTOT+QEV*3.14*D*DXF
      QRAT=QTOT/GFLOW
      PUNCH 113
      PUNCH 100, S, QEV, QTOT, QRAT
      PUNCH 115
      PUNCH 100, TG, PG, EXP9
      S=S+DX
500   CONTINUE
550   PUNCH 117
      GO TO 1
720   PUNCH 112
      GO TO 1
499   PUNCH 102
      GO TO 1
      END
```

APPENDIX E
PHYSICAL PROPERTIES

The viscosity, thermal conductivity, and specific heat at constant pressure for air are given in graphical form in Figures 28, 29, and 30, respectively. The data for temperatures below 3000 ^{o}F. were taken from tables in Kreith's Principles of Heat Transfer. The data above 3000 ^{o}F. were taken from references (15) and (28) in the Bibliography.

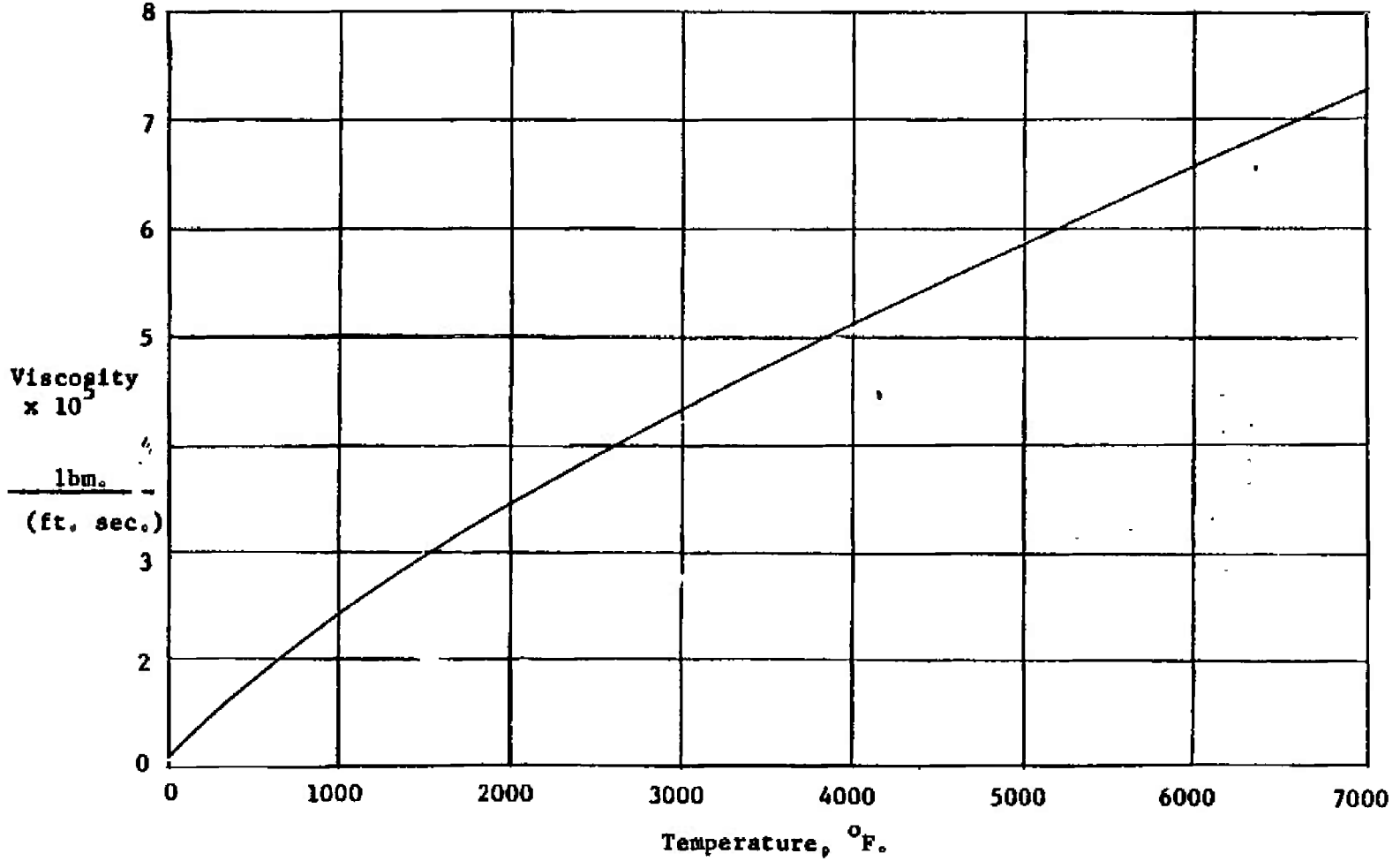

Fig. 28 Viscosity of Air as a Function of Temperature

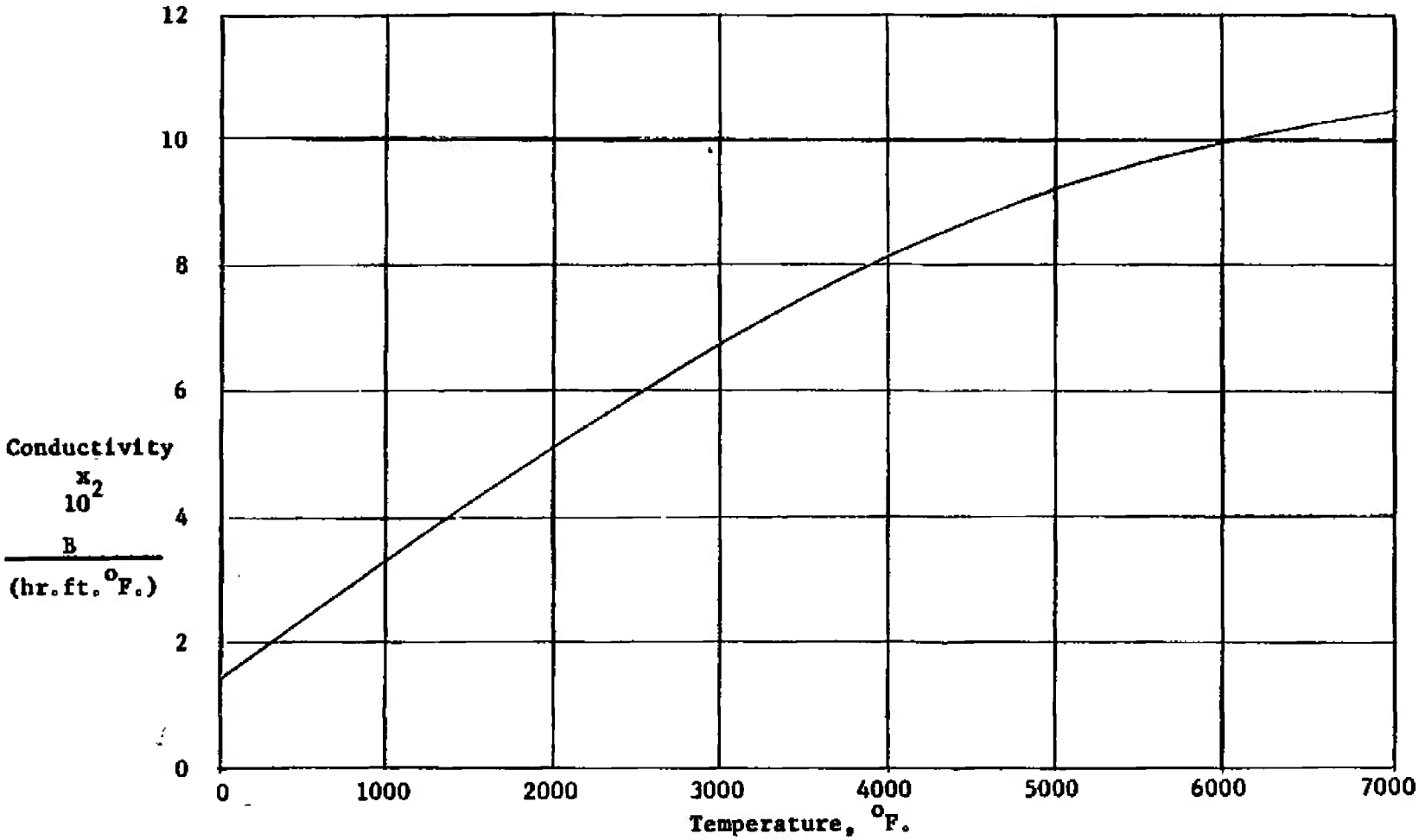

Fig. 29 Thermal Conductivity of Air as a Function of Temperature

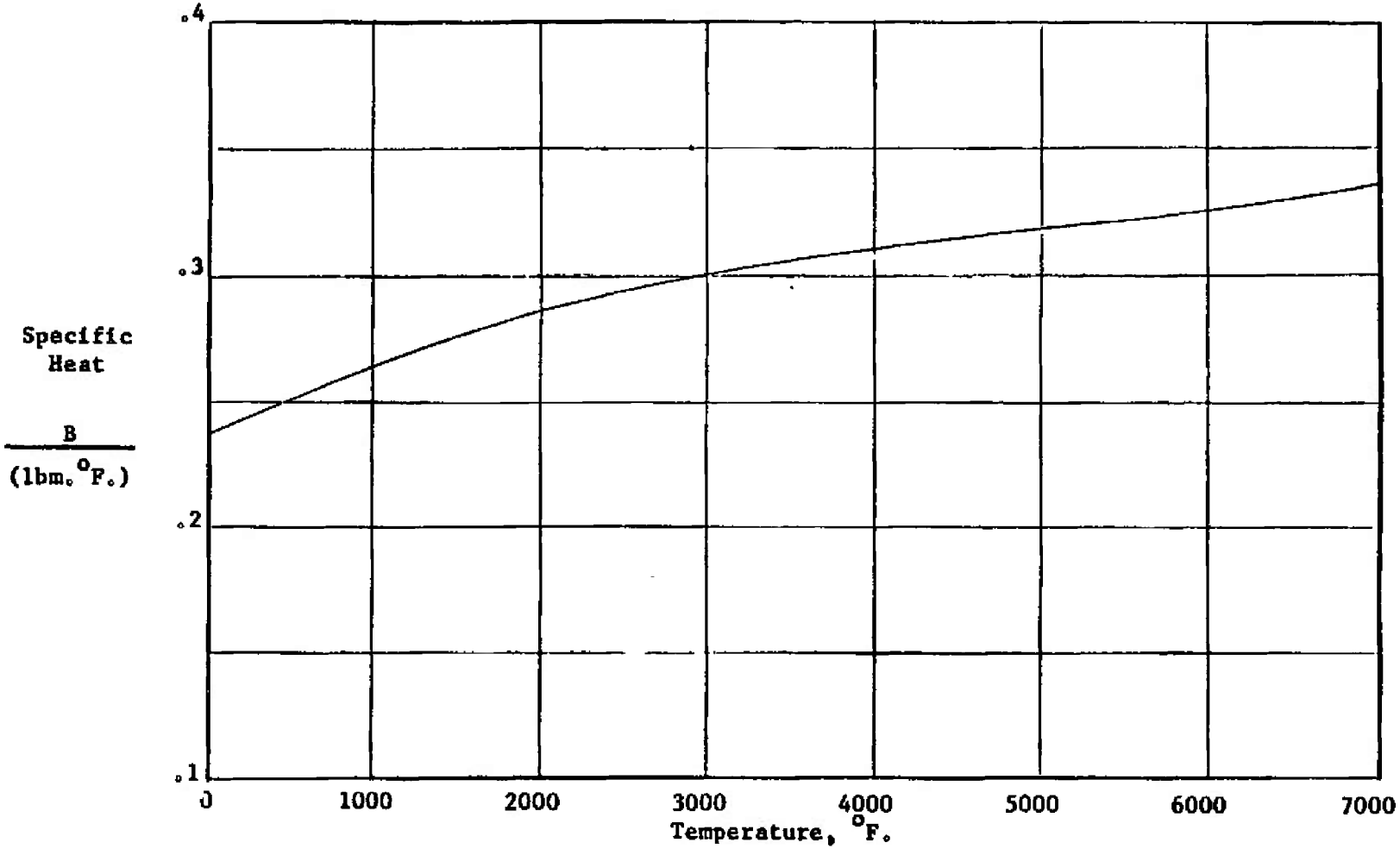

Fig. 30 Specific Heat of Air as a Function of Temperature

APPENDIX F
SAMPLE COMPUTER CALCULATIONS

This Appendix includes Tables VII, VIII, which are the sample computer calculation outputs for transpiration cooling using the gas film cooling program, transpiration cooling using the liquid or gas transpiration program, and the liquid film cooling calculation, respectively.

TABLE VII
SAMPLE CALCULATION FOR TRANSPIRATION
USING GAS FILM PROGRAM

INPUT DATA

```
   0.441E 03   0.300E 04   0.500E 00    20    20     0
   0.128E 01   0.342E 00   0.100E 00    0.200E-03    0.
   0.533E 02   0.190E 03   0.800E 00   320    20     1
   0.100E-01   0.150E 01   0.700E 00     2   320   320
   0.533E 02   0.150E-01   0.100E-01    0.100E 00    0.750E 02
   0.100E 03   0.100E 00
   0.170E-01   0.694E-05   0.139E-07   -0.717E-11    0.125E-14
  -0.262E 01   0.700E-01   0.233E-04    0.           0.
  -0.262E 01   0.700E-01   0.233E-04    0.           0.
   0.238E 00   0.233E-04   0.           0.           0.
   0.238E 00   0.233E-04   0.           0.           0.
    1
   0.          0.150E 01   0.180E 00    0.500E 04
   0.250E-01   0.150E 01   0.180E 00    0.500E 04
   0.500E-01   0.149E 01   0.160E 00    0.500E 04
   0.750E-01   0.148E 01   0.140E 00    0.500E 04
   0.100E 00   0.147E 01   0.110E 00    0.500E 04
   0.125E 00   0.145E 01   0.800E-01    0.500E 04
   0.150E 00   0.142E 01   0.500E-01    0.500E 04
   0.175E 00   0.139E 01   0.450E-01    0.500E 04
   0.200E 00   0.134E 01   0.400E-01    0.500E 04
   0.225E 00   0.130E 01   0.350E-01    0.500E 04
   0.550E 00   0.660E 00   0.300E-01    0.500E 04
   0.575E 00   0.610E 00   0.300E-01    0.500E 04
   0.600E 00   0.570E 00   0.300E-01    0.500E 04
   0.625E 00   0.540E 00   0.300E-01    0.500E 04
   0.650E 00   0.515E 00   0.300E-01    0.500E 04
   0.675E 00   0.505E 00   0.300E-01    0.500E 04
   0.700E 00   0.500E 00   0.300E-01    0.500E 04
   0.725E 00   0.505E 00   0.300E-01    0.500E 04
   0.750E 00   0.515E 00   0.300E-01    0.500E 04
   0.302E 01   0.200E 01   0.140E 00    0.500E 04
   0.127E 03   0.135E 04
   0.122E 03   0.127E 04
   0.119E 03   0.118E 04
   0.116E 03   0.111E 04
   0.115E 03   0.103E 04
   0.113E 03   0.965E 03
   0.111E 03   0.902E 03
   0.110E 03   0.844E 03
   0.108E 03   0.791E 03
   0.107E 03   0.743E 03
```

TABLE VII (Continued)

0.106E 03	0.699E 03
0.104E 03	0.659E 03
0.103E 03	0.623E 03
0.101E 03	0.590E 03
0.100E 03	0.560E 03
0.980E 02	0.534E 03
0.960E 02	0.509E 03
0.940E 02	0.484E 03
0.930E 02	0.468E 03
0.510E 02	0.237E 03
0.134E 03	0.149E 04
0.148E 03	0.168E 04
0.162E 03	0.187E 04
0.171E 03	0.204E 04
0.176E 03	0.220E 04
0.178E 03	0.235E 04
0.178E 03	0.248E 04
0.178E 03	0.259E 04
0.178E 03	0.268E 04
0.178E 03	0.275E 04
0.178E 03	0.281E 04
0.178E 03	0.285E 04
0.178E 03	0.289E 04
0.178E 03	0.291E 04
0.178E 03	0.294E 04
0.178E 03	0.296E 04
0.178E 03	0.298E 04
0.178E 03	0.299E 04
0.178E 03	0.300E 04
0.178E 03	0.300E 04

OUTPUT

QINJ	GFLOW
0.07537	0.75374

S	TSURF	Q/A	DISP.THCK.
0.500E-02	0.248E 03	0.	0.157E-01
0.105E 00	0.312E 03	0.	0.144E-01
0.205E 00	0.353E 03	0.	0.139E-01
0.305E 00	0.411E 03	0.	0.134E-01
0.405E 00	0.484E 03	0.	0.122E-01
0.505E 00	0.582E 03	0.	0.107E-01
0.605E 00	0.701E 03	0.	0.865E-02
0.705E 00	0.804E 03	0.	0.740E-02
0.805E 00	0.800E 03	0.	0.716E-02
0.905E 00	0.801E 03	0.	0.772E-02
0.100E 01	0.781E 03	0.	0.868E-02
0.110E 01	0.768E 03	0.	0.977E-02

TABLE VII (Concluded)

0.120E 01	0.756E 03	0.	0.112E-01
0.130E 01	0.698E 03	0.	0.122E-01
0.140E 01	0.686E 03	0.	0.137E-01
0.150E 01	0.673E 03	0.	0.153E-01
0.160E 01	0.603E 03	0.	0.163E-01
0.170E 01	0.594E 03	0.	0.180E-01
0.180E 01	0.544E 03	0.	0.191E-01
0.190E 01	0.515E 03	0.	0.206E-01
0.200E 01	0.510E 03	0.	0.226E-01
0.210E 01	0.444E 03	0.	0.232E-01
0.220E 01	0.440E 03	0.	0.251E-01
0.230E 01	0.431E 03	0.	0.265E-01
0.240E 01	0.371E 03	0.	0.275E-01
0.250E 01	0.377E 03	0.	0.298E-01
0.260E 01	0.340E 03	0.	0.305E-01
0.270E 01	0.311E 03	0.	0.320E-01
0.280E 01	0.322E 03	0.	0.347E-01
0.290E 01	0.262E 03	0.	0.344E-01
0.300E 01	0.263E 03	0.	0.366E-01

TABLE VIII
SAMPLE CALCULATION FOR TRANSPIRATION USING
LIQUID OR GAS TRANSPIRATION PROGRAM

```
INPUT DATA
   0.100E-04   0.100E-07   0.000E-38   0.000E-38   0.000E-38
   0.900E-02   0.300E-04   0.000E-38   0.000E-38   0.000E-38
   0.133E-01   0.170E-04   0.000E-38   0.000E-38   0.000E-38
   0.700E 00   0.000E-38   0.000E-38   0.000E-38   0.000E-38
   0.450E 03   0.250E 04   0.500E 00   0.500E 03   0.100E 01
   0.140E 01   0.400E 00   0.110E 01   0.533E 02   0.460E 00
   0.180E 02   0.100E 01   0.500E-01   0.700E 00
  110   10   23    1
NOZZLE TABLE
   0.000E-38   0.150E 01   0.400E-01
   0.100E 01   0.590E 00   0.400E-01
   0.103E 01   0.550E 00   0.400E-01
   0.105E 01   0.520E 00   0.400E-01
   0.108E 01   0.495E 00   0.400E-01
   0.110E 01   0.485E 00   0.400E-01
   0.113E 01   0.480E 00   0.400E-01
   0.115E 01   0.485E 00   0.400E-01
   0.117E 01   0.495E 00   0.400E-01
   0.313E 01   0.200E 01   0.160E 00
LIQUID COOLANT TABLE
   0.200E 00   0.531E 02   0.212E 02   0.108E 04
   0.500E 00   0.796E 02   0.476E 02   0.110E 04
   0.100E 01   0.102E 03   0.697E 02   0.111E 04
   0.200E 01   0.126E 03   0.940E 02   0.112E 04
   0.400E 01   0.153E 03   0.121E 03   0.113E 04
   0.700E 01   0.177E 03   0.145E 03   0.114E 04
   0.120E 02   0.202E 03   0.170E 03   0.115E 04
   0.200E 02   0.228E 03   0.196E 03   0.116E 04
   0.400E 02   0.267E 03   0.236E 03   0.117E 04
   0.700E 02   0.303E 03   0.273E 03   0.118E 04
   0.100E 03   0.328E 03   0.298E 03   0.119E 04
   0.150E 03   0.358E 03   0.331E 03   0.119E 04
   0.250E 03   0.401E 03   0.376E 03   0.120E 04
   0.350E 03   0.432E 03   0.410E 03   0.120E 04
   0.500E 03   0.467E 03   0.449E 03   0.120E 04
   0.700E 03   0.503E 03   0.491E 03   0.120E 04
   0.100E 04   0.545E 03   0.542E 03   0.119E 04
   0.150E 04   0.596E 03   0.612E 03   0.117E 04
   0.200E 04   0.636E 03   0.672E 03   0.114E 04
   0.250E 04   0.668E 03   0.731E 03   0.109E 04
   0.290E 04   0.690E 03   0.785E 03   0.104E 04
   0.310E 04   0.700E 03   0.825E 03   0.993E 03
```

TABLE VIII (Concluded)

0.321E 04	0.705E 03	0.903E 03	0.903E 03
OUTPUT			
GFLOW			
0.841E 00			
S	QEV	QTOT	QRAT
0.250E-01	0.139E 00	0.223E-03	0.265E-03
TG	PG	EXP9	
0.250E 04	0.449E 03	0.589E 00	
S	QEV	QTOT	QRAT
0.750E-01	0.189E 00	0.518E-03	0.616E-03
TG	PG	EXP9	
0.250E 04	0.448E 03	0.759E 00	
S	QEV	QTOT	QRAT
0.125E 00	0.183E 00	0.794E-03	0.944E-03
TG	PG	EXP9	
0.250E 04	0.448E 03	0.693E 00	
S	QEV	QTOT	QRAT
0.175E 00	0.201E 00	0.109E-02	0.129E-02
TG	PG	EXP9	
0.250E 04	0.448E 03	0.718E 00	
S	QEV	QTOT	QRAT
0.225E 00	0.212E 00	0.139E-02	0.165E-02
TG	PG	EXP9	
0.250E 04	0.448E 03	0.711E 00	
S	QEV	QTOT	QRAT
0.275E 00	0.227E 00	0.170E-02	0.202E-02
TG	PG	EXP9	
0.250E 04	0.447E 03	0.713E 00	
S	QEV	QTOT	QRAT
0.325E 00	0.242E 00	0.201E-02	0.239E-02
TG	PG	EXP9	
0.250E 04	0.447E 03	0.713E 00	
S	QEV	QTOT	QRAT
0.375E 00	0.260E 00	0.234E-02	0.279E-02
TG	PG	EXP9	
0.250E 04	0.446E 03	0.714E 00	
S	QEV	QTOT	QRAT
0.425E 00	0.280E 00	0.268E-02	0.319E-02
TG	PG	EXP9	
0.250E 04	0.446E 03	0.715E 00	
S	QEV	QTOT	QRAT
0.475E 00	0.302E 00	0.303E-02	0.361E-02
TG	PG	EXP9	
0.250E 04	0.445E 03	0.716E 00	
S	QEV	QTOT	QRAT
0.525E 00	0.327E 00	0.340E-02	0.404E-02

TABLE IX
SAMPLE CALCULATION FOR LIQUID FILM COOLING

INPUT DATA

0.000E-38	0.000E-38	0.200E-03	0.000E-38	0.000E-38
0.100E 01	0.000E-38	0.000E-38	0.000E-38	0.000E-38
0.375E 00	0.000E-38	0.000E-38	0.000E-38	0.000E-38
0.111E-04	0.850E-08	0.000E-38	0.000E-38	0.000E-38
0.600E 02	0.000E-38	0.000E-38	0.000E-38	0.000E-38
0.900E-02	0.300E-04	0.000E-38	0.000E-38	0.000E-38
0.133E-01	0.170E-04	0.000E-38	0.000E-38	0.000E-38
0.700E 00	0.000E-38	0.000E-38	0.000E-38	0.000E-38
0.300E 03	0.400E 04	0.480E 00	0.500E-02	0.700E 02
0.140E 01	0.400E 00	0.110E 01	0.533E 02	0.702E 01
0.190E 03	0.180E 02	0.200E 01	0.100E 01	0.100E 01
0.300E-01	0.113E 01	0.250E 00	0.858E 02	
120 10	10 1	20		
0.000E-38	0.150E 01	0.400E-01	0.500E 04	
0.100E 01	0.590E 00	0.400E-01	0.500E 04	
0.103E 01	0.550E 00	0.400E-01	0.500E 04	
0.105E 01	0.520E 00	0.400E-01	0.500E 04	
0.108E 01	0.495E 00	0.400E-01	0.500E 04	
0.110E 01	0.485E 00	0.400E-01	0.500E 04	
0.113E 01	0.480E 00	0.400E-01	0.500E 04	
0.115E 01	0.485E 00	0.400E-01	0.500E 04	
0.117E 01	0.495E 00	0.400E-01	0.500E 04	
0.313E 01	0.200E 01	0.160E 00	0.500E 04	
0.200E 00	0.531E 02	0.212E 02	0.108E 04	
0.500E 00	0.796E 02	0.476E 02	0.110E 04	
0.100E 01	0.102E 03	0.697E 02	0.111E 04	
0.200E 01	0.126E 03	0.940E 02	0.112E 04	
0.400E 01	0.153E 03	0.121E 03	0.113E 04	
0.700E 01	0.177E 03	0.145E 03	0.114E 04	
0.120E 02	0.202E 03	0.170E 03	0.115E 04	
0.200E 02	0.228E 03	0.196E 03	0.116E 04	
0.400E 02	0.267E 03	0.236E 03	0.117E 04	
0.700E 02	0.303E 03	0.273E 03	0.118E 04	
0.100E 03	0.328E 03	0.298E 03	0.119E 04	
0.150E 03	0.358E 03	0.331E 03	0.119E 04	
0.250E 03	0.401E 03	0.376E 03	0.120E 04	
0.350E 03	0.432E 03	0.410E 03	0.120E 04	
0.500E 03	0.467E 03	0.449E 03	0.120E 04	
0.700E 03	0.503E 03	0.491E 03	0.120E 04	
0.100E 04	0.545E 03	0.542E 03	0.119E 04	
0.150E 04	0.596E 03	0.612E 03	0.117E 04	
0.200E 04	0.636E 03	0.672E 03	0.114E 04	
0.250E 04	0.668E 03	0.731E 03	0.109E 04	

TABLE IX (Concluded)

OUTPUT (SELECTED)

QRAT	QI	GFLOW
0.01114235	0.00500000	0.35917528

S	Q/A	TB	NBOIL
0.150E-01	0.195E 04	0.703E 02	0
H	EXP9	TF2(NI)	NI
0.115E 03	0.111E 01	0.860E 02	1
S	Q/A	TB	NBOIL
0.215E 00	0.116E 06	0.907E 02	
H	EXP9	TF2(NI)	NI
0.124E 03	0.100E 01	0.119E 03	1
S	Q/A	TB	NBOIL
0.415E 00	0.324E 06	0.137E 03	0
H	EXP9	TF2(NI)	NI
0.179E 03	0.100E 01	0.193E 03	1
S	Q/A	TB	NBOIL
0.615E 00	0.474E 06	0.167E 03	0
H	EXP9	TF2(NI)	NI
0.206E 03	0.100E 01	0.248E 03	2
S	Q/A	TB	NBOIL
0.815E 00	0.597E 06	0.191E 03	0
H	EXP9	TF2(NI)	NI
0.487E 03	0.100E 01	0.281E 03	2
S	Q/A	TB	NBOIL
0.102E 01	0.671E 06	0.206E 03	0
H	EXP9	TF2(NI)	NI
0.712E 03	0.100E 01	0.301E 03	3
S	Q/A	TB	NBOIL
0.122E 01	0.739E 06	0.209E 03	0
H	EXP9	TF2(NI)	NI
0.703E 03	0.903E 00	0.313E 03	3
S	Q/A	TB	NBOIL
0.152E 01	0.760E 06	0.211E 03	1
H	EXP9	TF2(NI)	NI
0.391E 03	0.877E 00	0.314E 03	4
S	Q/A	TB	NBOIL
0.192E 01	0.748E 06	0.209E 03	1
H	EXP9	TF2(NI)	NI
0.236E 03	0.857E 00	0.252E 03	5
S	Q/A	TB	NBOIL
0.2[illegible]E 01	0.714E 06	0.206E 03	1
H	EXP9	TF2(NI)	NI
0.197E 03	0.851E00	0.206E03	5

APPENDIX G
DEVELOPMENT OF DIFFERENCE EQUATIONS FOR GAS FILM COOLING ANALYSIS

The difference equation for the momentum (or force) balance, Eq. (6), page 14, is developed by referring to Fig. 2 and evaluating the terms in Eq. (5).

The pressure force is the difference in pressure multiplied by the annular area of the layer projected in the axial direction, thus

$$\text{Pressure forces in } \Delta \text{ direction on coolant layer 1} = \pi d_1' \delta_1' (p_1 - p_2) \tag{86}$$

The inertia forces are the net rate of momentum flow into the volume element as a result of the axial mass flow rate and the velocity of the fluid. Thus,

$$\text{Inertia forces in } \Delta \text{ direction on coolant layer 1} = \frac{w_1'}{g_c} (v'1_1 - v'2_1) \tag{87}$$

The shear forces on the top and bottom of the coolant layer are calculated from the shear stress equation

$$\tau = \rho \epsilon \frac{dv}{dy} \tag{88}$$

Considering τ as the current of momentum and dv as the potential for momentum flow, Eq. (88) may be written as

$$\tau = \frac{dv}{(dy/\rho\epsilon)} \tag{89}$$

By analogy, the resistance to momentum flow is given by the denominator of Eq. (89). Since resistances in series are additive the shear stress on the top of the first coolant layer is given in finite difference form as

$$\tau_{top} = \frac{\frac{v_{1_1} + v_{2_1}}{2} - \frac{v'_{1_1} + v'_{2_1}}{2}}{\frac{\delta_1}{2\rho_1\epsilon_1} + \frac{\delta'_1}{2\rho'_1\epsilon'_1}} \tag{90}$$

Evaluation of the shear stress on the bottom of coolant layer 1 is determined in a similar manner. The shear forces are found by multiplying the stresses by appropriate areas.

$$\begin{aligned}\text{Shear forces on the top and bottom of coolant layer 1} &= \frac{\pi d'_1 \Delta (v_{1_1} + v_{2_1} - v'_{2_1} - v'_{1_1})}{\frac{\delta_1}{\rho_1\epsilon_1} + \frac{\delta'_1}{\rho'_1\epsilon'_1}} \\ &+ \frac{\pi d'_1 \Delta (v'_{1_2} + v'_{2_2} - v'_{1_1} - v'_{2_1})}{\frac{\delta'_1}{\rho'_1\epsilon'_1} + \frac{\delta'_2}{\rho'_2\epsilon'_2}}\end{aligned} \tag{91}$$

Equating the sum of Eqs. (86)(87)(91) to zero yields the momentum balance equation in finite difference form.

The difference equation for the steady state energy balance, Eq. (22), page 20, is developed in a similar manner. Refer to Fig. 2, page 16.

The enthalpy change in the axial direction of a layer is determined from the ideal gas laws as

$$\text{Enthalpy change in } \Delta \text{ direction of coolant layer 1} = w'_1 c'_1 (T'1_1 - T'2_1) \tag{92}$$

The change in kinetic energy is determined from the square of the velocities as

$$\text{Kinetic energy change in } \Delta \text{ direction of coolant layer 1} = \frac{w'_1}{2Jg_c} (v'1_1^2 - v'2_1^2) \tag{93}$$

The thermal energy conduction term is calculated using the temperature difference between layer. The resistance to the flow of heat is

$$\text{Thermal resistance} = \frac{\delta}{\rho c \varepsilon \psi}$$

Thus

$$\text{Thermal energy transfer from gas layer 1 to coolant layer 1 by diffusion} = \frac{\pi d_1 \Delta\left(\frac{T1_1 + T2_1}{2} - \frac{T'1_1 + T'2_1}{2}\right)}{\left(\frac{\delta_1}{2\rho_1 c_1 \varepsilon_1 \psi} + \frac{\delta'_1}{2\rho'_1 c'_1 \varepsilon'_1 \psi}\right)} \quad (94)$$

and a similar equation is written for the thermal energy transfer between coolant layer 1 and coolant layer 2.

In evaluating the work at the boundaries of the increment only shear stress effects are considered.

Thus

$$\text{Viscous work/unit volume} = \mu\left(\frac{dv}{dy}\right)^2 \quad (95)$$

Apply Eq. (95) to the first coolant layer, noting that the velocity gradient in difference terms is established using three layers

$$\text{work/unit volume} = \mu\left[\frac{\frac{v1_1 + v2_1}{2} - \frac{v'1_2 + v'2_2}{2}}{\frac{\delta_1}{2} + \delta'_1 + \frac{\delta'_2}{2}}\right]^2$$

Thus evaluating μ and multiplying by the layer volume of coolant layer 1 gives

$$\text{work at boundaries on coolant layer 1 from shear stress effects} = \frac{\pi d'_1 \Delta \delta'_1 \rho'_1 c'_1 (v1_1 + v2_1 - v'1_2 - v'2_2)^2}{J g_c (2\delta'_1 + \delta'_2 + \delta_1)^2} \quad (96)$$

Security Classification

DOCUMENT CONTROL DATA - R&D

(Security classification of title, body of abstract and indexing annotation must be entered when the overall report is classified)

1. ORIGINATING ACTIVITY (Corporate author)	2a. REPORT SECURITY CLASSIFICATION
Nuclear Engineering Department University of Tennessee Knoxville, Tennessee	UNCLASSIFIED
	2b. GROUP N/A

3. REPORT TITLE

FILM AND TRANSPIRATION COOLING OF NOZZLE THROATS

4. DESCRIPTIVE NOTES (Type of report and inclusive dates)

N/A

5. AUTHOR(S) (Last name, first name, initial)

Roland, H. C., Pasqua, P. F., and Stevens, P. N.
Nuclear Engineering Department, The University of Tennessee

6. REPORT DATE	7a. TOTAL NO. OF PAGES	7b. NO. OF REFS
June 1966	156	42

8a. CONTRACT OR GRANT NO.	9a. ORIGINATOR'S REPORT NUMBER(S)
AF40(600)-981 b. PROJECT NO. 7778	AEDC-TR-66-88
c. Program Element 62410034 d. Task 777805	9b. OTHER REPORT NO(S) (Any other numbers that may be assigned this report) N/A

10. AVAILABILITY/LIMITATION NOTICES

Qualified requesters may obtain copies of this report from DDC and distribution of this document is unlimited.

11. SUPPLEMENTARY NOTES	12. SPONSORING MILITARY ACTIVITY
N/A	Arnold Engineering Development Center(AEDC) Air Force Systems Command (AFSC) Arnold Air Force Station, Tennessee

13. ABSTRACT Analytical studies were made of liquid film cooling, gas film cooling, and liquid or gas transpiration cooling of hypersonic nozzles. Experimental studies of gas film cooling were performed on a small nozzle using air as both the mainstream and coolant gases. Based on the experimental results obtained and the development of satisfactory calculational techniques to implement the analyses given in the present study, the following conclusions were drawn: (1) Gas film cooling can be used to measurably lower the wall temperatures and the wall heat fluxes in the converging section and at the throat of a high-pressure high-temperature nozzle. Some gross mixing occurs at the injection point, the exact amount being some as yet undetermined function of the injection geometry, the relative velocities of the main gas stream and the coolant stream at the injection point, and the entering velocity profiles and turbulence conditions. (2) A straightforward boundary layer type analysis was developed and programmed which predicts with reasonable accuracy the nozzle wall temperatures and wall heat fluxes in the converging section and at the throat for gas film cooled nozzles. (3) Calculational techniques have been developed and programmed for predicting the effectiveness of liquid film cooling and liquid or gas transpiration cooling in nozzles. These techniques should be checked against experimental data before they are used for design purposes, however.

DD FORM 1 JAN 64 1473

Security Classification

14. KEY WORDS	LINK A		LINK B		LINK C	
	ROLE	WT	ROLE	WT	ROLE	WT
nozzles						
cooling - gas film						
cooling - liquid film						
transpiration						

INSTRUCTIONS

1. ORIGINATING ACTIVITY: Enter the name and address of the contractor, subcontractor, grantee, Department of Defense activity or other organization *(corporate author)* issuing the report.

2a. REPORT SECURITY CLASSIFICATION: Enter the overall security classification of the report. Indicate whether "Restricted Data" is included. Marking is to be in accordance with appropriate security regulations.

2b. GROUP: Automatic downgrading is specified in DoD Directive 5200.10 and Armed Forces Industrial Manual. Enter the group number. Also, when applicable, show that optional markings have been used for Group 3 and Group 4 as authorized.

3. REPORT TITLE: Enter the complete report title in all capital letters. Titles in all cases should be unclassified. If a meaningful title cannot be selected without classification, show title classification in all capitals in parenthesis immediately following the title.

4. DESCRIPTIVE NOTES: If appropriate, enter the type of report, e.g., interim, progress, summary, annual, or final. Give the inclusive dates when a specific reporting period is covered.

5. AUTHOR(S): Enter the name(s) of author(s) as shown on or in the report. Enter last name, first name, middle initial. If military, show rank and branch of service. The name of the principal author is an absolute minimum requirement.

6. REPORT DATE: Enter the date of the report as day, month, year, or month, year. If more than one date appears on the report, use date of publication.

7a. TOTAL NUMBER OF PAGES: The total page count should follow normal pagination procedures, i.e., enter the number of pages containing information.

7b. NUMBER OF REFERENCES: Enter the total number of references cited in the report.

8a. CONTRACT OR GRANT NUMBER: If appropriate, enter the applicable number of the contract or grant under which the report was written.

8b, 8c, & 8d. PROJECT NUMBER: Enter the appropriate military department identification, such as project number, subproject number, system numbers, task number, etc.

9a. ORIGINATOR'S REPORT NUMBER(S): Enter the official report number by which the document will be identified and controlled by the originating activity. This number must be unique to this report.

9b. OTHER REPORT NUMBER(S): If the report has been assigned any other report numbers *(either by the originator or by the sponsor)*, also enter this number(s).

10. AVAILABILITY/LIMITATION NOTICES: Enter any limitations on further dissemination of the report, other than those imposed by security classification, using standard statements such as:

(1) "Qualified requesters may obtain copies of this report from DDC."

(2) "Foreign announcement and dissemination of this report by DDC is not authorized."

(3) "U. S. Government agencies may obtain copies of this report directly from DDC. Other qualified DDC users shall request through _____."

(4) "U. S. military agencies may obtain copies of this report directly from DDC. Other qualified users shall request through _____."

(5) "All distribution of this report is controlled. Qualified DDC users shall request through _____."

If the report has been furnished to the Office of Technical Services, Department of Commerce, for sale to the public, indicate this fact and enter the price, if known.

11. SUPPLEMENTARY NOTES: Use for additional explanatory notes.

12. SPONSORING MILITARY ACTIVITY: Enter the name of the departmental project office or laboratory sponsoring *(paying for)* the research and development. Include address.

13. ABSTRACT: Enter an abstract giving a brief and factual summary of the document indicative of the report, even though it may also appear elsewhere in the body of the technical report. If additional space is required, a continuation sheet shall be attached.

It is highly desirable that the abstract of classified reports be unclassified. Each paragraph of the abstract shall end with an indication of the military security classification of the information in the paragraph, represented as *(TS), (S), (C), or (U)*.

There is no limitation on the length of the abstract. However, the suggested length is from 150 to 225 words.

14. KEY WORDS: Key words are technically meaningful terms or short phrases that characterize a report and may be used as index entries for cataloging the report. Key words must be selected so that no security classification is required. Identifiers, such as equipment model designation, trade name, military project code name, geographic location, may be used as key words but will be followed by an indication of technical context. The assignment of links, rules, and weights is optional.